

1. Report No.	2. Government Accession No.	3. Recipient's Catalog No.	
4. Title and Subtitle "Static and Buckling Analysis of Highway Bridges by Finite Element Procedures"		5. Report Date August 1973	6. Performing Organization Code
7. Author(s) C. Philip Johnson, Thaksin Thepchatri, and Kenneth M. Will		8. Performing Organization Report No. Research Report 155-1F	
9. Performing Organization Name and Address Center for Highway Research The University of Texas at Austin Austin, Texas 78712		10. Work Unit No.	11. Contract or Grant No. Research Project 3-5-71-155
12. Sponsoring Agency Name and Address Texas Highway Department Planning & Research Division P. O. Box 5051 Austin, Texas 78763		13. Type of Report and Period Covered Final September 1970 - August 1973	
15. Supplementary Notes Work done in cooperation with the Federal Highway Administration, Department of Transportation. Study Title: "Static and Buckling Analysis of Highway Bridges by Finite Element Procedures"		14. Sponsoring Agency Code	
16. Abstract This research focused on the application of finite element computer programs to complex bridge structures which may be idealized as an assemblage of one and two-dimensional elements. Each two-dimensional element may be either triangular or quadrilateral in shape. They may be arbitrarily located in space by merely specifying the coordinates at the corners of the elements. Each element contains a membrane and a bending stiffness. Assemblages of these elements are able to effectively represent three-dimensional structural behavior for a detailed determination of stresses and deflections for a wide range of highway structures. Demonstration analyses were performed on two highway bridges under the action of dead and live loads including prestressing forces. The influence of severely skewed supports, curvature along the bridge center line, lateral bracing and transverse diaphragms and concrete placing sequences on the structural response was studied. In addition, a buckling analysis of an interior steel girder was made in an effort to gain insight into bracing and stiffener requirements. A preliminary investigation of the influence of thermal stresses caused by daily variations in temperature was undertaken. The problem of temperature induced stresses is being addressed in more detail in a current project.			
17. Key Words static, buckling, highway bridges, finite element, skewed supports, computer program		18. Distribution Statement	
19. Security Classif. (of this report) Unclassified	20. Security Classif. (of this page) Unclassified	21. No. of Pages 154	22. Price

STATIC AND BUCKLING ANALYSIS OF HIGHWAY
BRIDGES BY FINITE ELEMENT PROCEDURES

by

C. Philip Johnson
Thaksin Thepchatri
Kenneth M. Will

Research Report 155-1F

Static and Buckling Analysis of Highway
Bridges by Finite Element Procedures

Research Project 3-5-71-155

conducted for

The Texas Highway Department

in cooperation with the
U. S. Department of Transportation
Federal Highway Administration

by the

CENTER FOR HIGHWAY RESEARCH
THE UNIVERSITY OF TEXAS AT AUSTIN

August 1973

The contents of this report reflect the views of the authors, who are responsible for the facts and the accuracy of the data presented herein. The contents do not necessarily reflect the official views or policies of the Federal Highway Administration. This report does not constitute a standard, specification, or regulation.

PREFACE

A finite element procedure for the analysis of complex bridge structures which may be idealized as an assemblage of one and two-dimensional elements has been presented. This procedure accounts for the effects of severely skewed supports, curvature along the bridge center line and the cross sectional shape as they influence the structural response.

Program SHELL was used to perform two demonstration analyses. Several individuals have made contributions in developing and testing this program over a period of several years. With regard to this project special thanks are due to John Panak, Hasan Akay, M. R. Abdelraouf and Steve Spoor. In addition, thanks are due to Nancy L. Pierce and the members of the staff of the Center for Highway Research for their assistance in producing this report.

This page replaces an intentionally blank page in the original.

-- CTR Library Digitization Team

ABSTRACT

This research focused on the application of finite element computer programs to complex bridge structures which may be idealized as an assemblage of one and two-dimensional elements. Each two-dimensional element may be either triangular or quadrilateral in shape. They may be arbitrarily located in space by merely specifying the coordinates at the corners of the elements. Each element contains a membrane and a bending stiffness. Assemblages of these elements are able to effectively represent three-dimensional structural behavior for a detailed determination of stresses and deflections for a wide range of highway structures.

Demonstration analyses were performed on two highway bridges under the action of dead and live loads including prestressing forces. The influence of severely skewed supports, curvature along the bridge center line, lateral bracing and transverse diaphragms and concrete placing sequences on the structural response was studied. In addition, a buckling analysis of an interior steel girder was made in an effort to gain insight into bracing and stiffener requirements. A preliminary investigation of the influence of thermal stresses caused by daily variations in temperature was undertaken. The problem of temperature induced stresses is being addressed in more detail in a current project.

KEY WORDS: static, buckling, highway bridges, finite element, skewed supports, computer program.

This page replaces an intentionally blank page in the original.

-- CTR Library Digitization Team

SUMMARY

Static and buckling computer programs have been applied to problems of current practical importance to the Texas Highway Department. Program SHELL which was used most extensively in the study is applicable to highway structures which may be idealized as an assemblage of one and two-dimensional elements. Complex geometries and supporting arrangements may be systematically treated inasmuch as elements and nodes can be arbitrarily positioned in space. This program was highly developed at the onset of this work. It was further modified and extended during the course of the research to enhance its application to highway structures.

A similar program, SHELL6 was used for check purposes. It is based on a six-degree-of-freedom nodal system of displacements while only five are used for program SHELL. Results from the two programs were in close agreement. During the latter part of the project, program SHELL was modified to account for six-degrees-of-freedom. The resulting program (PLS6DOF) reduces the required input but requires more storage and computation time than program SHELL. Program MESHPLT was developed to enable the user to check his input data. Moreover, a CAL-COMP plot routine was added for the purpose of plotting the finite element mesh. Program BASP was used for the buckling analyses.

Demonstration analyses were made for two highway bridges. The key results from these analyses are presented in this report. Input requirements and the associated output for an example problem are described in detail. The demonstration analyses were performed in close coordination with the engineers of the Bridge Division at the Texas Highway Department to enable continuing application of program SHELL for structures requiring this general treatment. The generality of programs SHELL and PLS6DOF allows one to determine analytically the structural response of proposed complex geometries for construction; thus enhancing the implementation of new bridge types which may be both efficient and pleasing in appearance.

This page replaces an intentionally blank page in the original.

-- CTR Library Digitization Team

IMPLEMENTATION STATEMENT

A finite element computer program (SHELL) for analyzing structures which may be idealized as an assemblage of one and two-dimensional flat plate elements has been modified and extended during the course of this research. The CDC 6600 computer at the University of Texas was used for this purpose. The final version of program SHELL has also been adapted to the IBM computer facilities of the Texas Highway Department. In particular this report contains:

- a) The Documentation of Program SHELL (Chapter 4)
- b) An Example Problem for Input and Output (Appendix 1)
- c) A Listing of the IBM Version (Appendix 2)

for the purpose of in-house use by the Texas Highway Department. Also, the two demonstration analyses which were performed and described herein should expedite the future use of this program. Programs BASP, MESHPLT and PLS6DOF which were not adapted to the computer facilities of the Texas Highway Department are available upon request. Program SHELL6 has been listed in a previous report.

The program is not restricted to any particular geometric form; thus the input requirements are quite substantial. Mesh generation options, however, which are an integral part of the program reduce and simplify the data preparation for a given problem.

All aspects of the demonstration analyses are successful. However, current research being performed under Research Project 3-5-74-23 clearly indicates a deficiency in the manner in which the temperature was represented. In particular the temperature distribution in a bridge slab is non-uniform over its depth. The ability to account for the non-uniform temperature distribution has recently been incorporated into PLS6DOF and is currently being evaluated. It is anticipated that the final version of PLS6DOF will be adapted to the Texas Highway Department computer facilities at the end of Research Project 3-5-74-23. This will provide the user with a choice of programs to use depending on the structure being analyzed.

This page replaces an intentionally blank page in the original.

-- CTR Library Digitization Team

TABLE OF CONTENTS

PREFACE	iii
ABSTRACT	v
SUMMARY	vii
IMPLEMENTATION STATEMENT	ix
CHAPTER 1. INTRODUCTION	
Nature of the Problem	1
Review of Analysis Procedures	2
Objectives of the Study	4
The Demonstration Analyses	5
CHAPTER 2. METHOD OF ANALYSIS	
General	11
The Structural Idealization	11
General Features of Program SHELL	13
Other Computer Programs Used in the Research	15
Program SHELL6	15
Program PLS6DOF	15
Program MESHPLT	16
Program BASP	16
Summary of Order of Presentation	16
CHAPTER 3. THE FINITE ELEMENT IDEALIZATION	
General	17
Finite Elements for Program SHELL	17
The Triangular Element	18
The Quadrilateral Element	18
The Out-of-Plane Rotational Stiffness for Program PLS6DOF	22
CHAPTER 4. DOCUMENTATION OF PROGRAM SHELL	
Purpose and Programming Information	27
Use of the Program	27
1.1 Mesh Construction	27
1.2 Coordinate Systems	29

1.3	Finite Element Types	32
1.4	Nodal Point Degrees of Freedom and Base Coordinates	33
1.5	Element Distributed Loads	34
1.6	Orthotropic Material Properties	36
	Preparation of Input Data	38
2.1	Title Card	38
2.2	Control Card	38
2.3	Nodal Coordinate Cards	39
2.4	Surface Coordinate Direction Cosine Cards	39
2.5	Element Nodal Point Number Cards	40
2.6	Element Material Table	41
2.7	Element Property Cards	41
2.8	Element Distributed Load Cards	42
2.9	Nodal Temperature Cards	42
2.10	Boundary Condition Cards	43
2.11	Control Card for Elastic Supports	43
2.12	Spring Constant Cards	43
2.13	Control Card for Nodal Point Loads	44
2.14	Nodal Point Load Cards	44
	Nodal Coordinate Generation	46
3.1	Straight Line	47
3.2	Circular Arc	49
3.3	Parabola	50
3.4	Ellipse	52
3.5	Incremental Generation -- TYPE 1	53
3.6	Incremental Generation -- TYPE 2	53
	Element Nodal Point Number Generation	56
4.1	TYPE 1	56
4.2	TYPE 2	56

CHAPTER 5. THE DEMONSTRATION ANALYSES

	The Gull-Winged Girder	57
	Summary	57
	Coordinate Systems and Finite Elements	60
	The Applied Loads	60
	The Load Cases	66
	Summary of the Results	66
	Load Case 1	66
	Load Case 2. (D.L. + P/S)	66
	Load Case 3. (D.L. + P/S + L.L. #1)	68
	Load Case 4. (D.L. + P/S + L.L. #2)	68
	Load Case 5. (D.L. + P/S + L.L. #3)	68
	The Three Girder Bridge	70
	The Structural Idealization	70
	The Dead Load	74
	The Live Load	74
	The Assumed Temperature Gradient	74

Summary of the Static Analyses	74
Load Case 1	74
Load Case 2	79
Load Case 3	79
Load Case 4	79
Load Case 5 and 6	79
A Two-Dimensional Analysis of the Actual Placing	
Sequence	85
Buckling Analysis	85
 CHAPTER 6. CONCLUSIONS AND RECOMMENDATIONS	 91
 REFERENCES	 93
 APPENDICES	
Appendix 1. An Example Problem for Input and Output	95
Appendix 2. A Listing of the IBM Version	111

CHAPTER 1. INTRODUCTION

Nature of the Problem

This report is intended to summarize the results of the research project "Static and Buckling Analysis of Highway Bridges by Finite Element Procedures," which was conducted during the period August 1, 1971, to August 31, 1973, under the sponsorship of the Texas Highway Department and the Federal Highway Administration. This project was motivated by the need for a general analysis procedure which would be applicable for predicting structural response of complex bridge structures.

Current bridge construction practice includes a variety of cross section types used in various plan configurations that require the use of a rather general procedure if a representative and accurate static analysis is to be made. The shape of the cross section when combined with either variable skew supports or curvature along the bridge center line is a source of three-dimensional structural response. In addition this behavior may be accentuated for bridges with widely spaced steel girders which are laced with complex diaphragms forming an integral three-dimensional structural assemblage with the slab and girders. Furthermore, the structural behavior is influenced by loadings which are eccentric to the bridge center line, thermal stresses caused by daily variations in temperature and buckling in regions having thin structural elements subjected predominately to compressive stresses.

The degree of accuracy in computing stresses, displacements, and buckling characteristics for such structures depends on how accurately the structure may be idealized as an assemblage of structural elements. To this end, the use of finite elements having arbitrary shape and position in space is required, together with the associated necessity that the individual elements have adequate stiffness properties so that the structural response may be accurately determined. Fortunately, highly developed finite element analysis programs were available at the onset of this work. Thus only minimal modifications and extensions were necessary to address problems of current interest.

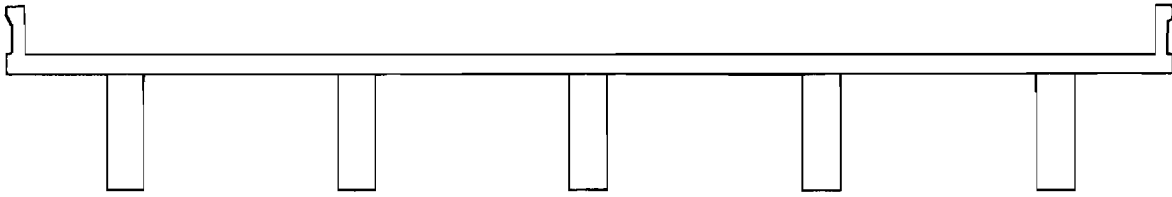
Review of Analysis Procedures

Historically highway bridges have been analyzed as continuous beams. When more detail is required to represent the shape of the cross section and supporting arrangement, the actual structure is often idealized as a two-dimensional plate structure or an assemblage of individual plates representing the slab and supporting girders. These idealizations for a typical slab-girder cross section are shown in Fig 1. Several analysis procedures are available for these idealizations. They may be grouped into four categories according to the structural idealization:

1. equivalent flat plate idealization (Fig 1b),
2. equivalent plate and beam idealization (Fig 1c),
3. folded plate method (Fig 1d), and
4. finite element method (Fig 1d).

The literature on analysis procedures for the four categories is extensive and will not be reviewed in detail here. However, characteristics of each category will be discussed and representative analysis procedures will be cited.

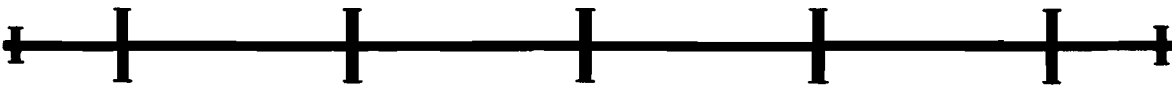
The equivalent flat plate idealization involves "smearing" the variable cross section properties into an equivalent uniform plate as shown in Fig 1b. Transverse and longitudinal bending stiffnesses are assigned empirically and the uniform plate is analyzed as a two-dimensional plate structure. An alternative idealization consists of empirical assignment of variable inertias for the slab, girders, and parapets as shown in Fig 1c. The resulting idealization is then analyzed as a plate with embedded beams in which the geometric center lines of the equivalent composite beams representing the parapets and girders are assumed to lie in the plane of the equivalent plate. Thus, both procedures approximate the eccentrically connected parapets and girders by a two-dimensional structural system. Analysis procedures for skewed anisotropic slabs are discussed extensively in Ref 1 by a finite element method and in Ref 2 by a discrete element technique. The principal shortcoming of either of the above procedures lies in the difficulty of assigning inertias to the equivalent system to accurately model the actual behavior. Furthermore, these analyses only yield bending moments in the equivalent bending structure which only approximates the actual distributions of longitudinal and transverse



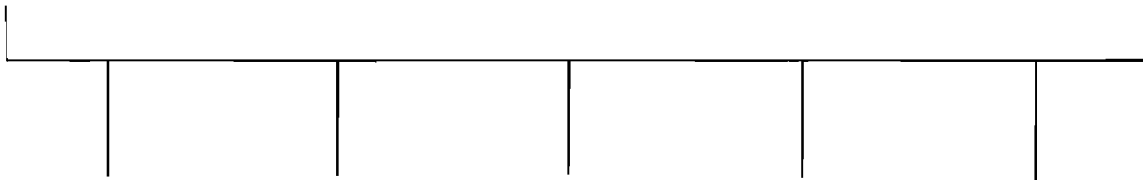
(a). Slab-girder section.



(b). Equivalent flat plate idealization.



(c). Equivalent plate and beam idealization.



(d). Folded plate and finite element idealization.

Fig 1. Typical slab-girder section and various idealizations.

stresses over the depth of the cross section.

The folded plate method, as described for example in Ref 3, is an efficient and accurate procedure for analyzing structures consisting of intersecting plates. For example, this procedure would provide a more accurate analysis of the cross section of Fig 1a as compared to the equivalent flat plate and beam idealizations as described above. This procedure necessitates a structural idealization as shown in Fig 1d and is able to accurately determine the distribution of stress over the cross section. Unfortunately, the folded plate method is based on a number of simplifying assumptions which limit its application to structures having regular geometries and supports, and so this method is essentially confined to treating cross sections which are constant over the entire bridge and to plan configurations which are rectangular.

The finite element method is now a highly developed procedure for the analysis of complex structures. Even this procedure introduces approximations in the manner in which the structure is idealized and the subsequent evaluation of the stiffness properties of the idealized structure. When planar elements are used, the structural idealization is similar to the folded plate method but is generalized by merely subdividing the structure into several elements or pieces in both the transverse and longitudinal directions. The accuracy and range of application of a particular procedure must be evaluated in light of the approximations introduced in the formulation (i.e., element shapes and their stiffness properties). Representative procedures applicable to a class of highway structures may be found in Refs 4 and 5.

The subject finite element procedure was an outgrowth of an effort to analyze curved shell structures (6,7,8,9) as an assemblage of planar triangular and quadrilateral elements. Since the shape of the individual elements and their orientation in space are arbitrary, they may be assembled to represent structures with arbitrary geometric forms. This procedure which has been further refined not only for static analysis (10) but also for structural buckling (11,12,13,14) was selected for this work.

Objectives of the Study

The application of static and buckling computer programs to study problems of current practical importance to the Texas Highway Department was the central

objective of this research. Demonstration analyses were performed on the structures shown in Figs 2 and 3. Emphasis was placed on accurately modeling these structures as an assemblage of one and two-dimensional finite elements in determining the displacements and stresses under the action of dead and live loads including prestressing forces.

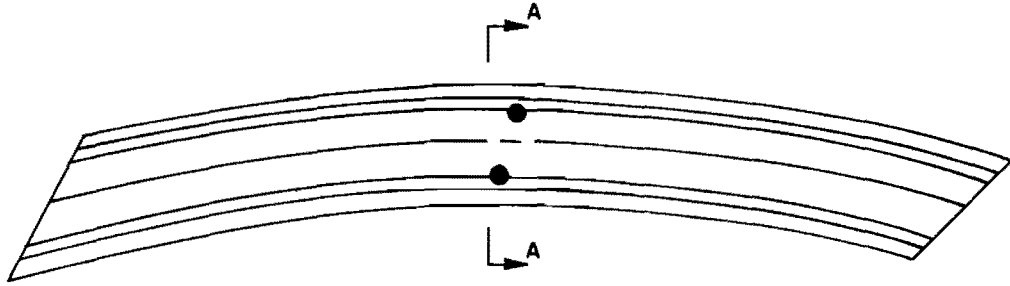
Demonstration analyses were made for the two highway bridges to determine the applicability of the subject procedure to complex bridge structures. These studies were performed in close coordination with the engineers of the Bridge Division of the Texas Highway Department. In addition to gaining insight into the static and buckling structural response of a special class of bridge structures, the experience thus gained could enable continuing application by the Texas Highway Department and others for structures requiring this general treatment.

The Demonstration Analyses

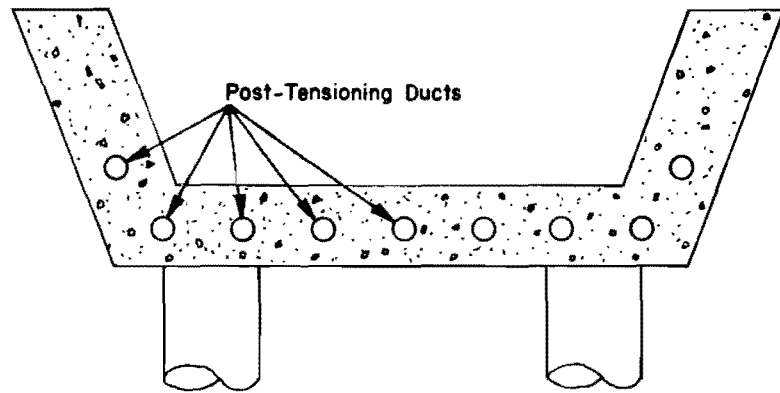
The gull-winged girder of Fig 2 was analyzed for dead load, prestressing forces and three live load cases. This structure is a post-tensioned railway structure continuous over three severely skewed supporting bents. The structure is slightly curved. A companion analysis was made for a straight structure with orthogonal supports. The final results showed that the behavior of the actual structure was significantly different from the assumed one. It was concluded that the severely skewed supports were the principal source of the differing behavior. In general, it was found that the skewed structure had smaller deflections than the straight orthogonally supported structure.

A second demonstration analysis was performed on a bridge having three widely spaced girders braced with truss-type diaphragms. It is continuous over three spans with skewed supports. The plan view and cross section are shown in Figs 3a and 3b. The structural idealization consisted of two-dimensional elements for the slab and the webs of the girders while the flanges of the girders, vertical stiffeners, lateral bracing and transverse diaphragms were represented by one-dimensional (truss) elements. A total of 584 nodal points and 1629 elements were included in this mesh layout.

This bridge was analyzed for dead load by simplifying the actual placing sequence to two placings. Also two live load cases were considered. Analyses

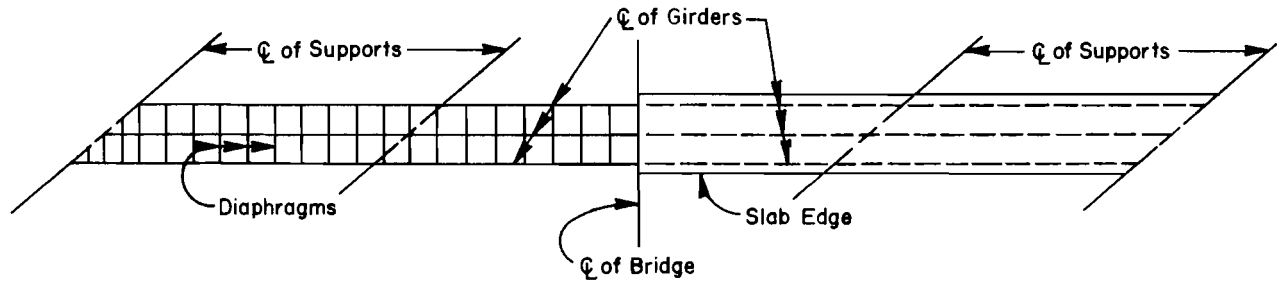


(a). Plan view.

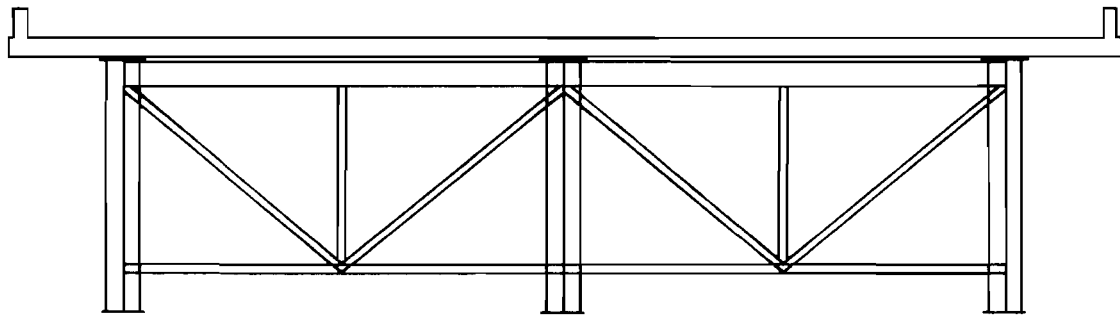


(b). Section A-A.

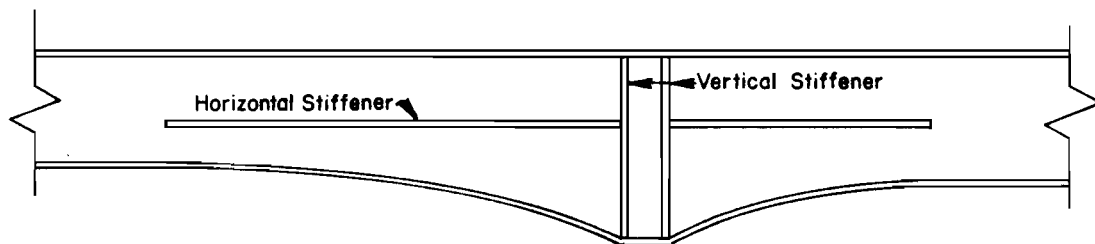
Fig 2. Post-tensioned curved bridge.



(a). Plan view of bridge with diaphragms.



(b). Bridge cross section at a typical diaphragm.

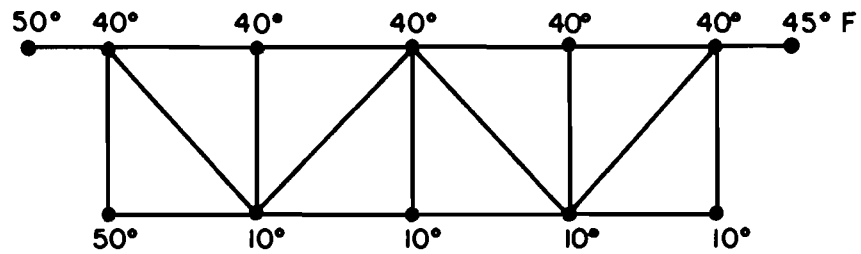


(c). Elevation of girder at interior support.

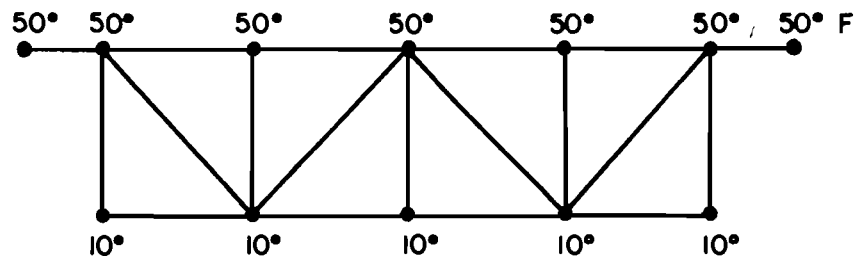
Fig 3. Skewed bridge with widely spaced girders.

were made with and without lateral bracing and transverse diaphragms. Also, a two-dimensional idealization (14) was employed in an effort to determine the effect of the skewed supports on the structural response. Analyses were also made for two assumed sets of temperatures as shown in Fig 4. The temperature gradient was assumed to be linear over the depth of the cross section. It was concluded that skewed supports had little influence on the overall structural response.

Also a buckling analysis of the interior girder (Fig 3c) of the three-girder bridge was made using the procedure of Ref 14. The buckling analysis was made for total dead load without regard to placing sequences. Several refinements in the mesh were used due to the highly localized nature of buckling in the web of the girder. Analyses were made with and without the longitudinal half-stiffener. Comparison of the results clearly indicated the importance of this stiffener in increasing the load at which the web buckles.



a. Uneven temperature rise.



b. Even temperature rise.

Fig 4. Idealized cross section with diaphragm and approximate temperature rise in degree Fahrenheit.

This page replaces an intentionally blank page in the original.

-- CTR Library Digitization Team

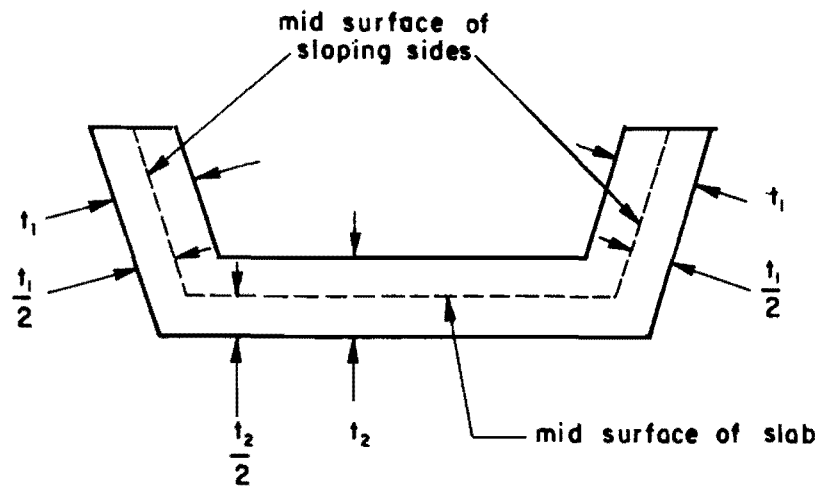
CHAPTER 2. METHOD OF ANALYSIS

General

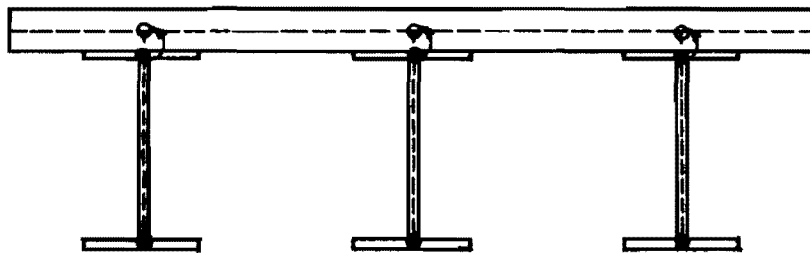
The program which was used most extensively in this research is called SHELL. As stated earlier, this program was available for the study since it had already found a wide range of applications for shell structures which could be idealized as an assemblage of two-dimensional flat plate elements to approximate the shell surface. These elements may be either triangular or quadrilateral in shape. They may be arbitrarily located in space by merely specifying the coordinates at the corners of the element. Each element contains a membrane stiffness and a bending stiffness. These stiffnesses are uncoupled at the element level.

The Structural Idealization

In order to apply this program to highway bridges, the bridge must first be idealized as an assemblage of two-dimensional elements. In most cases, this is done on an intuitive basis. For example, the finite element idealization of the cross section of the gull-winged structure of Fig 5a is taken as the mid-surface of the slab and the sloping sides. Thus, the juncture regions of the slab and the sloping sides are only approximated by the mid-surface representation. The finite element idealization for the cross section of the Fig 5b was taken as the mid-surface of the slab and the webs of the girders. In addition, the stiffness of the flanges was simulated with truss elements located at the mid-depth of the flanges. In this case, the mid-surface of the slab and the truss do not coincide. Thus the truss elements were shifted up to the mid-surface of the slab. In this case, the cross-sectional moment of inertia of the finite element idealization differed from that of the actual cross section by 2.9 percent. While the finite element idealizations described above are relatively straight-forward, more thought may have to be given, for example, in the case of the cross section of Figs 6a and b. The difficulty here lies in the region of the slab, sidewalk and



a. Concrete section.



● Truss elements simulating the flange

○ Shifted position of truss elements

b. Concrete and steel section.

Fig 5. Finite element representations for bridge cross sections.

parapet. Two possible idealizations are shown in Fig 6. These kinds of approximations in the structural idealization could be overcome by using three-dimensional finite elements with a heavy penalty paid in computation effort.

General Features of Program SHELL

The theoretical development for program SHELL is available in Ref 7. The program resulting from that work (7) was extended and documented in Ref 8. The principal extensions included element pressure load and mesh generation options for simplification of input data. Additional features were incorporated into the program and described in Ref 10. These included:

1. Variable thickness over the individual elements,
2. Orthotropic material properties,
3. Overlay features,
4. Element distributed loads (gravity forces),
5. Iterative procedure for improving the displacement solution, and
6. Calculation of reactive nodal point forces.

The above versions of SHELL employed a five-degree-of-freedom (DOF) nodal system of displacements. The five-DOF consisted of three translations but only two rotations at each node point. While the five-DOF system yields economy in the solution process as compared to a six-DOF system, judgement is required in selecting the orientation of the two nodal rotations. This is discussed in more detail in Chapters 4 and 5.

During the course of this work the following were incorporated into program SHELL:

7. The capacity of the program was increased to accommodate 800 nodes and 1200 elements.
8. Truss elements were added.
9. An improved membrane element (QM5) was added.
10. A mechanism to account for linear variations in temperature over the elements mid-surface was added.
11. An option was made available for the calculation of element principal stresses.

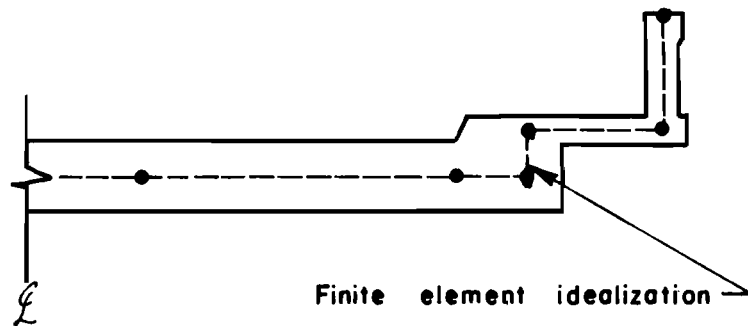
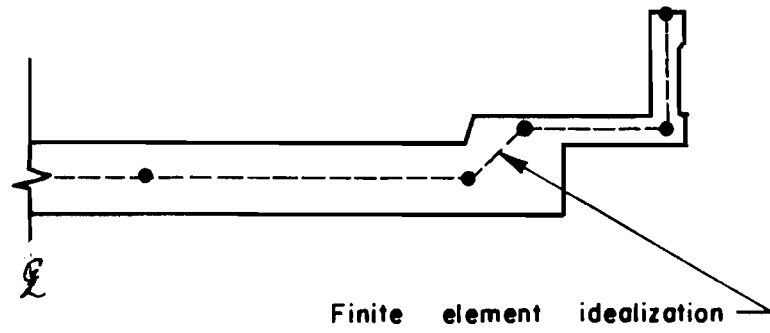


Fig 6. Two possible finite element idealizations for slab, sidewalk and parapet.

12. Nodes with zero stiffness in the equilibrium equations were made acceptable (this was useful in analyzing the placing sequences for the three-girder bridge).

The CDC version of this program has been adapted to the IBM computer facilities of the Texas Highway Department. A documentation of the program and a listing of the IBM version are included in this report.

Other Computer Programs Used in the Research

In addition to Program SHELL, four other programs were used during the course of this research. General characteristics of each are described below.

Program SHELL6 -- This program employs the same structural idealization as SHELL. It has an option which enables the use of a refined membrane and bending element in the analysis. It employs a six-DOF nodal system of displacements. This program was useful in this work in assessing the effects of the five-DOF of SHELL for the gull-winged girder. This was accomplished by comparative analyses using both programs. SHELL6 is based on isotropic material properties and constant element thickness. The theoretical development, user's guide and program listing may be found in Ref 15.

Program PLS6DOF -- This program was developed during the course of this research. It is identical to SHELL in all respects except that an element stiffness was added so that all three rotations could be dealt with in the analysis, thus resulting in a six-DOF nodal system. The chief attribute of PLS6DOF as compared to SHELL is the fact that a set of rather cumbersome inputs (those required to define the two rotations in SHELL) have been eliminated. It should be noted that PLS6DOF is currently being extended to include a more accurate representation of nonlinear temperature gradients through the element's thickness. This is being accomplished in Research Project 23, "Temperature Induced Stresses in Highway Bridges by Finite Element Analysis and Field Tests." Implementation of the final version of this program will thus enable the use of either a five or six-DOF nodal system in the analysis. The manner in which the additional stiffness was specified is described later in this report.

Program MESHPLT -- This program was developed to enable the user to check his input data before performing an analysis with either SHELL or PLS6DOF. To this end, the portions of these programs which read and print the data required to describe a finite element idealization were extracted to form MESHPLT. Moreover, a CAL-COMP plot routine was added for the purpose of plotting the finite element mesh. By exercising the appropriate option, a region of the mesh can be isolated and plotted to a larger scale. The plotting capability is very valuable in insuring that the elements and nodal coordinates have been correctly specified.

Program BASP -- This program is based on a two-dimensional structural model which consists of plate elements and one-dimensional beam elements. It may be used for an in-plane stress analysis as well as an out-of-plane buckling analysis. The development of this program may be found in Refs 11 and 14. It was further extended during the course of this work to enable mesh refinement in regions exhibiting local buckling as well as plotting of the finite element mesh. It was used in this project to determine the buckling characteristics of the interior girder of the three-girder bridge of Fig 3.

Summary of Order of Presentation

General characteristics of the analysis procedures have been described above. Since the emphasis of this project centered around using existing programs to address problems of current importance, much of the background information on the subject programs is contained in the previously cited references. However, for continuity in the presentation as well as bringing to light the developments as a result of this project, the finite elements used in Programs SHELL and PLS6DOF are described in the subsequent chapter. This is followed by documentation for SHELL and the results from the demonstration analyses.

CHAPTER 3. THE FINITE ELEMENT IDEALIZATION

General

In addition to the approximations introduced by the structural idealization that applies to any structural analysis problem, the finite element method includes another approximation which is due to the manner in which the stiffness properties of the individual elements are evaluated. Element stiffnesses are constructed by permitting the element to undergo prescribed sets of displacement patterns. Inasmuch as the structure is divided into several elements, the behavior of the entire structure can in general be closely approximated by using "simple" displacement patterns for each element. In this context "simple" displacement patterns are generally understood to mean linear variations of in-plane displacements (for the membrane stiffness) and cubic variations for out-of-plane displacements (for the bending stiffness). This results in a five-DOF nodal system for the element consisting of two in-plane translations for the membrane stiffness and one out-of-plane translation and two in-plane rotations for the bending stiffness.

Refined elements result from using more "complex" displacement patterns. This generally results in an improvement of the element stiffness properties but additional degrees-of-freedom are introduced. With this approach fewer elements are required to achieve the desired accuracy. This advantage is offset when the structural idealization itself governs the number of elements required to accurately model the geometry and supporting arrangements of a particular structure. The approach used in developing the subject procedures was based on "simple" displacement patterns. In this regard, however, care was exercised in selecting elements with improved stiffness properties while maintaining a five-DOF nodal system of displacements.

Finite Elements for Program SHELL

This program allows the use of triangular elements or quadrilateral elements. The quadrilateral element should be used when possible because its stiffness properties have been shown to be superior to that of the triangle.

The triangle was maintained only because it is sometimes required in the structural idealization. The membrane stiffness is based on plane stress while the bending stiffness follows from the Kirchhoff plate bending assumptions.

The Triangular Element -- The membrane stiffness of the triangle is derived from linear displacement patterns as shown in Fig 7. Each corner has two in-plane DOF. This element is called the CST (Constant Strain Triangle). The bending stiffness of the triangle is constructed from cubic displacement patterns as shown in Fig 8. This element was presented in Ref 16 and is termed the HCT (after Hsieh, Clough, and Tocher). It has 3 DOF at each corner consisting of a normal translation and two in-plane rotations. Cubic displacement functions are assigned to each sub-element of the triangle, thus resulting in 27 generalized coordinates for the triangle. The reduction to 9 DOF is accomplished by applying internal compatibility constraints between the sub-elements. This element is fully compatible for plate bending problems since the normal slopes along the element edges are constrained to be linear.

The Quadrilateral Element -- Two versions of the quadrilateral element are contained in SHELL as indicated in Figs 9 and 10. In each case its bending stiffness consists of four HCT's. Thus the bending DOF are three at each corner node and the central interior node. The membrane stiffness for the quadrilateral of Fig 9 is a result of an assemblage of four triangles. The stiffness of each triangle is derived from quadratic displacement functions and by constraining the four external sides of Fig 9 to displace linearly. The quadratic functions for Triangle 1 and its DOF system are shown in Fig 11. This element has 12 DOF (two at each corner node and at each mid-side node) and is termed the LST (Linear Strain Triangle (17)). The stiffness of Triangle 1 (Figs 9 and 12) results from setting $u_0 = (u_1 + u_2)/2$ and $v_0 = (v_1 + v_2)/2$ in Fig 11. This eliminates the 2 DOF at the external mid-side node (i.e., Point 0 in Fig 11), and the resulting triangle has 10 DOF as shown in Fig 12. This element is called the CLST (Constrained Linear Strain Triangle (6)). For the assembled quadrilateral of Fig 9, there are 33 DOF (15 bending DOF and 18 membrane DOF). The 13 DOF contained in the interior of the element are eliminated by static condensation; thus the condensed element has 20 DOF (five at each exterior corner node).

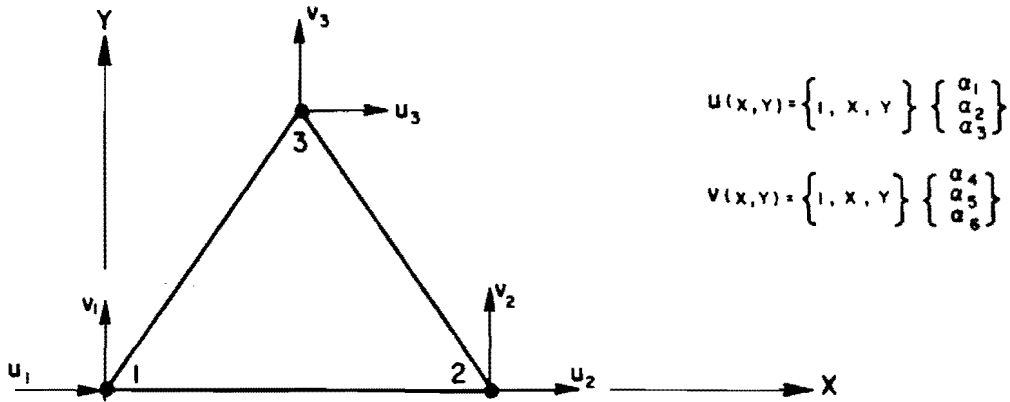


Fig 7. Constant strain triangle with 6 degrees of freedom.

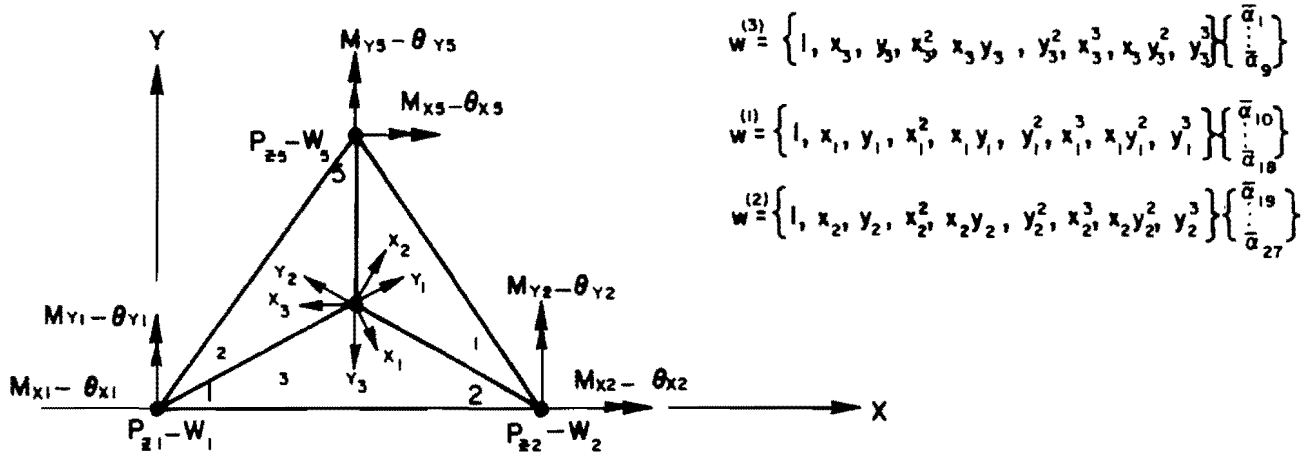


Fig 8. Displacement functions and nodal point systems for triangular plate elements.

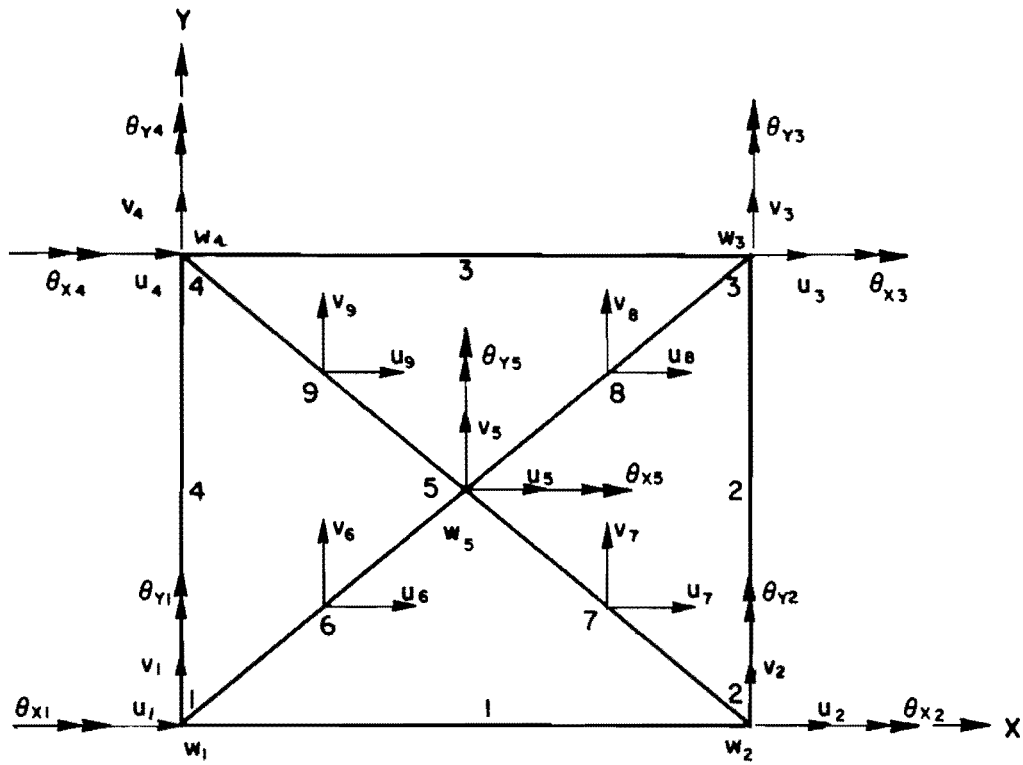


Fig 9. Planar quadrilateral with 33 DOF.

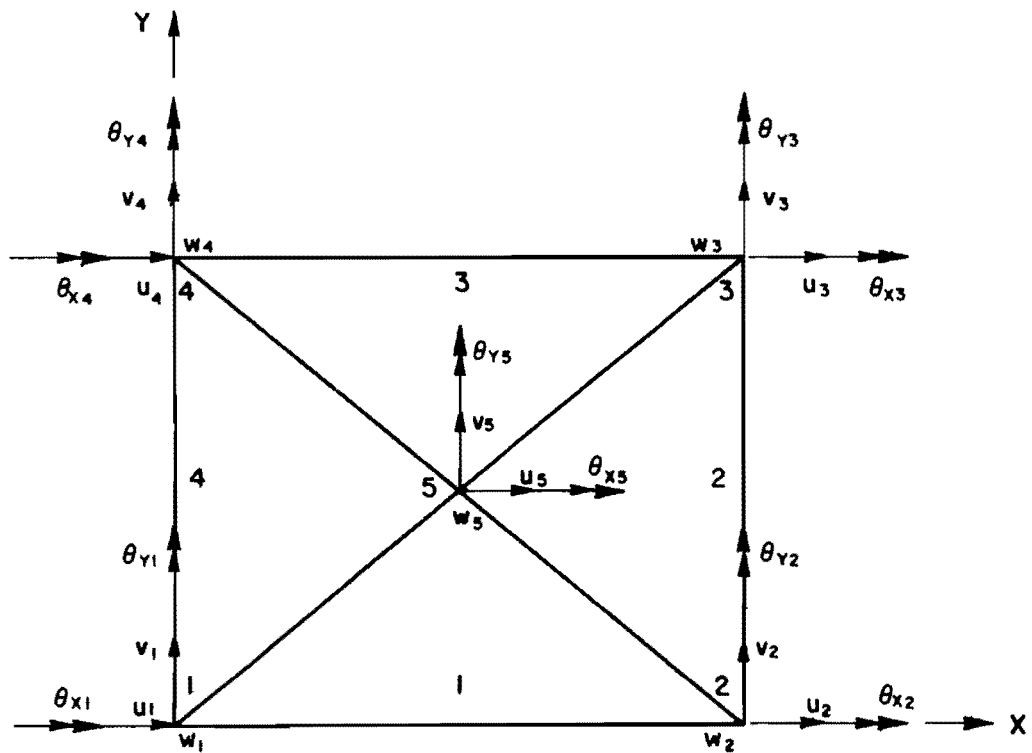


Fig 10. Planar quadrilateral with 25 DOF.

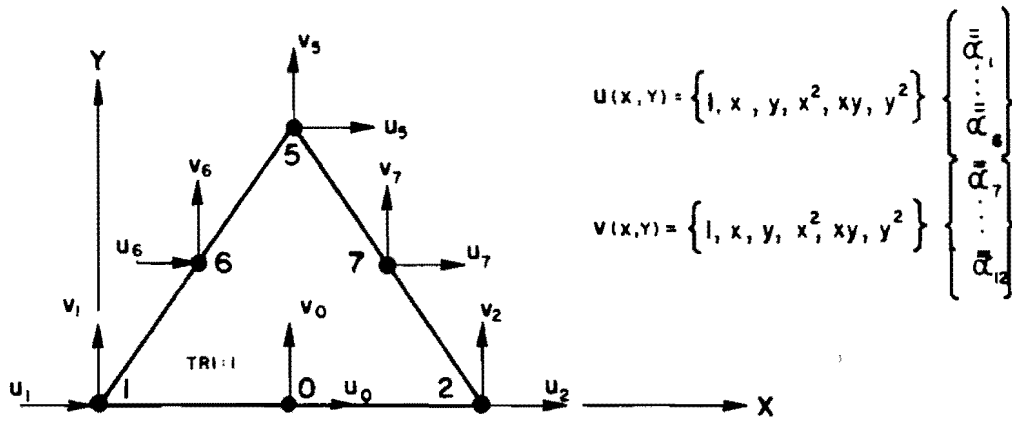


Fig 11. Linear strain triangle with 12 DOF.

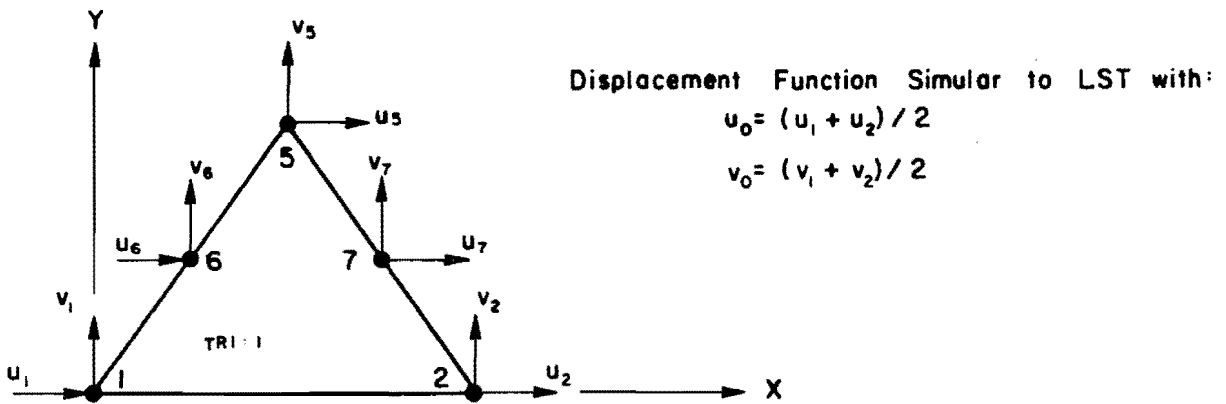


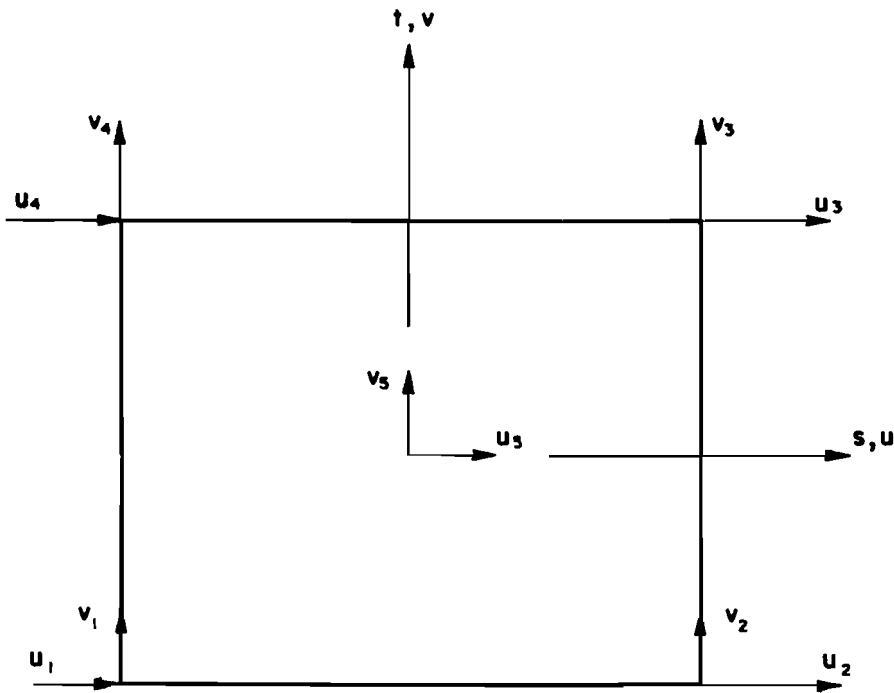
Fig 12. Constrained linear strain triangle with 10 DOF.

The membrane stiffness of the quadrilateral of Fig 10 is constructed from bi-linear polynomials with one additional higher term in each expansion as shown in Fig 13. These expansions cause each edge to displace linearly. Since each expansion has five terms, a total of 10 DOF are necessary. They consist of 2 DOF at each corner and the central interior point. This element was presented in Ref 18 and was referred to as the QM5. The assembled quadrilateral of Fig 10 has 25 DOF. The 5 DOF of the central interior node are eliminated by static condensation.

The QM5 is very effective in capturing bending modes of deformation that occur, for example, in the web of I-beams in flexure. Further, its stiffness properties remain acceptable with increasing aspect ratios (a/b). Aspect ratios up to 4 to 1 have been found acceptable. On the other hand, its stiffness properties deteriorate when the element geometry differs markedly from a rectangle. As a general guideline, the quadrilateral of Fig 10 is recommended when the element geometry is nearly rectangular while the quadrilateral of Fig 9 should be used for highly skewed quadrilaterals.

The Out-of-Plane Rotational Stiffness for Program PLS6DOF. The planar elements previously described have only five-DOF at the element level. In program SHELL only five-DOF were maintained in describing the stiffness of the element assemblage. These DOF are described in Secs. 1.2 and 1.4. In order to include, in a systematic way, six-DOF for the stiffness of the element assemblage an approach similar to that of Refs 19 and 20 was employed. This approach yields a rotational DOF normal to the element (about the z-axis) at each corner as shown in Fig 14; thus giving rise to six-DOF at the element level. These rotational DOF follow from a fictitious set of rotational stiffness coefficients which are assigned to the element (19). These rotational stiffness coefficients were constructed such that equilibrium is preserved in element coordinates and were defined for the triangular element as:

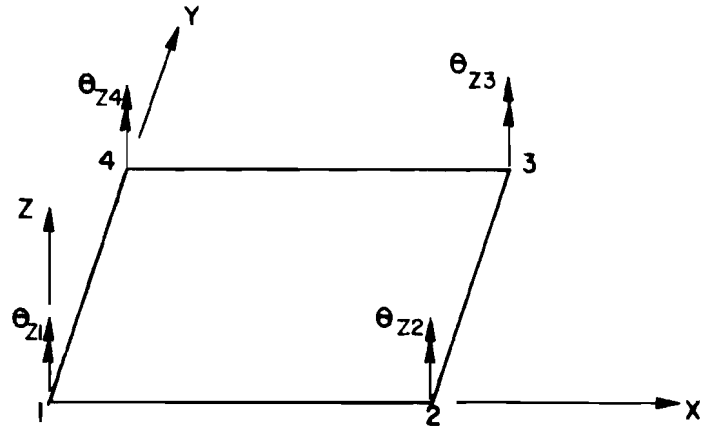
$$\begin{Bmatrix} M_{z1} \\ M_{z2} \\ M_{z3} \end{Bmatrix} = \alpha E t A \begin{bmatrix} 1 & -0.5 & -0.5 \\ & 1 & -0.5 \\ \text{sym} & & 1 \end{bmatrix} \begin{Bmatrix} \theta_{z1} \\ \theta_{z2} \\ \theta_{z3} \end{Bmatrix}$$



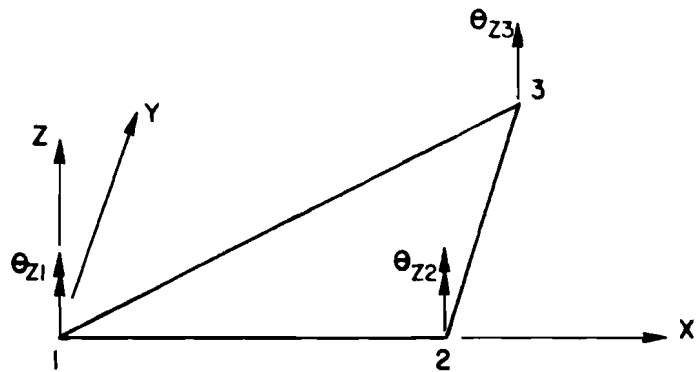
$$u = a_0 + a_1 s + a_2 t + a_3 st + a_4 (1-s^2)(1-t^2)$$

$$v = b_0 + b_1 s + b_2 t + b_3 st + b_4 (1-s^2)(1-t^2)$$

Fig 13. Quadrilateral membrane element - QM5.



a. Quadrilateral with 24 DOF.



b. Triangle with 18 DOF.

Fig 14. Planar elements.

and for quadrilateral element as:

$$\begin{Bmatrix} M_{z1} \\ M_{z2} \\ M_{z3} \\ M_{z4} \end{Bmatrix} = \alpha E t A \begin{bmatrix} 1.5 & -0.5 & -0.5 & -0.5 \\ & 1.5 & -0.5 & -0.5 \\ & & 1.5 & -0.5 \\ \text{sym} & & & 1.5 \end{bmatrix} \begin{Bmatrix} \theta_{z1} \\ \theta_{z2} \\ \theta_{z3} \\ \theta_{z4} \end{Bmatrix}$$

where E is the elastic constant

A is the area of the element

t is the average thickness over the element

α is a constant

The effects of varying α between very wide limits have been shown to be quite small (20). A value of $\alpha = 0.02$ was selected for use in PLS6DOF.

This page replaces an intentionally blank page in the original.

-- CTR Library Digitization Team

CHAPTER 4. DOCUMENTATION OF PROGRAM SHELL

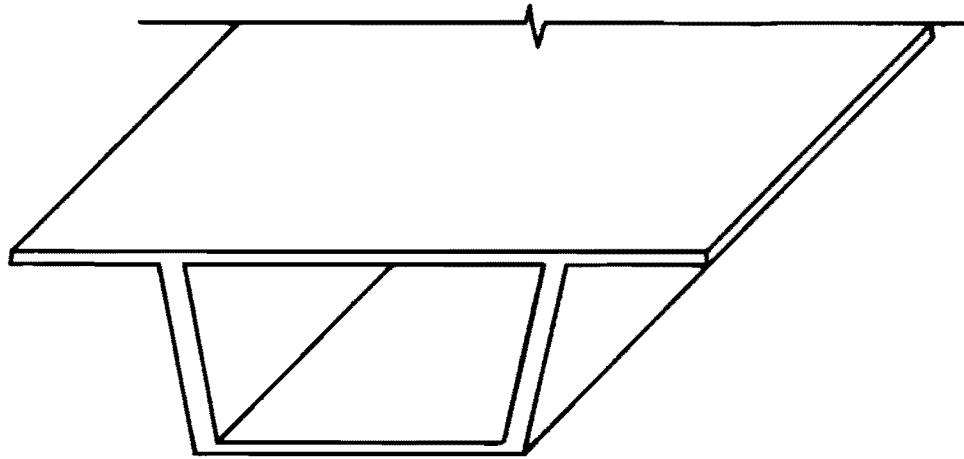
Purpose and Programming Information

The purpose of this finite element computer program is to provide a general capability for the analysis of complex structures which may be idealized as an assemblage of one and two-dimensional elements. The analysis includes the determination of nodal displacements, element stress and moment resultants, element stresses and principal stresses and nodal point reactions. Arbitrary loadings and support conditions, as well as variable thickness over the individual elements and orthotropic material properties, may be accounted for. Temperature effects may be approximated. In this regard, temperature is linear over the element's mid-surface but constant over its thickness. This program has been designed for large capacity; 800 nodes and 1200 elements are possible in the structural idealization. Automatic mesh generation options reduce and simplify the task of preparing input data to the program.

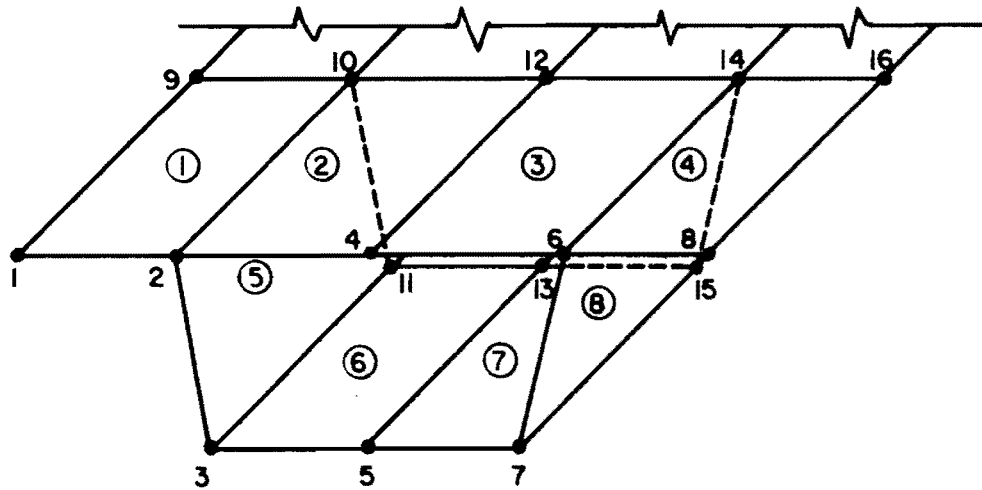
The program is written in FØRTRAN IV. It is divided into a main program and 35 subroutines. Overlay features are utilized to save storage. There are four overlays which are called sequentially by the resident (MAIN) program. Six FØRTRAN logical units are used for intermediate storage during the execution of the program. DOUBLE PRECISION is used for all real variables in the IBM version presented in this report.

Use of the Program

1.1 Mesh Construction. A finite element mesh is obtained by subdividing the structure into quadrilateral or triangular elements. An example of a finite element mesh for a typical segment used in segmental bridge construction is shown in Fig 15. Element nodes lie in the mid-surface of the individual plates comprising the segment. Although the exact proportions of the individual elements are arbitrary, care should be taken to insure that the element proportions do not become overly exaggerated.



a. Partial three-dimensional view.



b. Partial finite element idealization.

Fig 15. Box girder bridge.

The nodal point numbering should run in the direction with the smallest number of elements as shown in Fig 15 in order to minimize the nodal point half band width (maximum element nodal difference plus one) of the entire assemblage. The program is dimensioned for a maximum nodal point half band width of 20. The element numbering should follow the general path of the nodal point numbering to insure successful formation of the structural stiffness of the assemblage. Recommended nodal and element numbering for the typical segment is shown in Fig 15.

When the entire mesh or a portion of it has the same number of subdivisions in two directions throughout as shown in Fig 16, a reduction of the required input is possible. The assumed nodal and element numbering for a mesh of this type, which is referred to herein as a regular mesh, is illustrated in Fig 16. Element nodal point numbers for a regular mesh may be generated with a single input data card as described in Sec. 2.5. Element nodal points I, J, K and L are numbered counterclockwise with node I having the smallest number as illustrated for element 1 in Fig 16 for a regular mesh. Regular meshes should be used when possible. This simplifies the required input, thereby reducing possibilities of error in preparing the input data. Moreover, regular meshes usually result in minimum nodal point half band width, hence reducing storage and the computation time for a given problem.

The mesh may require refinement, i.e., reduction in element size, in regions having steep stress and moment gradients. A regular mesh is graded by a gradual decrease in element sizes. In addition, a mesh may be graded by the use of triangular elements. However, this type of gradation results in "branches" of the nodal numbering sequence which increases the nodal point half band width; thus limiting the usefulness of this refinement procedure.

1.2 Coordinate Systems. A global coordinate system x, y, z , for example, as shown in Fig 17, must be chosen for the structure which is to be analyzed. This choice is arbitrary; however, simplification of input nodal coordinates usually dictates the proper orientation for this coordinate system.

In addition, another set of coordinates ξ_1, ξ_2 and ξ_3 (Fig 17), called surface coordinates, must be selected. This coordinate system is used to characterize the two rotations of the five-DOF nodal system (also see Sec. 1.4). The rotation about ξ_3 is assumed to be zero; thus care should be exercised

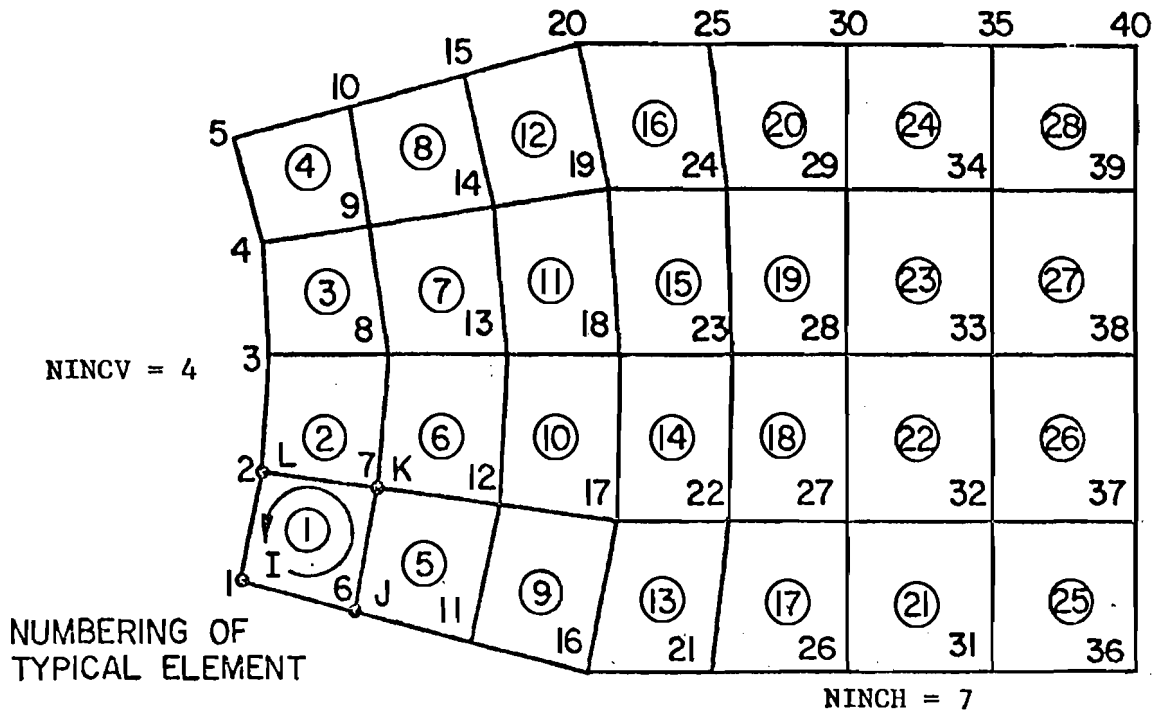


Fig 16. Regular mesh with nodal and element numbering.

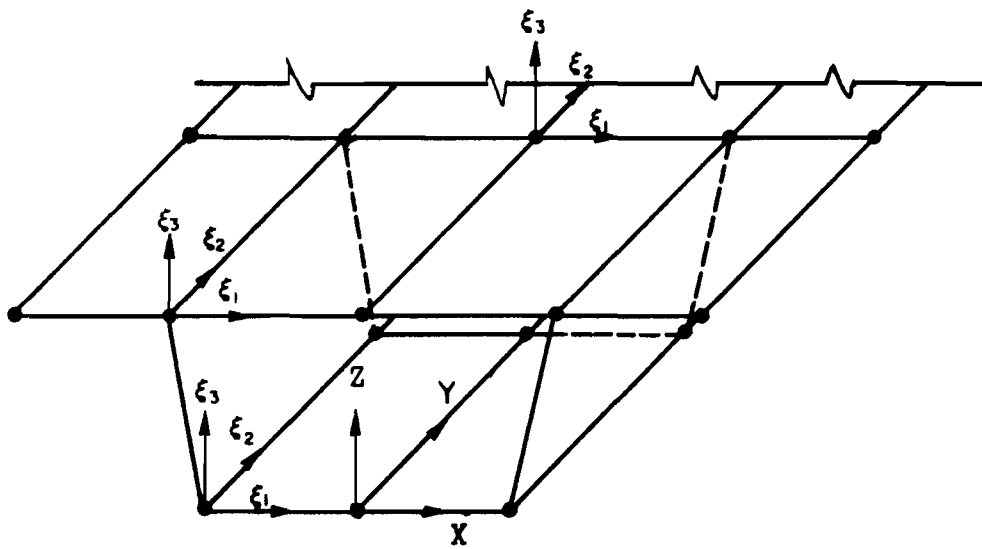


Fig 17. Surface coordinate systems for box girder bridge.

in selecting its orientation. For points where all adjacent elements form a plane, ξ_3 should be normal to that plane. In this case the five-DOF nodal system does not introduce any additional approximations since only five-DOF were used in the construction of the individual element stiffnesses. On the other hand for points where all elements at a point are not contained in a single plane, ξ_3 should be located in the direction of the smaller of the three rotations to minimize the rotational constraints imposed by the omission of the third rotation. One possible orientation of the surface coordinates for the typical segment is shown in Fig 17. In this case ξ_3 is directed vertically at the juncture of the horizontal and sloping plates. For gravity loads this is a good selection since the actual rotation about the gravity axis is in all likelihood a small effect. Furthermore, this simplifies the required input (see Sec. 2.4). As an additional note, if the sloping plates of Fig 17 were subdivided into more than one element, ξ_3 should be specified normal to the nodes contained on the interior of the sloping plates.

Local coordinates (\bar{x} , \bar{y} , and \bar{z}) for each triangle are constructed automatically by the program as shown in Fig 18. This coordinate system is referred to as element coordinates and is defined as follows: The coordinate \bar{x} is directed along side I-J while the coordinate \bar{y} lies in the plane of the element and is directed toward node K. The coordinate \bar{z} is constructed normal to the plane of the element to complete a right-handed system for the coordinates \bar{x} , \bar{y} and \bar{z} .

Another local coordinate system (η_1 , η_2 , and η_3) for each quadrilateral is constructed automatically as shown in Fig 19. This coordinate system is referred to as η -coordinates and is constructed as follows. The coordinate, η_1 , bisects sides I-L and J-K, while $\bar{\eta}_2$ bisects sides I-J and K-L. Positive directions for η_1 and $\bar{\eta}_2$ are shown in Fig 19. Subsequently, η_3 is constructed normal to the η_1 - $\bar{\eta}_2$ plane and then η_2 is taken normal to the η_1 - η_3 plane to complete the right handed system (η_1 , η_2 , η_3).

These two local systems, i.e., element and η -coordinates, must be considered in specifying orthotropic material orientations and element distributed loadings, and also, in determining the orientations of stress and moment resultants which are output by the program.

1.3 Finite Element Types. In addition to a truss element, three types of finite elements are available in the program, all of which include membrane and bending stiffnesses.

- a. Triangular Element
 - Membrane stiffness . . . Constant strain triangle (CST)
 - Bending stiffness . . . Fully compatible plate bending element after Hsieh, Clough and Tocher (HCT).
- b. Nonplanar Quadrilateral Element
 - Membrane stiffness . . . An assemblage of four linear strain triangles with linear displacements along exterior sides (CLST).
 - Bending stiffness . . . An assemblage of four bending elements as per a. above.
- c. Planar Quadrilateral Element
 - Membrane stiffness . . . A refined membrane element (QM5).
 - Bending stiffness . . . Same as for nonplanar quadrilateral.
- d. One-Dimensional Element . . . Axial stiffness only.

The superior stiffness properties of the quadrilateral versus the triangle motivate the general use of the quadrilateral.

1.4 Nodal Point Degrees of Freedom and Base Coordinates. A five-degree-of-freedom nodal point displacement system for the assemblage is utilized. These five degrees of freedom consist of three linear translations and two rotations, and are defined as follows:

- D1 \equiv Translation in either global x-dir. or surface ξ_1 - dir.,
- D2 \equiv Translation in either global y-dir. or surface ξ_2 - dir.,
- D3 \equiv Translation in either global z-dir. or surface ξ_3 - dir.,
- D4 \equiv Rotation about ξ_1 coordinate.,
- D5 \equiv Rotation about ξ_2 coordinate.

It should be noted that all translations are either in global coordinates or surface coordinates.

Base coordinates are defined as the coordinates in which the five degrees of freedom at each nodal point of the assemblage are expressed. From the above description, it is evident that the two options for base coordinates are:

- a. Global coordinates for the three translations and surface coordinates for the two rotations.

- b. Surface coordinates for both the three translations and the two rotations.

1.5 Element Distributed Loads. Equivalent nodal forces are automatically generated for element unit weight and pressure load for each element of the assemblage. Only translational nodal force components are considered to result from element weight and pressure load. The element nodal forces are computed by assuming linear variations of in-plane and out-of-plane displacements over each triangle and each subelement of the quadrilateral. The nodal forces resulting from both shell weight and pressure are assumed to be LOAD CASE 1 (see Sec. 2.13); hence, input nodal forces which are designated as LOAD CASE 1 will be superimposed onto the loads resulting from shell weight and pressure loads.

Element unit weight is considered uniform over each triangle and each quadrilateral in the idealization, but may have a different value for each element. Element weight per surface area is computed by multiplying the element unit weight by the element thickness at each corner of the triangular element and each subelement of the quadrilateral. Therefore, a linear variation in element weight is accounted for in the program. Positive element weight is assumed to act in the positive global z-direction.

The pressure load is assumed to act normal to each triangular element. For the quadrilateral, the pressure load is assumed to act normal to each of the four subelements. Input positive pressure is assumed to act in the \bar{z} -direction for the triangle while input positive pressure for the quadrilateral is assumed to produce loads in each subelement which act in the positive η_3 direction for a planar quadrilateral. For a nonplanar quadrilateral positive pressure on each subelement produces loads which have positive components in the direction of η_3 ; however, in this case, components will result in the $\eta_1 - \eta_2$ plane, since the normal component for each subelement is not exactly parallel to η_3 . The pressure load may vary linearly over each triangular element and linearly over each subelement of the quadrilateral since the pressure at the central interior node is taken as the average of the pressure at the four exterior nodes. See Figs 18 and 19 for triangular and quadrilateral coordinate definition.

Temperature effects are accounted for by computing "equivalent" element nodal point forces from the specified temperatures. For the triangle the temperature is assumed linear over its mid-surface and the "equivalent" forces

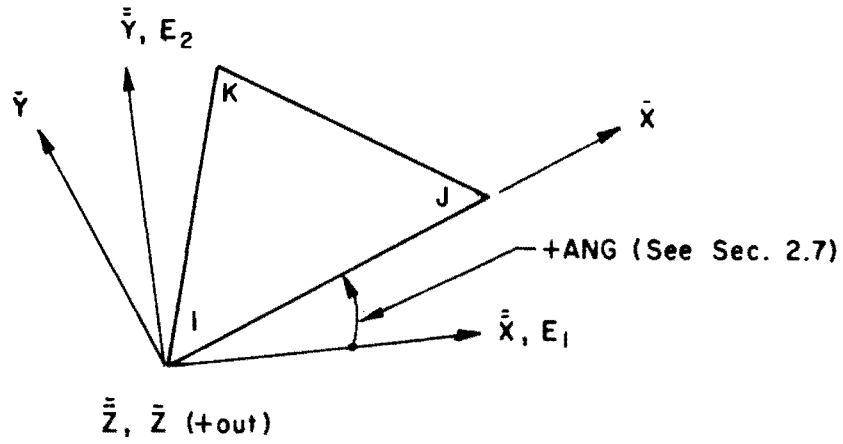


Fig 18. Definition of \bar{x} - \bar{y} coordinates for triangle and orientation of orthotropic moduli, E_1 and E_2 .

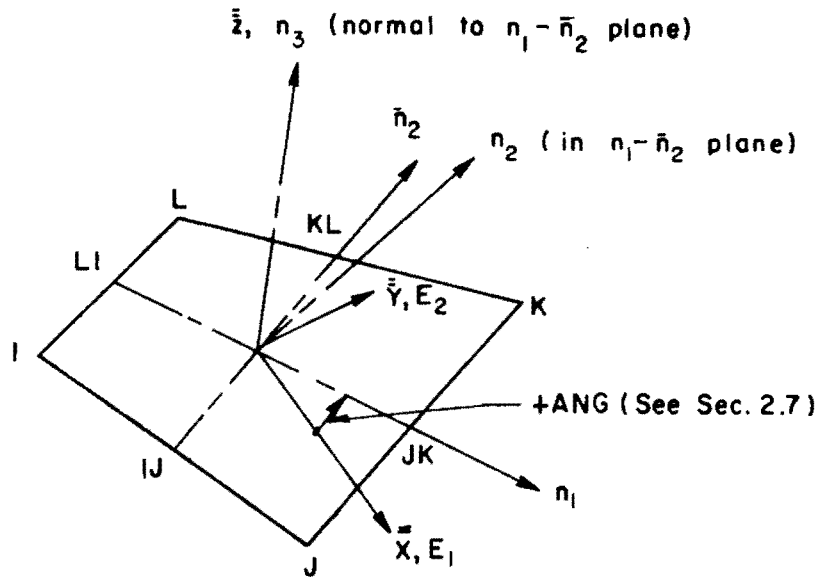


Fig 19. Definition of τ -coordinates for quadrilateral and orientation of orthotropic moduli, E_1 and E_2 .

are computed using the displacement patterns of the constant strain triangle. Equivalent forces for each of the four triangles comprising the quadrilateral are computed in the same way. As previously stated, the temperature is assumed to be constant over the thickness of the element. Temperature is specified by node point and thus the corners of elements sharing a common node have the same temperature. The reference temperature is assumed to be zero.

1.6 Orthotropic Material Properties. The principal elastic axes for the orthotropic properties are \bar{x} , \bar{y} , \bar{z} , as shown in Figs 18 and 19. The principal elastic axes may have arbitrary orientation with respect to the quadrilateral and triangular coordinates as shown in Figs 18 and 19. The angle, ANG, between the principal elastic axes and element coordinates is measured from the principal elastic axis, \bar{x} to η_1 and \bar{x} for the quadrilateral and triangle, respectively. Positive angles are indicated in Figs 18 and 19.

The stress-strain relation referred to the principal elastic axes is

$$\begin{Bmatrix} \sigma_{\bar{x}} \\ \sigma_{\bar{y}} \\ \tau_{\bar{x}\bar{y}} \end{Bmatrix} = \begin{bmatrix} E_1/X & E_2\nu_{12}/X & \cdot \\ E_1\nu_{21}/X & E_2/X & \cdot \\ \cdot & \cdot & G_{12} \end{bmatrix} \begin{Bmatrix} \epsilon_{\bar{x}} \\ \epsilon_{\bar{y}} \\ \gamma_{\bar{x}\bar{y}} \end{Bmatrix}$$

where

E_1, E_2 are principal elastic moduli in the \bar{x} and \bar{y} directions, respectively;

$$\nu_{12}, \nu_{21} = \text{Poisson's ratios } (E_2\nu_{12} = E_1\nu_{21})$$

$$X = (1 - \nu_{12}\nu_{21})$$

G_{12} is the shear modulus.

To simplify the input, the following material constants will be defined

$$\begin{aligned}
 E &= \sqrt{E_1 E_2} && \text{mean modulus;} \\
 \rho &= E_1/E_2 && \text{modulus ratio;} \\
 \nu &= \sqrt{\nu_{12}\nu_{21}} && \text{mean Poisson's ratio;} \\
 \nu_{G12} &= \left[E/(2G_{12}) \right] - 1 && \text{fictitious Poisson's ratio associated} \\
 &&& \text{with } G_{12}.
 \end{aligned}$$

The in-plane stress-strain relation in the principal elastic axes becomes

$$\begin{Bmatrix} \bar{\sigma}_x \\ \bar{\sigma}_y \\ \bar{\tau}_{xy} \end{Bmatrix} = \frac{E}{1-\nu^2} \begin{bmatrix} \sqrt{\rho} & \nu & \cdot \\ \nu & 1/\sqrt{\rho} & \cdot \\ \cdot & \cdot & \frac{1-\nu^2}{2(1+\nu_{G12})} \end{bmatrix} \begin{Bmatrix} \bar{\epsilon}_x \\ \bar{\epsilon}_y \\ \bar{\gamma}_{xy} \end{Bmatrix}$$

The moment curvature relation is obtained by multiplying this matrix by $t^3/12$, where t is the plate thickness, and by associating a factor of two with the twisting curvature.

If the material is isotropic, $E_1 = E_2 = E$, $\nu_{12} = \nu_{21} = \nu = \nu_{G12}$ and $\rho = 1.0$. For the isotropic case, ANG (Figs 18 and 19) is arbitrary and should be input as zero or simply left blank.

Preparation of Input Data

Abbreviations: A = alphanumeric field.
 I = integer value (must be packed to the right of the field).
 F = floating point number (must be punched with a decimal).

2.1 Title Card (A) - Alphanumeric information for problem identification.

2.2 Control Card

Cols.	1- 4 (I)	NUMEL	=	Number of elements (2000 max)
	5- 8 (I)	NUPTS	=	Number of nodal points (800 max)
	9-12 (I)	NUBPTS	=	Number of points with displacement boundary conditions (100 max)
	13-16 (I)	IBANDP	=	<u>Nodal point half band width</u> : Max. element nodal difference +1 (20 max)
	17-20 (I)	NDFRE	=	Nodal point degrees of freedom \equiv 5
	21-24 (I)	IFLAG	=	Base coordinates for translations; If 0, translations are in global coordinates. If 1, translations are in surface coordinates.
	25-28 (I)	NUMAT	=	Number of different material types (30 max)
	29-32 (I)	ISHEAR	=	This field must be left blank.
	33-36 (I)	NRED	=	Number of cycles for correcting displacement solution; If 0, no correction is made.
	37-40 (I)	IREACT	=	Specifies if the nodal forces and reactions are to be printed; If = 0, reactions are suppressed If > 0, reactions are printed

NOTE: IREACT MUST BE INPUT AS ZERO IF MORE THAN ONE LOAD CASE IS SPECIFIED.
 (see Sec. 2.13)

41-44 (I)	LPROB	Specifies if another problem is to follow: If 0, this is the last problem, If 1, another problem follows.
45-48 (I)	IGEN	IGEN, which may have values of 0,1,2,3 or 4, governs the level of output desired, for example, when IGEN = 0, maximum amount of output is obtained, when IGEN = 4, minimum amount of output is obtained.
49-52 (I)	ISIG	Specifies whether element stress and moment resultants or element stresses and principal stresses are to be printed. Refer to Appendix 1 for definitions of the quantities. If 0 stress and moment resultants are printed. If 1 stresses and principal stresses are printed.

2.3 Nodal Coordinate Cards. One card per nodal point, except when mesh generation options are used. These cards need not be input in numerical sequence; however, the node having the largest number must be input last.

Cols.	1- 4 (I)	Nodal point number.
	18-24 (F)	Global x-coordinate.
	25-31 (F)	Global y-coordinate.
	32-38 (F)	Global z-coordinate.

For generation options see Nodal Coordinate Generation (Secs. 3.1-3.6).

2.4 Surface Coordinate Direction Cosine Cards. The surface coordinate direction cosines as described in Sec. 1.2 are specified by this set of cards. From the input cosines described below, ξ_3 is automatically constructed by a cross-product of ξ_1 and $\bar{\xi}_2$, and $\bar{\xi}_2$ is then determined by the cross-product of ξ_3 and ξ_1 to insure a right-handed orthogonal system.

When none of the generation options of Secs. 3.1-3.6 are used, one card per nodal point is required. When the options of Secs. 3.1-3.6 are exercised, each point for which coordinates are generated will also be assigned direction cosines. If only some of the nodes are generated as per Secs. 3.1-3.6, the direction cosines must be input for all other nodes. These cards need not be input in numerical sequence. A blank card must be used to terminate this data set.

Cols.	1- 4 (I)	Nodal point number I	
	5- 8 (I)	LIM	
	9-12 (I)	MOD	
	18-24 (F)	Component in global x-dir. of unit vector	ξ_1 *
	25-31 (F)	Component in global y-dir. of unit vector	ξ_1
	32-38 (F)	Component in global z-dir. of unit vector	ξ_1
	39-45 (F)	Component in global x-dir. of unit vector	ξ_2 **
	46-52 (F)	Component in global y-dir. of unit vector	ξ_2
	53-59 (F)	Component in global z-dir. of unit vector	ξ_2

*If Cols. 18-38 are left blank, input cosines for ξ_1 are suppressed.

**If Cols. 39-59 are left blank, input cosines for ξ_2 are suppressed.

The suppression option allows one to redefine one set of previously established cosines (either from input or generation options) without changing the other at a given point.

If $LIM > I$ and $MOD > 0$, then the direction cosines of points

$$I + MOD, I + 2*MOD, \dots, LIM$$

will be set equal to these specified for point I.

2.5 Element Nodal Point Number Cards. One card per element, except when mesh-generation options are used. These cards need not be input in numerical sequence; however, the element having the largest number must be input last.

Cols.	1- 4 (I)	Element Number	N
	5- 8 (I)	Element nodal point	I
	9-12 (I)	Element nodal point	J
	**13-16 (I)	Element nodal point	K
	*17-20 (I)	Element nodal point	L
	21-24 (I)	NINCV = number of elements in direction of nodal numbering, see Fig 16.	

25-28 (I) NINCH = number of layers with similar element nodal numbering, see Fig 16.

*A triangular element is assumed if Cols. 17-20 are left blank.

**A truss element is assumed if Cols. 13-20 are left blank.

If $NINCV > 0$ and $NINCH > 0$, a regular mesh will be constructed for the quadrilateral elements N through $N + NINCV * NINCH - 1$, as shown in Fig 16. Care should be taken to order the node numbers I, J, K, and L for the N'th element as shown in Fig 16.

See Secs. 4.1-4.2 for additional generation options.

2.6 Element Material Table. One card per element type must be input. Material properties are assumed constant over each individual element. See Sec. 1.6 for definition of terms used below.

Cols.	1- 4 (I)	Element material type
	11-20 (F)	Mean modulus = $\sqrt{E_1 E_2}$
	21-30 (F)	Modulus ratio = E_1 / E_2
	31-40 (F)	Mean Poisson's ratio = $\sqrt{\nu_{12} \nu_{21}}$
	41-50 (F)	Fictitious Poisson's ratio = $\left[\sqrt{E_1 E_2} / (2G_{12}) \right] - 1$
	51-60 (F)	Field <u>must</u> be left blank
	61-70 (F)	Field <u>must</u> be left blank
	71-80 (F)	Thermal coefficient of expansion

2.7 Element Property Cards. One card per element, except when mesh generation options are used. These cards need not be input in numerical sequence; however, the element having the largest number must be input last.

Cols.	1- 4 (I)	Element number N
	5- 8 (I)	Element material type (see Sec. 2.6)
	9-12 (I)	LIM
	13-16 (I)	MOD
	17-20 (I)	Specifies type of membrane stiffness for the quadrilateral. If 0, four CLST's are used (see Sec. 1.3b). If 1, a QM5 is used (see Sec. 1.3c)
	21-30 (F)	Thickness at node I (or cross-sectional area for a truss member).
	31-40 (F)	Thickness at node J

- 41-50 (F) Thickness at node K
 51-60 (F) Thickness at node L
 61-70 (F) ANG = Angle in degrees between principal elastic axis and element coordinates; see Figs 18 and 19.

If $LIM > N$ and $MOD > 0$, then the element type, thicknesses and ANG of elements

$N + MOD, N + 2*MOD, \dots, LIM$

will be set equal to those specified for element N .

2.8 Element Distributed Load Cards. One card per element, except when mesh generation options are used. Loads acting on all elements must be specified (elements with zero loads must be included). These cards need not be input in numerical sequence; however, the element having the largest number must be input last.

Cols.	1- 4 (I)	Element number N	
	5- 8 (I)	LIM	
	9-12 (I)	MOD	
	21-30 (F)	Element unit weight (positive in global z-direction.)	
	31-40 (F)	Pressure at node I	
	41-50 (F)	Pressure at node J	Note: See Sec. 1.5 for sign conventions
	51-60 (F)	Pressure at node K	
	61-70 (F)	Pressure at node L	

If $LIM > N$ and $MOD > 0$, then the element unit weight and pressures of elements

$N + MOD, N + 2*MOD, \dots, LIM$

will be set equal to those specified for element N .

2.9 Nodal Temperature Cards.

Cols.	1- 4 (I)	Nodal point number I
	5- 8 (I)	LIM
	9-12 (I)	MOD
	16-25 (F)	Temperature at Node I

If $LIM > I$ and $MOD > 0$, then the temperature at points

$$I + MOD, I + 2*MOD, \dots, LIM$$

will be set equal to those specified for Node I. Temperatures need not be input in numerical sequence but they must be specified for all nodes. A blank card must be used to terminate this data set.

2.10 Boundary Condition Cards. One card per nodal point having a specified displacement component (whether zero or nonzero), except when mesh generation options are used. Boundary condition cards need not be input in numerical sequence. The five degrees of freedom are ordered as follows:

Cols.	1- 4 (I)	Nodal point number I
	7 (I)	1 for specified value for D1; 0 otherwise
	8 (I)	1 for specified value for D2; 0 otherwise
	9 (I)	1 for specified value for D3; 0 otherwise
	10 (I)	1 for specified value for D4; 0 otherwise
	11 (I)	1 for specified value for D5; 0 otherwise
	13-16 (I)	LIM
	17-20 (I)	MOD
	21-30 (F)	Specified value for D1*
	31-40 (F)	Specified value for D2
	41-50 (F)	Specified value for D3
	51-60 (F)	Specified value for D4
	61-70 (F)	Specified value for D5

*Specified value may be nonzero.

If $LIM > I$ and $MOD > 0$, then values for points

$$I + MOD, I + 2*MOD, \dots, LIM$$

will be set equal to those specified for element I.

2.11 Control Card for Elastic Supports.

Cols. 1- 4 (I) Number of points with elastic supports (Max. 50)

2.12 Spring Constant Cards. If the number of points with elastic springs is specified as zero no cards are required for this set. These cards need not be input in numerical sequence.

Cols. 1- 4 (I) Nodal point number I
 5- 8 (I) LIM
 9-12 (I) MOD
 21-30 (F) Spring constant for D1 displacement
 31-40 (F) Spring constant for D2 displacement
 41-50 (F) Spring constant for D3 displacement
 51-60 (F) Spring constant for D4 rotation
 61-70 (F) Spring constant for D5 rotation

If $LIM > 1$ and $MOD > 0$, then values for points

$I + MOD, I + 2*MOD, \dots, LIM$

will be set equal to those specified for node I. This set is terminated when the number of points specified in Sec 2.11 have been input.

2.13 Control Card for Nodal Point Loads A maximum of three independent load cases for a single problem may be specified on this card. A blank card must follow this card.

Cols. 1- 4 (I) Number of independent load cases (must be at least 1)
 5- 8 (I) Number of loaded nodes for load case 1
 9-12 (I) Number of loaded nodes for load case 2
 13-16 (I) Number of loaded nodes for load case 3

Joints with all five applied force components equal to zero need not be included as a loaded joint. Nodal forces are input as described below.

2.14 Nodal Point Load Cards. Input nodal forces correspond in an energy sense to the nodal point displacement components, i.e., $P_i D_i$, $i = 1,5$. The number of input cards for each load case must equal the number specified in Sec. 2.13 above, except when mesh generation options are used. The input format for each load case is as follows:

Cols. 1- 4 (I) Nodal point number I
 5- 8 (I) LIM
 9-12 (I) MOD
 21-30 (F) Value of P1 which corresponds to D1
 31-40 (F) Value of P2 which corresponds to D2
 41-50 (F) Value of P3 which corresponds to D3
 51-60 (F) Value of P4 which corresponds to D4
 61-70 (F) Value of P5 which corresponds to D5

These cards need not be input in numerical sequence, but all cards for each load case must be grouped together, in the sequence: Load case 1, 2, 3.

If $LIM > I$ and $MOD > 0$, then loads for points;

$I + MOD, I + 2*MOD, \dots, LIM$

will be set equal to those specified for point I.

Nodal Coordinate Generation

The previous section provided a general input format by which all the information which is necessary to completely define a given problem is input via data cards. The generation options in Secs. 3.1-3.6 and Secs. 4.1-4.2 are intended to simplify and to reduce the amount of that required input.

Six types of automatic generation options are available. The first four types treat surface generations which occur frequently in structures; straight lines, circular arcs, parabolas and ellipses. Nodal numbering along each generator must be in increasing order and the difference between adjacent nodes must be constant over the entire generator. The fifth and sixth types of generation are useful when the coordinates of a set of points may, by constant increments (in nodal numbering and global coordinates), be defined from a previous set of points which have been input.

If any of these six types of generation are used, then two sets of direction cosines are generated. The procedure for the generation of these direction cosines is described below for each type of coordinate generation. In many cases, these generated direction cosines will correspond with the chosen surface coordinates ξ_1 and ξ_2 , thereby eliminating the need of inputting these direction cosines; in other cases, the generated direction cosines will have to be replaced by manually computed values.

3.1 Straight Line (Fig 20).

Cols.	1- 4 (I)	Node I of straight line
	5- 8 (I)	Node J of straight line
	9-12 (I)	Increment between successive nodes $\equiv K$
	16 (I)	= 1
	18-24 (F)	Global x-coordinate of point I
	25-31 (F)	Global y-coordinate of point I
	32-38 (F)	Global z-coordinate of point I
	39-45 (F)	Global x-coordinate of point J
	46-52 (F)	Global y-coordinate of point J
	53-59 (F)	Global z-coordinate of point J

The straight line is subdivided into $(J-I)/K$ equal parts and the intermediate global nodal coordinates are computed.

The two sets of direction cosines are computed by

- a. Assuming ξ_1 is in the direction from point I to point J.
- b. Assuming ξ_2 lies in the x-y plane and is normal to the line obtained by projecting line I-J onto the x-y plane, i.e., $\xi_2 \equiv \bar{y}$ (Fig 20), and by ensuring a right-handed system for \bar{x} , \bar{y} , \bar{z} .

For example, if the numbering had required a reversed direction for \bar{x} and hence ξ_1 , then \bar{y} and ξ_2 would be reversed in order to maintain a right-handed system without changing the direction of ξ_3 . In the case where ξ_1 is parallel to z (either direction), then ξ_2 is assumed to be in the same direction as the global y-coordinate.

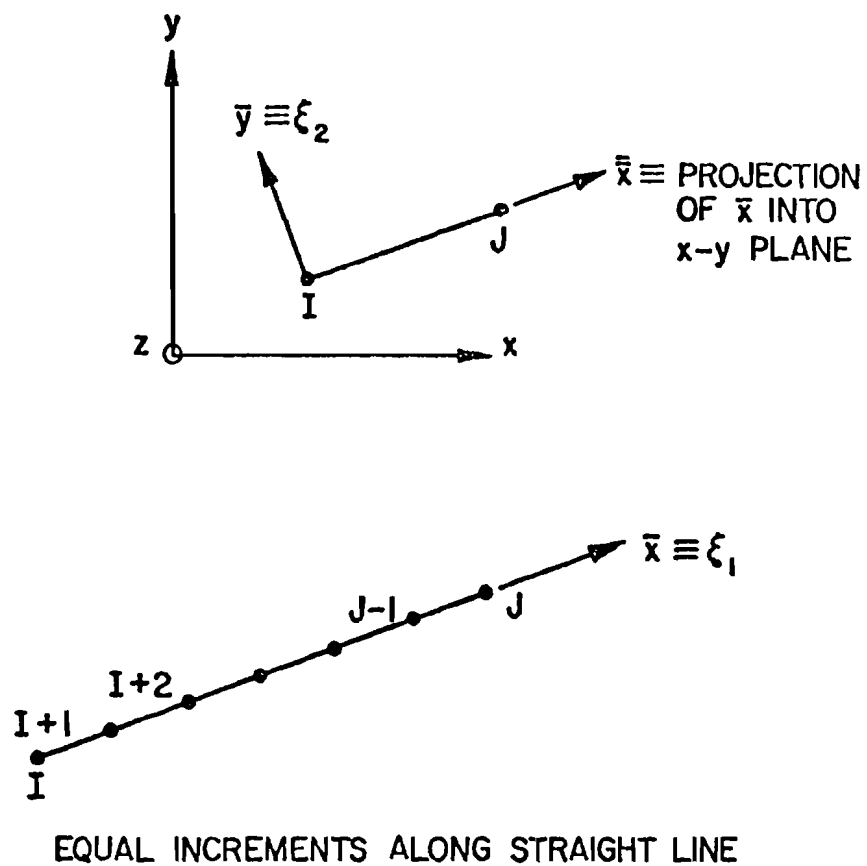


Fig 20. Straight line.

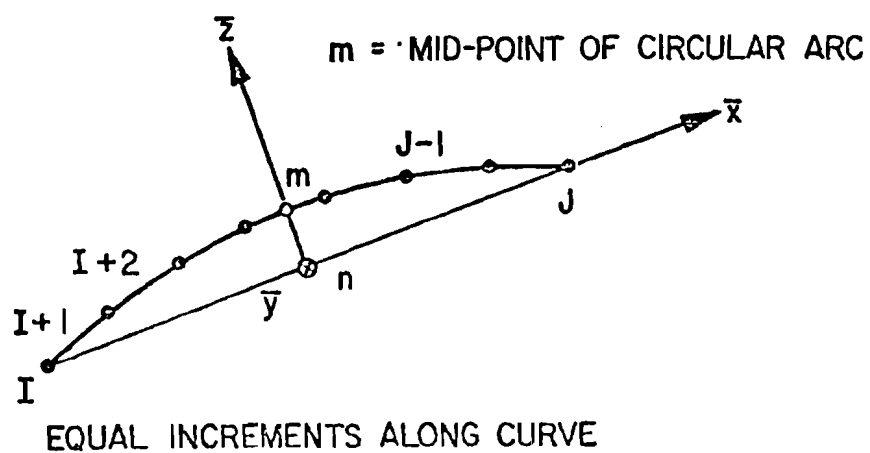


Fig 21. Circular arc.

3.2 Circular Arc (Fig 21).

Cols.	1- 4 (I)	Node I of circular arc
	5- 8 (I)	Node J of circular arc
	9-12 (I)	Increment between successive nodes $\equiv K$
	16 (I)	= 2
	18-24 (F)	Global x-coordinate of point I
	25-31 (F)	Global y-coordinate of point I
	32-38 (F)	Global z-coordinate of point I
	39-45 (F)	Global x-coordinate of point m
	46-52 (F)	Global y-coordinate of point m
	53-59 (F)	Global z-coordinate of point m
	60-66 (F)	Global x-coordinate of point J
	67-73 (F)	Global y-coordinate of point J
	74-80 (F)	Global z-coordinate of point J

The circular arc is subdivided into $(J-I)/K$ parts of equal arc length and the intermediate global nodal coordinates are computed. The local right-handed Cartesian coordinate system \bar{x} , \bar{y} , \bar{z} is constructed as follows:

- a. \bar{x} is positive from I to J.
- b. \bar{z} is positive from n, a point equidistant from I and J, to point m, the midpoint of the circular arc.
- c. \bar{y} is established by a cross-product of \bar{x} and \bar{z} (+inward as shown in Fig 21).

Surface coordinate direction cosines are computed by assuming

- d. ξ_1 lies in the plane \bar{x} - \bar{z} and is tangent to the circular arc at each node. It is directed along the arc going from I to J.
- e. ξ_2 is assumed to be in the positive direction of \bar{y} . Note that if the nodal point numbers had increased from right to left in Fig 21, \bar{y} , and hence ξ_2 , would be positive outward.

The circular arc may have an arbitrary orientation with respect to the global coordinates.

3.3 Parabola (Fig 22).

Cols.	1- 4 (I)	Node I of parabola
	5- 8 (I)	Node J of parabola
	9-12 (I)	Increment between successive nodes $\equiv K$
	16 (I)	= 3
	18-24 (F)	Global x-coordinate of origin point 0
	25-31 (F)	Global y-coordinate of origin point 0
	32-38 (F)	Global z-coordinate of origin point 0
	39-45 (F)	Local \bar{x} -coordinate of point I
	46-52 (F)	Local \bar{x} -coordinate of point J
	53-59 (F)	Largest absolute value of \bar{z}_i and \bar{z}_j
	60-66 (F)	Counterclockwise angle ω (in degrees) from x to \bar{x}

The horizontal distance between I and J is subdivided into $(J-I)/K$ equal intervals and the intermediate global nodal coordinates are computed.

The local coordinate system \bar{x} , \bar{y} , and \bar{z} is constructed as follows:

- a. \bar{x} is positive in the direction from I to J
- b. \bar{z} is parallel and in the same direction as z
- c. \bar{y} forms a counterclockwise angle of $\omega + 90^\circ$ from the global x-axis

Surface coordinate direction cosines are computed by assuming

- d. ξ_1 lies in the plane \bar{x} - \bar{z} and is tangent to the parabola at each node. It is directed along the parabola going from I to J
- e. ξ_2 is parallel to and in the same direction as \bar{y}

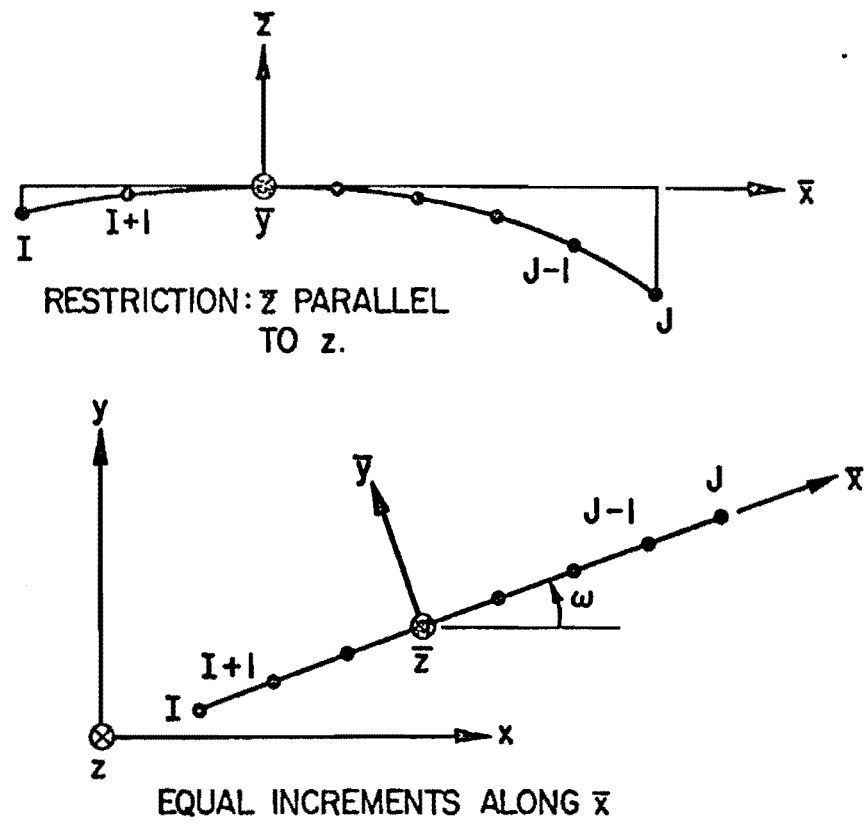


Fig 22. Parabola

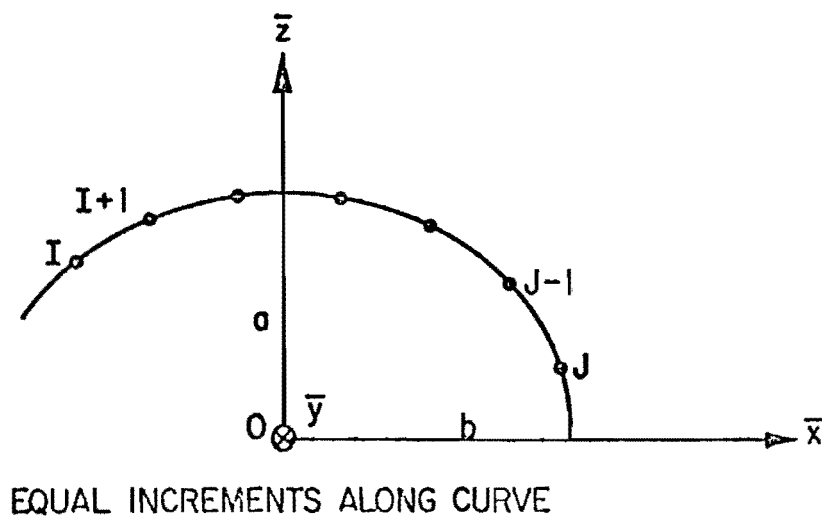


Fig 23. Ellipse .

3.4 Ellipse (Fig 23).

Cols.	1- 4 (I)	Node I of ellipse
	5- 8 (I)	Node J of ellipse
	9-12 (I)	Increment between successive nodes $\equiv K$
	16 (I)	=4
	18-24 (F)	Global x -coordinate of origin point 0
	25-31 (F)	Global y -coordinate of origin point 0
	32-38 (F)	Global z -coordinate of origin point 0
	39-45 (F)	Local \bar{x} -coordinate of point I
	46-52 (F)	Local \bar{x} -coordinate of point J
	53-59 (F)	Distance, a , from 0 to ellipse along \bar{z}
	60-66 (F)	Distance, b , from 0 to ellipse along \bar{x}
	67-73 (F)	Counterclockwise angle from x to \bar{x} in degrees

The ellipse arc length between nodes I and J is subdivided into $(J-I)/K$ equal arc lengths and the intermediate global nodal coordinates are computed.

The local coordinate system \bar{x} , \bar{y} , and \bar{z} is constructed as follows:

- \bar{x} is positive in the direction from I to J
- \bar{z} is parallel and in the same direction as z
- \bar{y} forms a counterclockwise angle of $\omega + 90^\circ$ from the global x -axis.

Surface coordinate direction cosines are computed by assuming

- ξ_1 lies in the plane \bar{x} - \bar{z} and is tangent to the ellipse at each node. It is directed along the parabola going from I to J
- ξ_2 is parallel to and in the same direction as \bar{y} .

Restriction: \bar{z} must be parallel to the global z axis and angle $\angle IOJ \leq 180^\circ$

3.5 Incremental Generation -- TYPE 1.

Cols.	1- 4 (I)	Node I of generator
	5- 8 (I)	Node J of generator
	9-12 (I)	-MOD, where MOD = Nodal difference of adjacent generators
	13-16 (I)	-LIM, where LIM = Number of new lines to be generated
	18-24 (F)	XINC = Increment in x-dir. from old to new generator
	25-31 (F)	YINC = Increment in y-dir. from old to new generator
	32-38 (F)	ZINC = Increment in z-dir. from old to new generator

This card causes $(J-I)*LIM$ points to be generated as follows:

$$\begin{aligned} X_K &= X_{K-MOD} + XINC * L & (\xi_1)_K &= (\xi_1)_{K-MOD} \\ Y_K &= Y_{K-MOD} + YINC * L & \text{AND} & (\xi_2)_K &= (\xi_2)_{K-MOD} \\ Z_K &= Z_{K-MOD} + ZINC * L & (\xi_3)_K &= (\xi_3)_{K-MOD} \end{aligned}$$

where $L = 1, 1, LIM$ and $K = (I+MOD*(L-1)), 1, (J+MOD*(L-1))$.

This option assumes that XINC, YINC, and ZINC are constant for all generators considered. Also nodal numbering as for a regular mesh is assumed as shown in Fig 24. Assuming that Line 1 (Fig 24) had been generated, then the following would generate the remaining Lines 2-6:

$$\begin{aligned} I &= 5, J = 8, MOD = 4, LIM = 5 \text{ and} \\ XINC &= X_5 - X_1, YINC = Y_5 - Y_1, ZINC = Z_5 - Z_1 \end{aligned}$$

3.6 Incremental Generation -- TYPE 2.

Cols.	1- 4 (I)	Node I of generator
	5- 8 (I)	Node J of generator
	9-12 (I)	MOD (same as for TYPE 1)
	13-16 (I)	-LIM, where LIM = Number of new lines to be generated
	18-24 (F)	XINC
	25-31 (F)	YINC
	32-38 (F)	ZINC
		} same as for TYPE 1

This card causes $((J-I)/MOD)*MOD*LIM$ points to be generated as follows:

$$\begin{aligned} X_K &= X_{K-1} + XINC * L & (\xi_1)_K &= (\xi_1)_{K-1} \\ Y_K &= Y_{K-1} + YINC * L & \text{and} & (\xi_2)_K &= (\xi_2)_{K-1} \\ Z_K &= Z_{K-1} + ZINC * L & (\xi_3)_K &= (\xi_3)_{K-1} \end{aligned}$$

where $L = 1, 1, LIM$ and $K = (I+L-1), MOD, (J+L-1)$

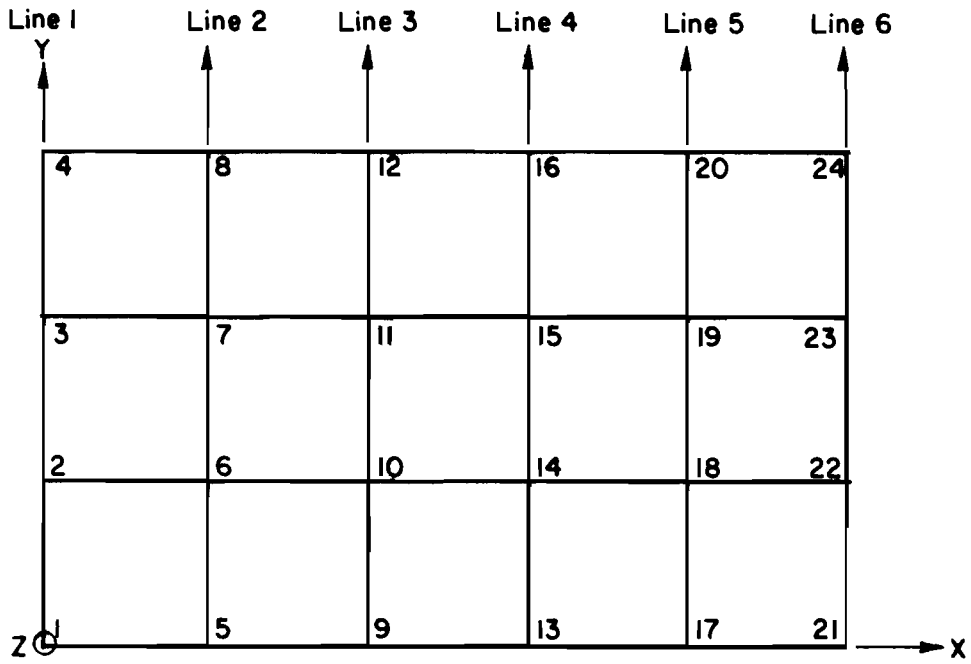


Fig 24. Sample for nodal point generation.

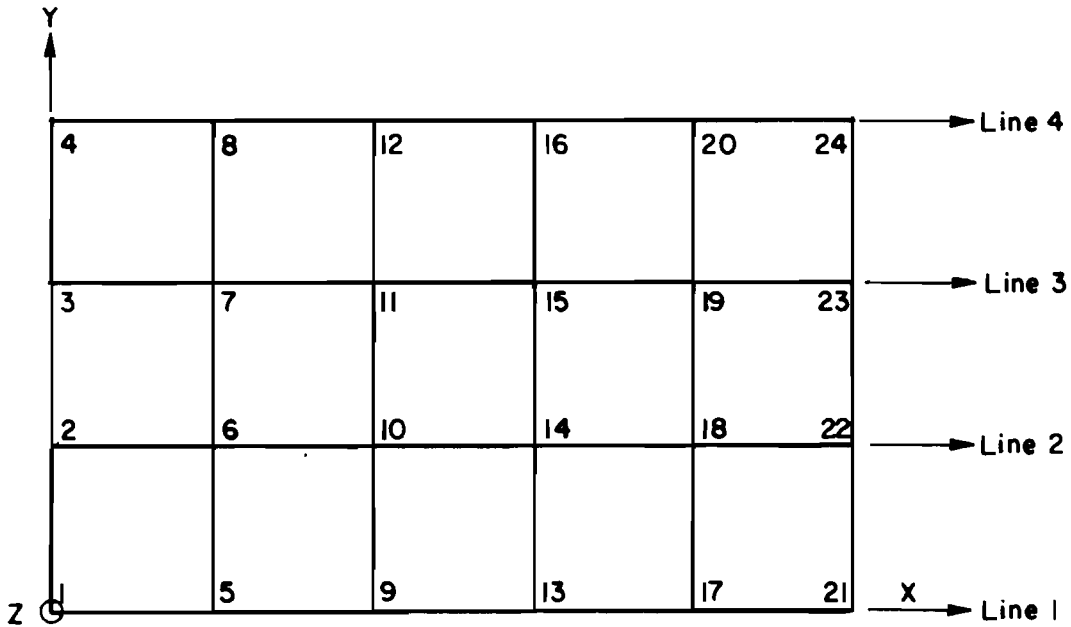


Fig 25. Sample for nodal point generation.

As for TYPE 1 a regular mesh is assumed as shown in Fig 25; however, TYPE 2 generates lines opposite to the direction of nodal numbering. Assuming that Line 1 (Fig 25) had been generated, then the following would generate the remaining lines 2-4:

$$I = 2, J = 22, MOD = 4, LIM = 3$$

Element Nodal Point Number Generation

4.1 TYPE 1. If M element cards are omitted with $NINCV = NINCH = 0$ in Sec. 2.5, these missing elements will be generated by increasing the nodal numbers I, J, K, L of each of the preceding elements by 1.

4.2 TYPE 2. If on the card for element N (Sec. 2.5) we specify

Cols. 21-24 (I) -MOD
25-28 (I) NLAY
29-32 (I) LASTEL

then elements $N + NLAY, N + 2 * NLAY, \dots, LASTEL$ will be constructed by adding MOD to the nodal numbers of each preceding element. If $LASTEL$ equals $NUMEL$, the input of the element nodal point numbers will be terminated.

CHAPTER 5. THE DEMONSTRATION ANALYSES

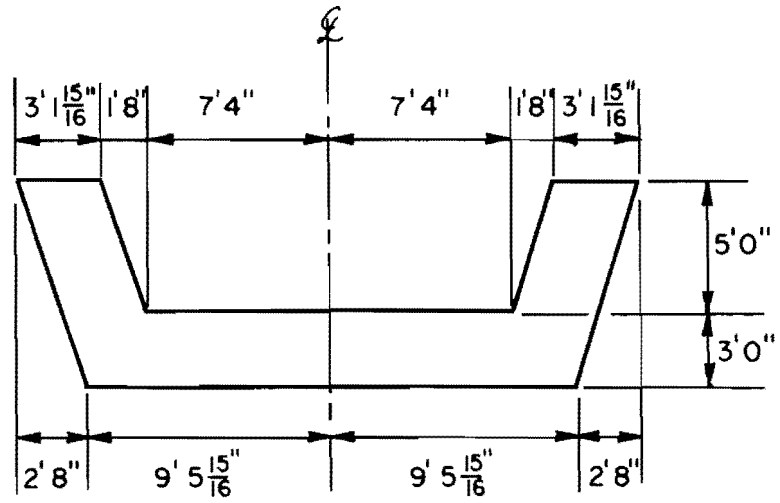
The Gull-Winged Girder

Summary. The post-tensioned railway bridge which was considered has a cross section as shown in Fig 26a with a constant thickness of 3.0 feet. In plan, the bridge center-line follows a horizontal circular curve with a radius of 616.4 feet. The bridge is continuous over two spans with two overhanging ends as shown in Fig 26b. The center line span length between supports of the left span was 93.565 feet while that of the right span was 78.879 feet. The bridge was assumed to be isotropic with a Young's modulus of 0.6192×10^6 ksf and a Poisson's ratio of 0.15.

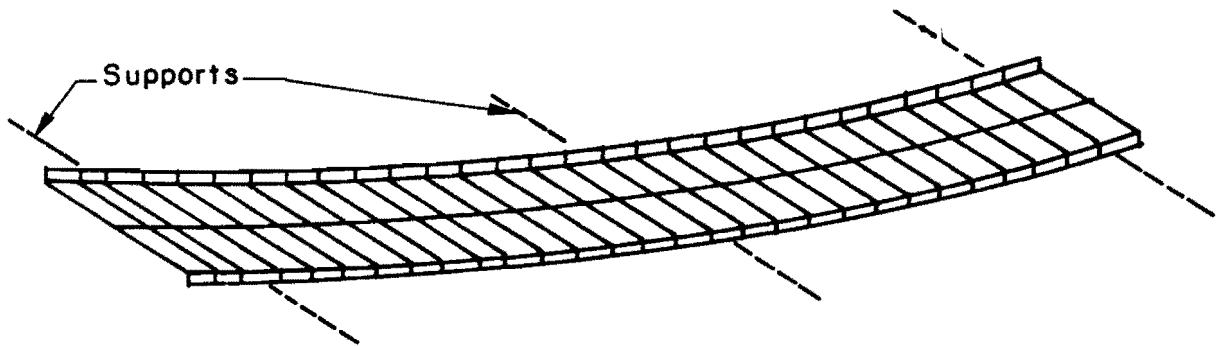
An analysis was made using program SHELL with the finite element idealization shown in Fig 27. In this idealization eight divisions were used transversely and 29 divisions longitudinally. The longitudinal divisions are in the form of two equal divisions for the left end overhang, 14 equal divisions for the left span, 12 equal divisions for the right span, and one division for the right end overhang. The transverse dividing lines are parallel to the support lines in the slab part of the bridge while in the wings these lines lie in radial planes. Thus skewed quadrilateral elements are used in the slab part while rectangular elements were used in the two wings.

In addition, analyses were made using program SHELL6 (15) and PLS6DOF utilizing the same mesh as described above. These solutions were in agreement within expected small differences. The differences were primarily due to the difference in the membrane element stiffness evaluations in the programs as well as the nodal point degrees of freedom considered (five-DOF for SHELL and six-DOF for SHELL6 and PLS6DOF).

Another analysis was made, using program SHELL6, in which the elastic properties of the supports were taken into consideration. This analysis was carried out for the case of dead load plus prestressing forces and it gave considerable change in the deflections compared to those with rigid supports while the stresses were not significantly changed. This happened because the

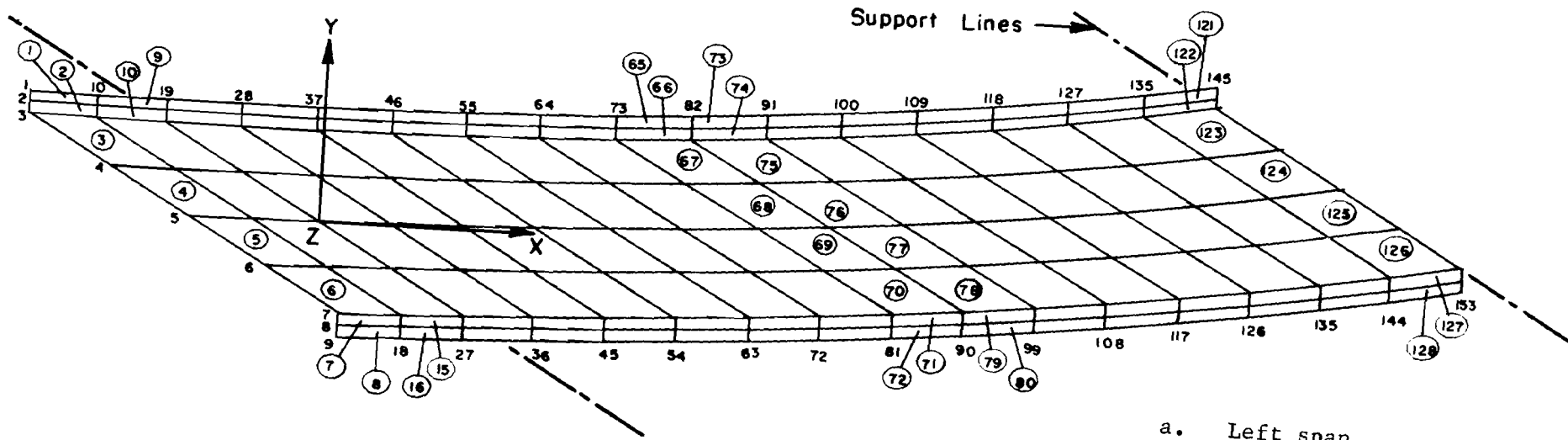


a. Cross section.

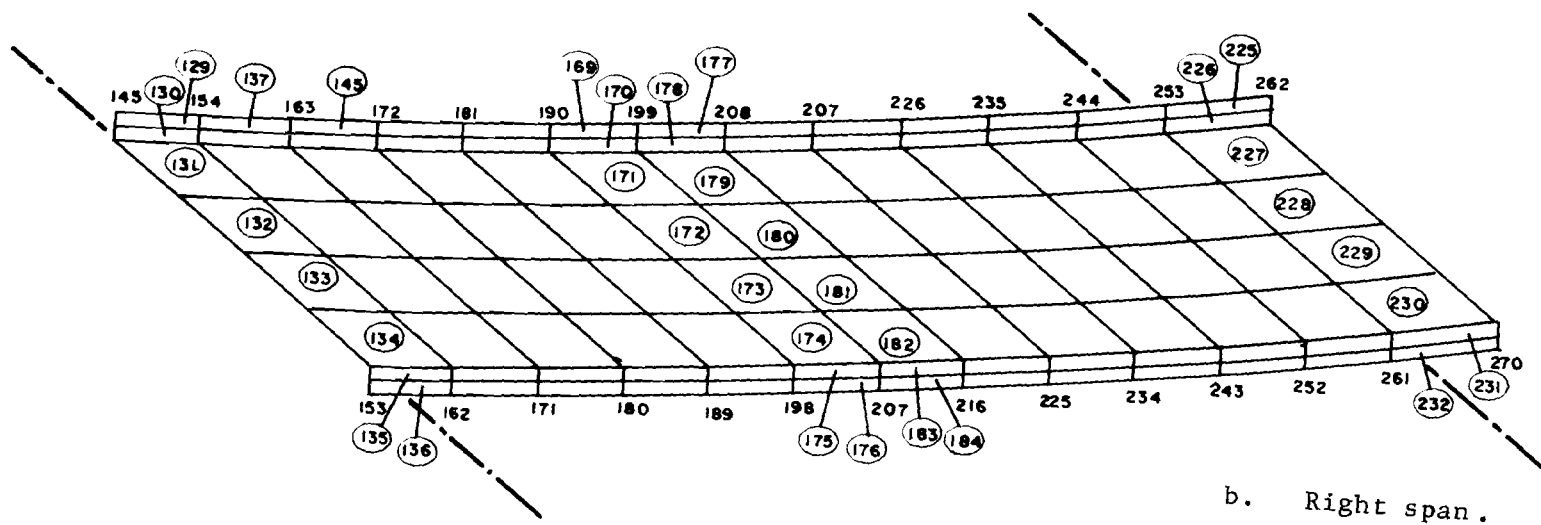


b. Complete plan view.

Fig 26. Gull wing bridge.



a. Left span.



b. Right span.

Fig 27. Finite element mesh.

change in the deflections is in the form of approximately uniform downward settlement of the supports.

The effects of skewed supports and curvature were evaluated by analyzing a straight bridge (with orthogonal supports) having the same cross-sectional dimensions and span lengths as the bridge in question. The straight bridge was analyzed by using SHELL and SHELL6 as well as a straight beam-column analysis using program BMCOL 51 (21). Comparisons of deflections from the three analyses of the straight bridge were very favorable.

Coordinate Systems and Finite Elements. The global coordinates x , y and z which were used in the analysis are shown in Fig 27a. Nodal point coordinates and the computed nodal point displacements are expressed in global coordinates. In the analysis using program SHELL, the surface coordinates ξ_1 , ξ_2 and ξ_3 were selected to be in the x , y and z directions respectively. The constraints of the five-DOF of SHELL for this structure were shown to be small. The QM5 was used for the membrane stiffness of the quadrilaterals comprising the wings while four CLST's were employed for the skewed quadrilaterals of the slab. All fifteen points along the skewed supports were supported in the vertical direction. In order to make the structure stationary in the horizontal plane, which is a requirement of the analysis procedure, the horizontal displacements (in the x - and y -directions) at the five points along the central support were set to zero. All other points were allowed to displace in the x - y plane.

The Applied Loads. The bridge was subjected to three types of loads: (a) distributed loads, (b) concentrated loads and (c) prestressing forces.

- (a) The distributed loads consist of the weight of the concrete and the weight of the track and ballast. The weight of the concrete (150 lbs/ft^3) was input as element unit weight. This value was input with a negative sign, since it is acting in the opposite direction of the global z -axis (see Sec. 1.5). The weight of the track and ballast was assumed to be uniformly distributed on the horizontal portion of the finite element idealization. The total weight of the ballast and track is listed below:

Ballast weight	=	2.262	k/ft
Track weight	=	<u>0.200</u>	k/ft
Total weight	=	2.462	k/ft

thus producing an equivalent distributed load of $2.462/16.82 = 0.1464 \text{ k/ft}^2$. This weight was input as a pressure load with a negative sign since it is in the opposite direction of η_3 (see Sec. 1.5).

- (b) The concentrated loads consist of the train loads or live loads. Three positions of the train were considered. These positions were determined by using a BMCOL 51 analysis (21) to give the following maximum effects.

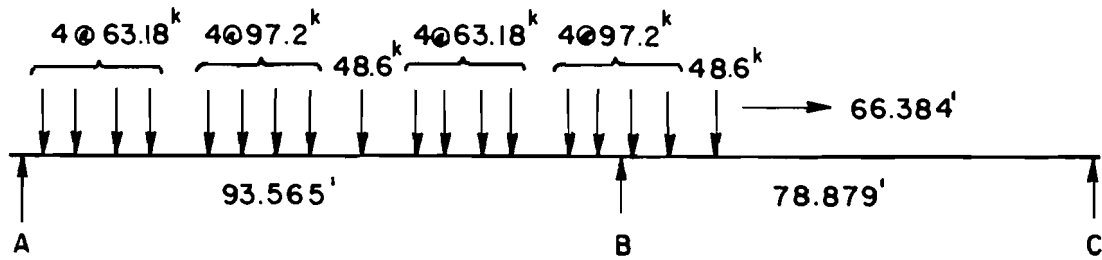
- i - The maximum positive bending moment in the long span. This position is as shown in Fig 28a and is denoted live load case #1.
- ii - The maximum positive bending moment in the short span. This is live load case #2 and it is as shown in Fig 28b.
- iii - The maximum negative bending moment. This is live load case #3 and it is as shown in Fig 28c.

For each of the load cases, the wheel loads were replaced by proportional loads (based on tributary areas) acting at the nodal points. These were calculated by hand and input as described in Sec. 2.13 and 2.14.

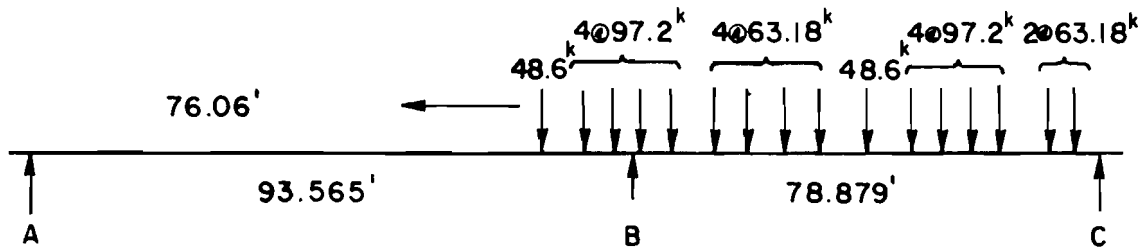
- (c) The prestressing forces were also converted to equivalent nodal forces by hand calculations. The profile of the cable used in this structure was controlled by the variation of the external moment as computed from the effect of dead load and live loads. The analysis of the prestressing force was accomplished by replacing the forces along the cable by equivalent uniform loads. Forces after losses were used in the analysis. An equivalent uniform load is applied to the structure in those regions where the cable has non-zero curvature. The total force for a typical region is given by

$$W = 2F \sin \frac{\theta}{2} = F\theta$$

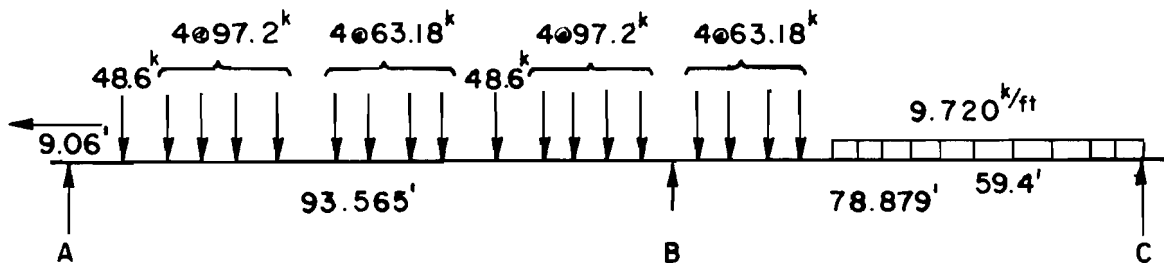
and $w = \frac{W}{L}$



To produce: a. Maximum positive moment in the left span.

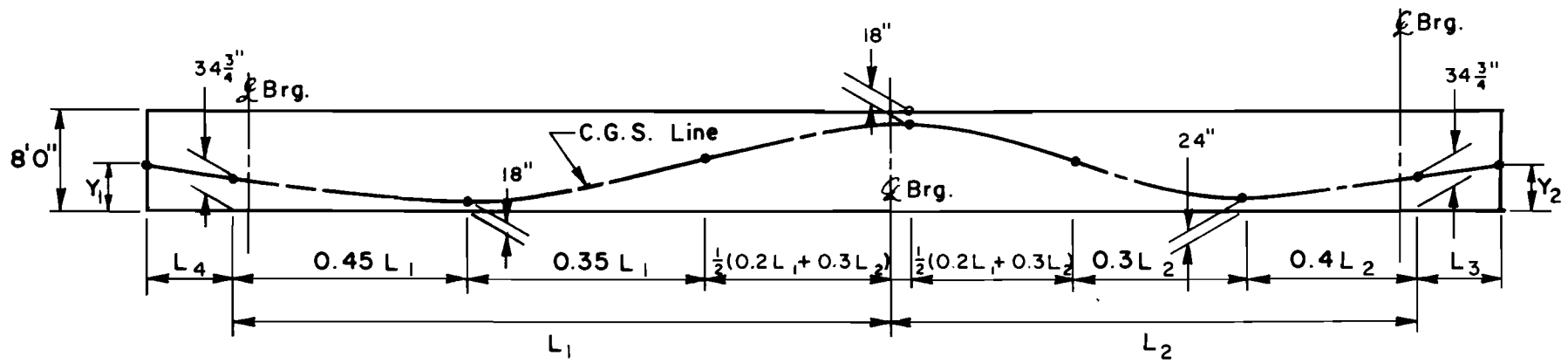


To produce: b. Maximum positive moment in the right span.



To produce: c. Maximum negative moment at the interior support.

Fig 28. Positions of live load.



	Lt. Tendon	Rt. Tendon
L_1	98.597'	92.928'
$0.45 L_1$	44.368'	41.817'
$0.35 L_1$	34.509'	32.525'
L_2	82.276'	79.610'
$0.40 L_2$	32.910'	31.844'
$0.30 L_2$	24.683'	23.883'
$\frac{1}{2}(0.2 L_1 + 0.3 L_2)$	22.201'	21.234'
L_4	2.665'	16.382'
L_5	10.146'	2.265'
Y_1	3.065'	3.992'
Y_2	3.759'	3.096'

Fig 29. Prestressing cable layout along wings.

where W = total force,
 w = equivalent uniform distributed load,
 F = average prestressing force after losses,
 L = length being considered, and
 θ = change of slope of cable in length L .

Since friction loss and other losses are taken into account the prestressing force will not be constant but will vary along the length of the tendon. Thus to simplify the analysis an average force, F , after losses was used in the above equation. The prestressing forces were applied as concentrated forces at the adjacent nodal points by proportion. A portion of the side-view and a cross section of the idealized structure are shown in Fig 30. Equivalent vertical forces, P_1 , at each wing are computed first. For example, the force acting at point a (Fig 30b) is

$$P_1 = w \times l_{ij}$$

where P_1 = vertical force

l_{ij} = half of the length between nodes i and j , for this case, 102 and 120 respectively

Since the wings are inclined, the force due to prestressing must therefore lie in the direction of the force P as shown in Fig 30b. The slope of both wings is 1:3; therefore a horizontal force P_2 , equal to one-third of the vertical force, P_1 , also exists at point a . These two forces are then proportioned to nodal points 110 and 111.

This structure is curved in plan; therefore, the prestressing force produces uniform radial force. This force can be computed as

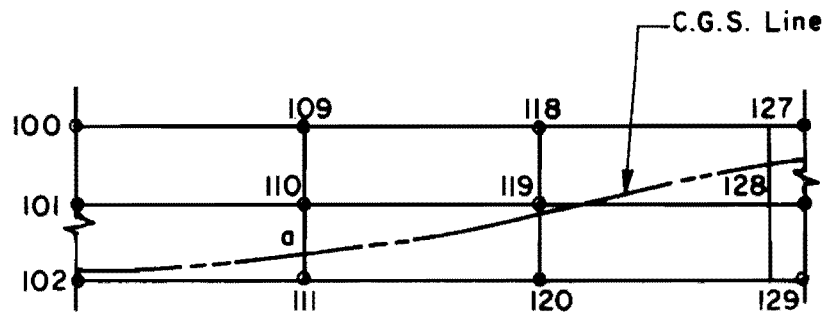
$$p = \frac{H}{R}$$

where H = average of horizontal forces at each end,

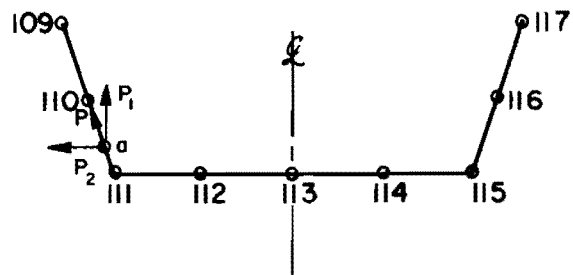
R = radius of curvature,

p = uniform radial force.

After the component p was computed, the above procedure was applied to obtain the input nodal forces. The forces thus obtained are in the radial direction which necessitates a transformation into the global x - and y -directions for the computer input. In addition to the prestressing forces



a. Partial left wing elevation.



b. Cross section.

Fig 30. Finite element idealization.

described above, nodal forces were used at the ends of the bridge to simulate the end effects of the tendons.

The Load Cases. Five load cases were considered for analysis as follows:

1. Dead load. This load case cannot exist by itself, but was used in the early studies for the purpose of comparison of results of the different computer solutions.
2. Dead load plus prestressing forces.
3. Dead load plus prestressing forces plus live load case #1 (with the train mainly on the long span).
4. Dead load plus prestressing forces plus live load case #2 (with the train mainly on the short span).
5. Dead load plus prestressing forces plus live load case #3 (with the train loads covering the two spans).

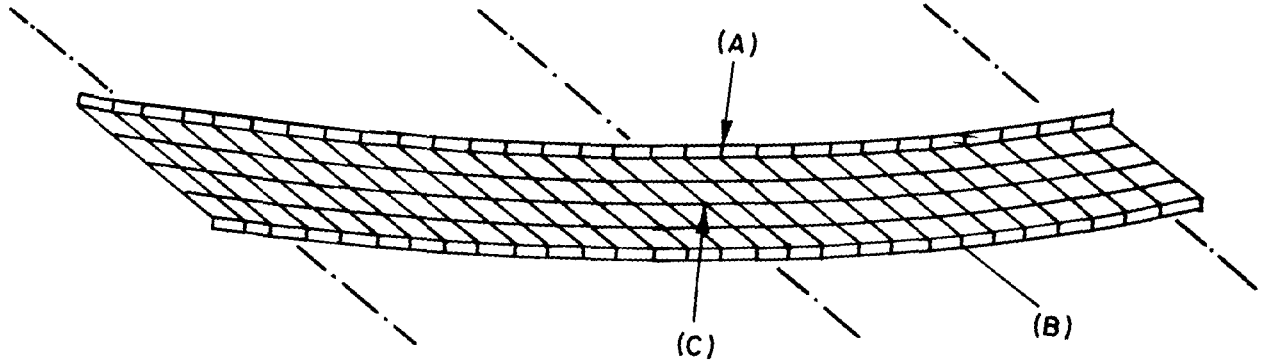
Summary of the Results. The results of the analyses for the five load cases listed above are summarized as follows:

Load Case 1. The finite element solutions by program SHELL6 and program SHELL were very close. Program SHELL yielded a slightly stiffer behavior (with a maximum difference of about 2.6% in the deflections). The deflections along the center line of the bridge as computed by the finite element solutions are very close to the beam-column solution (for the straight bridge) in the short span while considerable difference (about 21%) occurs in the long span. Also considerable twisting deformations are indicated in the two spans by the finite element solutions. It was felt that these differences are due to the stiffening effect of the skewed supports and the effect of the curvature. This was confirmed by the results of the finite element solutions of the straight bridge which were very close to the beam-column analysis.

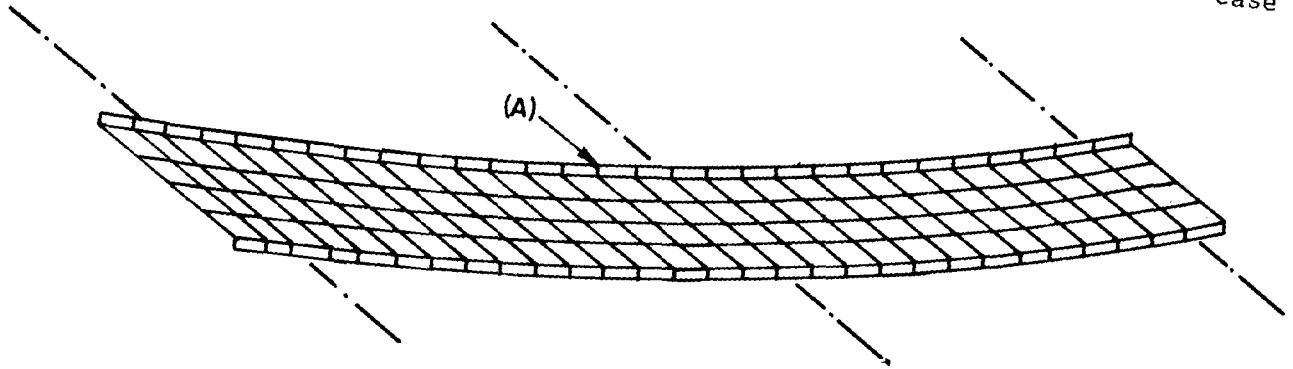
Load Case 2. (D.L. + P/S). The two finite element solutions for this case were quite close and yielded a maximum upward deflection of 0.28 inch in the long span (at left wing and slab juncture) and 0.17 inch upward in the short span (at right wing and slab juncture). Considerable torsional deformations, similar to those under dead load, are apparent in both spans.

The maximum compressive stress under this loading condition is located in the longitudinal direction at location (A) as shown in Fig 31a and equals

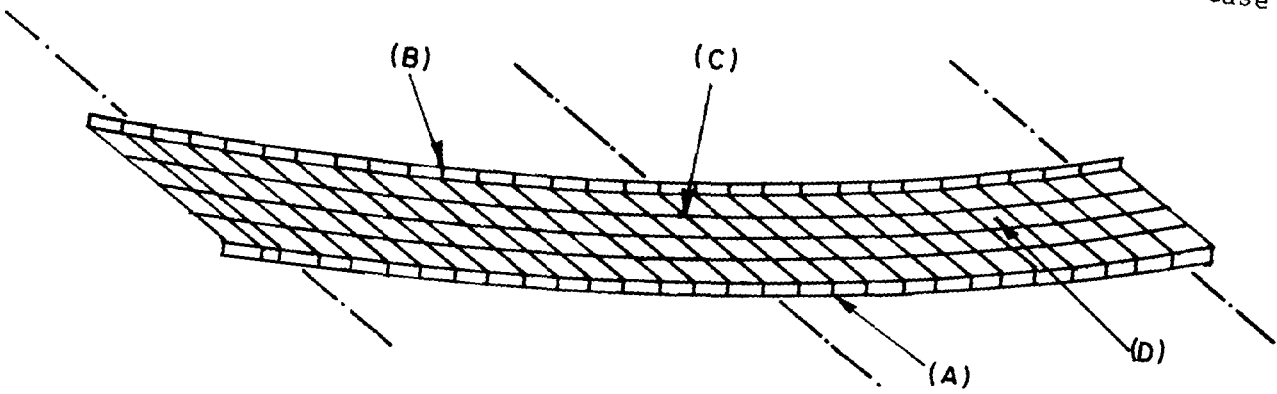
Support Lines



a. Load case 2.



b. Load case 3.



c. Load case 4.

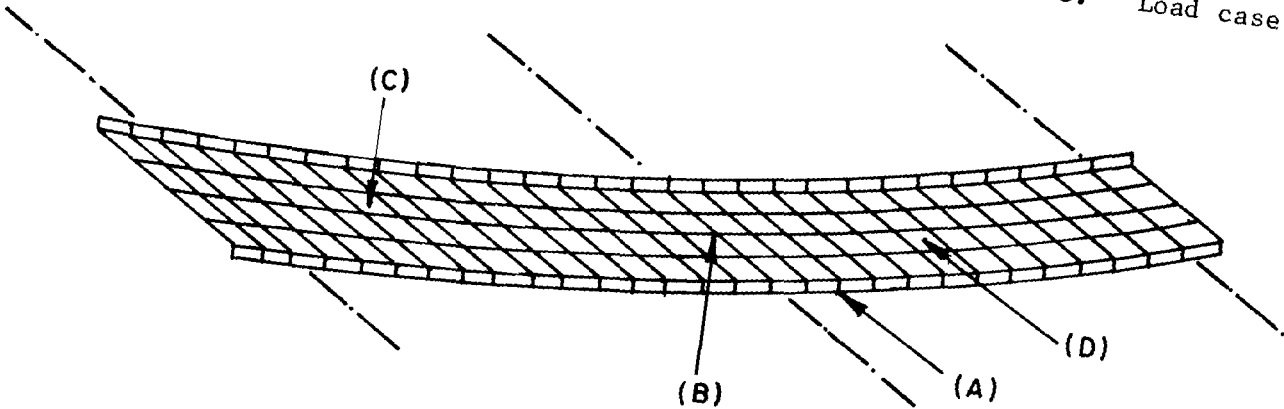


Fig 31. Locations of interest.

d. Load case 5.

1430 psi. In the longitudinal direction a maximum of 167 psi tensile stress (location (B), Fig 31a) was computed at the top of the right wing in the short span. In the transverse direction tensile stresses of considerable magnitude were computed at and near the supports. The maximum tensile stress occurs at the middle support and equals 306 psi (principal stress) (location (C), Fig 31a).

Load Case 3. (D.L. + P/S + L.L. #1). The two finite element solutions gave small downward deflections in the long span (where the L.L. exists) and upward deflections in the short span with a maximum value of 0.22 inch along the right wing. Here some twisting deformations were evident.

The maximum compressive stress for this case was 1010 psi and occurred at location (A), Fig 31b. Considerable tensile stresses result at the same locations as for load case 2. At the top of the right wing in the short span, the longitudinal tensile stress reached a maximum value of 390 psi and at the middle support the maximum tensile stress was 349 psi (principal stress). The variations along the bridge of the longitudinal stresses at the top of the wings and at the centerline of the bridge for this case are as shown in Fig 32.

Load Case 4. (D.L. + P/S + L.L. #2). This load case produced the largest deflection (upward) in the long span. The maximum value of deflection was 0.31 inch at the left wing and slab juncture. Again considerable twisting deformations were observed. In the short span (the loaded span), the maximum downward deflection is 0.10 inch.

Still no severe compressive stresses were evident for this case (the maximum value is 1320 psi in the longitudinal direction location (A) in Fig 31c). In the longitudinal direction a maximum tensile stress of 222 psi occurred at location (B) in Fig 31c at the top of the wing. Considerable tensile stresses were observed also in the transverse direction at the middle support (location (C), Fig 31c) the maximum value of the tensile stress was 348 psi (principal stress) and at location (D), Fig 31c it was 262 psi (principal stress).

Load Case 5. (D.L. + P/S + L.L. #3). This load case produces the least deflections over the entire bridge. Small deflections (upward) occur in the short span, with a maximum of 0.087 inch. The deflection in the long span was 0.038 inch upward.

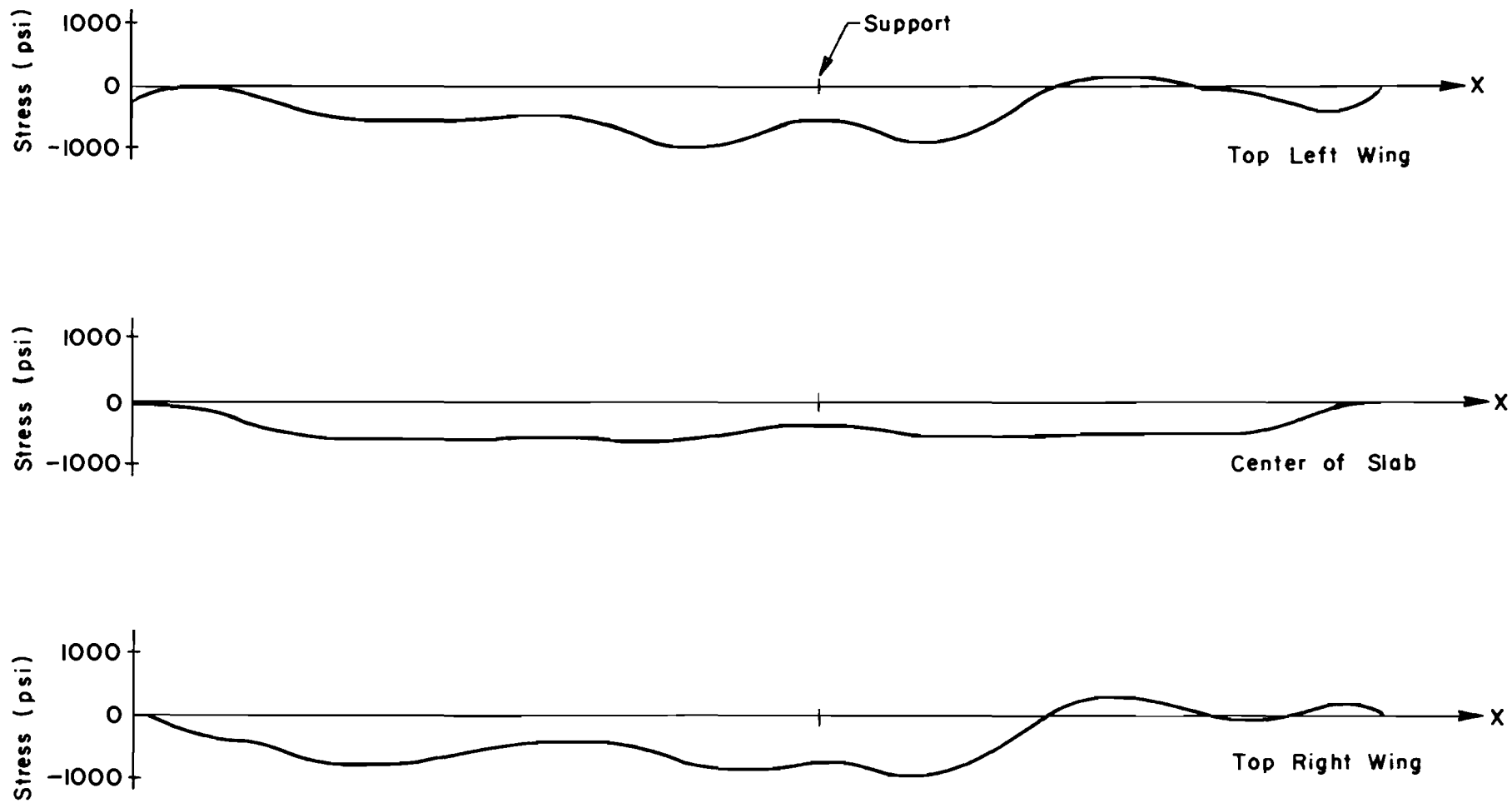


Fig 32. Longitudinal stress distributions under load case 3.

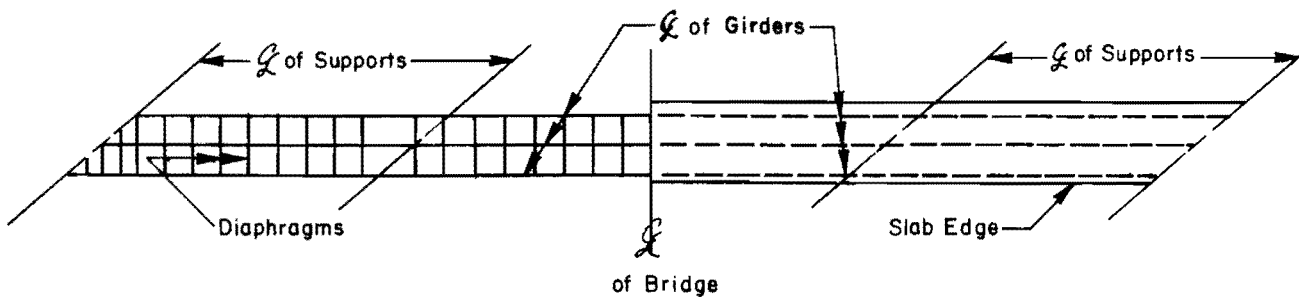
The maximum compressive stress in this case was 1070 psi in the longitudinal direction at location (A), Fig 31d. No tensile stresses are shown in the longitudinal direction. In the transverse direction, considerable tensile stresses are calculated at the supports and around mid-span sections. At the middle support a maximum value of tensile stress of 342 psi (principal stress was observed (location (B), Fig 31d); at the middle of the long span a maximum value of 246 psi (principal stress) (location (C), Fig 31d); and at the middle of the short span (location (D), Fig 31d) a maximum value of about 212 psi (principal stress) was computed.

The values of stresses for all the cases discussed above are those obtained by program SHELL. Program SHELL6 gave slightly different values for stresses which were usually somewhat higher than those given by program SHELL.

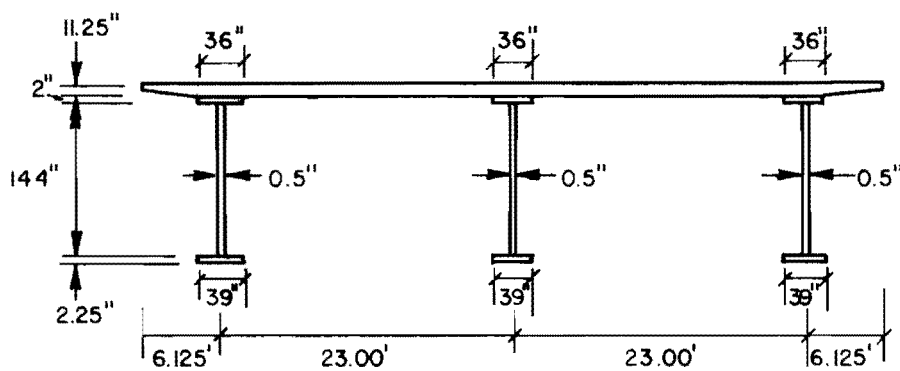
The Three Girder Bridge

The Structural Idealization. This bridge has three widely spaced girders braced with truss-type diaphragms. It is continuous over three skewed supports. The plan view and cross section are shown in Figs 33a and 33b. Also, the idealized cross section which was used in the finite element analysis is shown in Fig 33c. As stated earlier this idealization is about two percent stiffer than the actual cross section of Fig 33b, since the length from the mid-depth of the concrete slab to the mid-depth of the bottom flange of the girder was considered as the depth of the idealized structure.

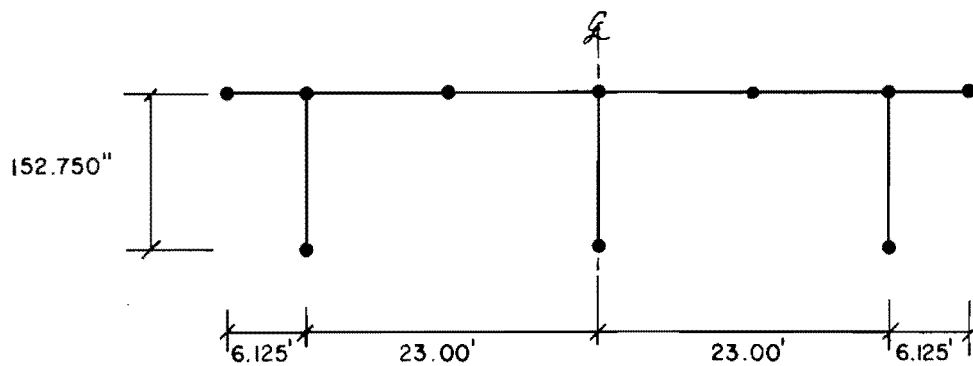
In the analysis, the slab and the webs of the girders were idealized with two-dimensional elements while the flanges, the vertical stiffeners, the lateral bracing system and the diaphragms were idealized by one-dimensional (truss) elements. The mesh layout for the slab and the upper girder is partially shown in Fig 34a and Fig 34b respectively. The QM5 was used for the membrane stiffness of all the quadrilaterals. It should be noted that only one element was used over the depth of the girders. A plan view of the wind bracing is partially shown in Fig 35a while the idealization of a typical diaphragm is depicted in Fig 35b. A total of 584 nodal points and 1629 elements were included in the mesh layout. This idealization was analyzed by program SHELL.



a. Plan view with diaphragms.

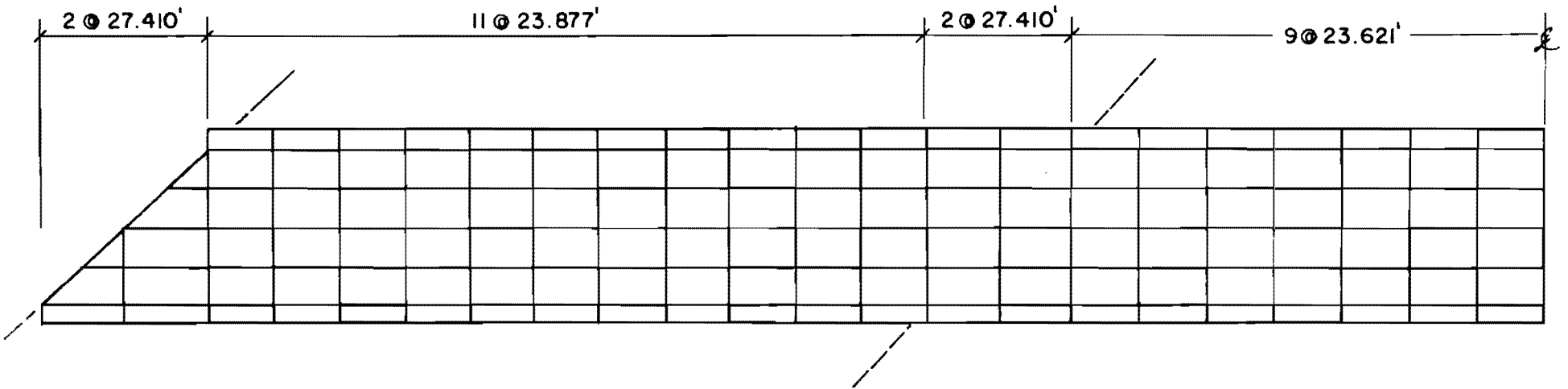


b. Actual end cross section.

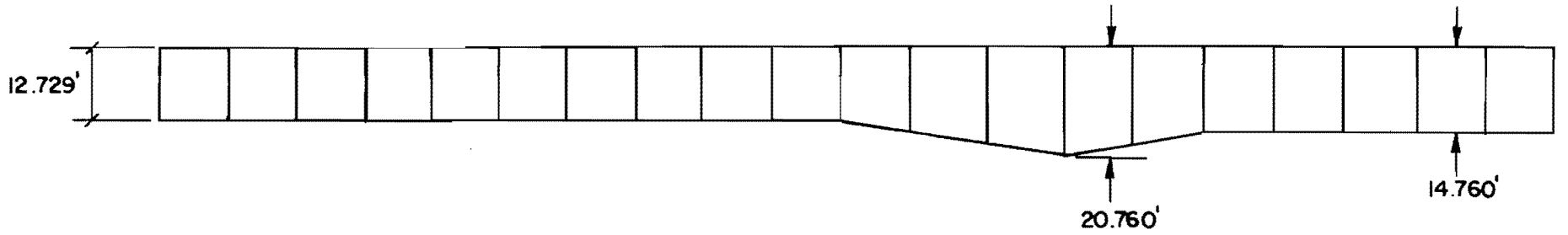


c. Idealized cross section.

Fig 33. Three girder bridge.

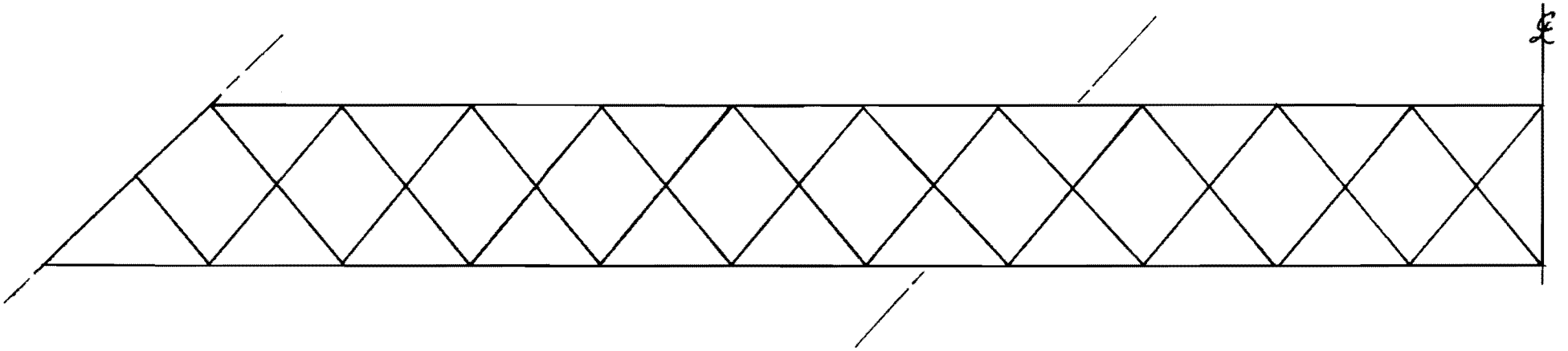


a. Plan view.

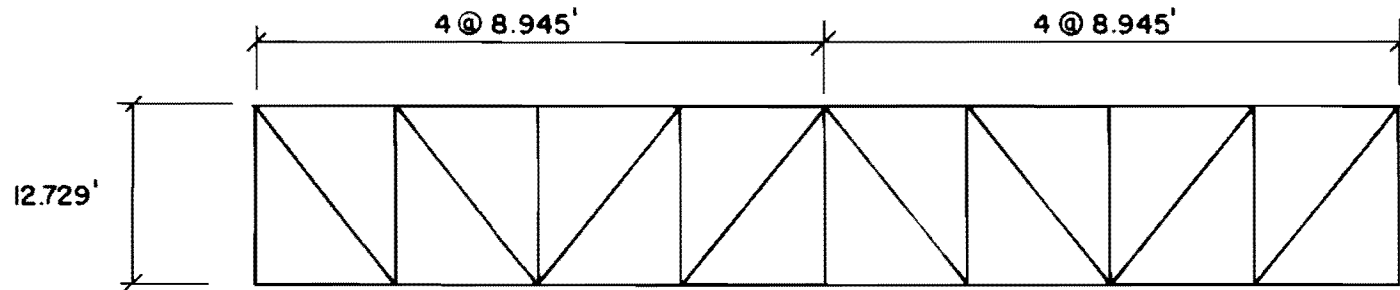


b. Elevation view of upper girder.

Fig 34. Partial mesh idealization.



a. Plan view of wind bracings.



b. Elevation view of typical diaphragm.

Fig 35. Partial mesh idealization.

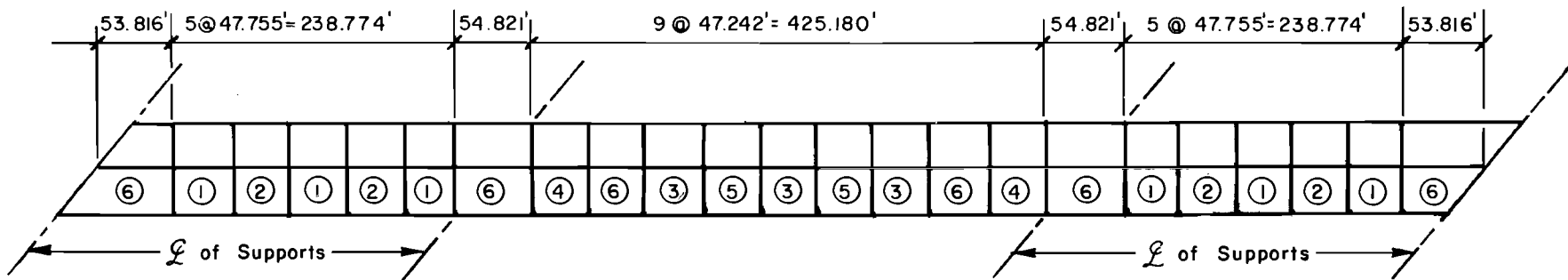
The Dead Load. The dead load included the steel weight and the weight of the concrete. In the actual construction of the slab six placing sequences were employed as shown in Fig 36a. To simplify the finite element analysis, the actual placing sequence was approximated by two placing sequences as shown in Fig 36b. The first placing sequence included most of the exterior panels (Fig 36b) while the second sequence included all remaining concrete panels. While a sequence of concrete is being placed it is assumed to have no stiffness, however, previous placements were assumed to be set and their contribution to the structural stiffness was considered. In the analysis the concrete was considered to have equal stiffness in both tension and compression.

The Live Load. Lane loads consisting of a uniform load per linear foot of traffic lane combined with either one or two concentrated loads were considered. As shown in Fig 37a. The uniform and concentrated loads were further considered to be distributed over a ten foot transverse width. Three lanes were loaded and positioned transversely as shown in Fig 37b. The loads were positioned for maximum positive moment as shown in Fig 37c and for maximum negative moment as shown in Fig 37d. By considering reduction of load intensity due to three lanes being loaded and impact factors according to AASHO specifications the load intensities shown in Figs 37c and 37d were obtained.

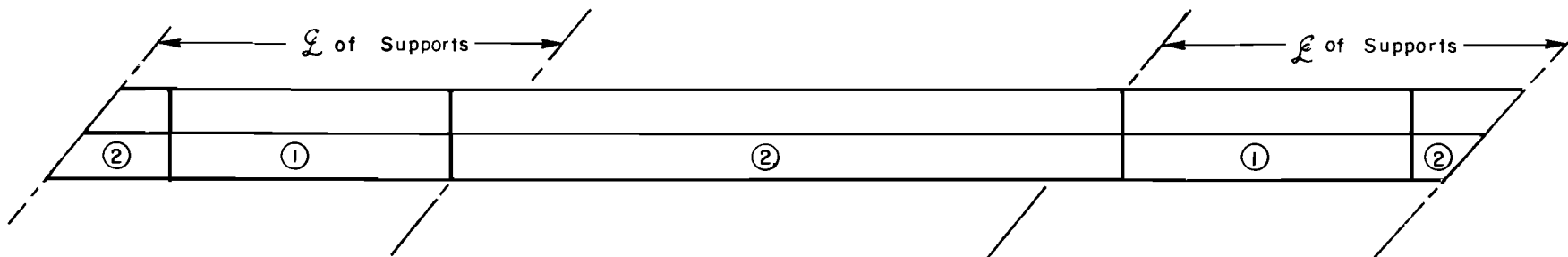
The Assumed Temperature Gradient. The estimated set of temperatures which were considered are shown in Fig 4a and 4b. They were assumed to be constant over the length of the bridge and were assumed to vary linearly over the depth of the section. Although the assumed differential temperatures of 30°F (Fig 4a) and 40°F (Fig 4b) correspond with results reported in Ref 22, the distribution of temperature over the bridge section is nonlinear. Most of the temperature change takes place in the top portion of the slab. The nonlinear characteristics of temperature over the depth is currently being addressed in the previously mentioned Research Project 23.

Summary of the Static Analyses. A total of six load cases were analyzed using program SHELL which are described below and summarized in Table 1.

Load Case 1. The loads applied included the weight of the concrete from the first placing sequence (Fig 36b) and the steel weight. Deflections and stresses for Load Case 1 are plotted in Figs 38 and 39. The maximum downward deflection was 0.97 ft in span A-B (see Table 1). The maximum

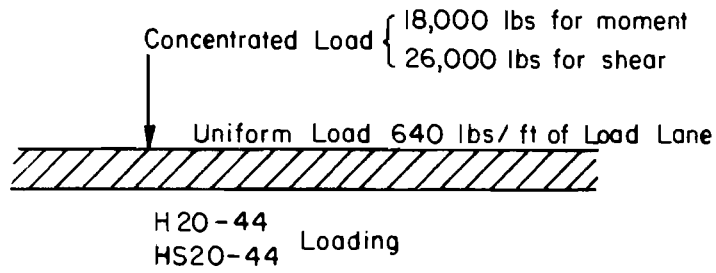


a. Actual placing sequences.

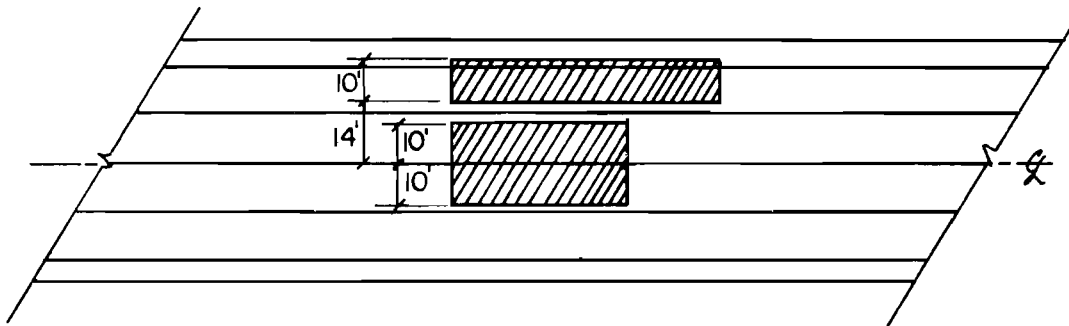


b. Placing sequences used in the analyses.

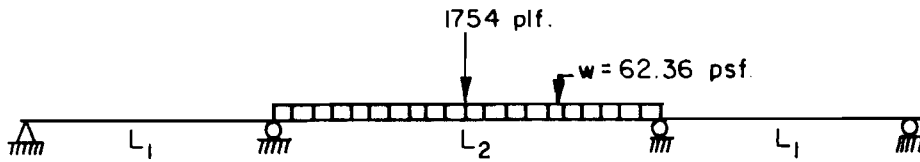
Fig 36. Concrete placing sequences.



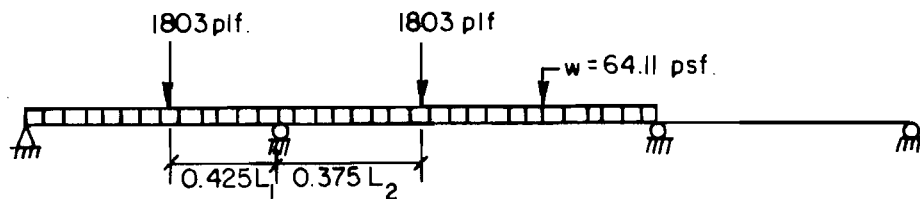
a. Lane loading.



b. Plan view showing transverse positioning of three lanes.



c. Position for maximum positive moment in the center span.



d. Position for maximum negative moment at the interior support.

Fig 37. Live load.

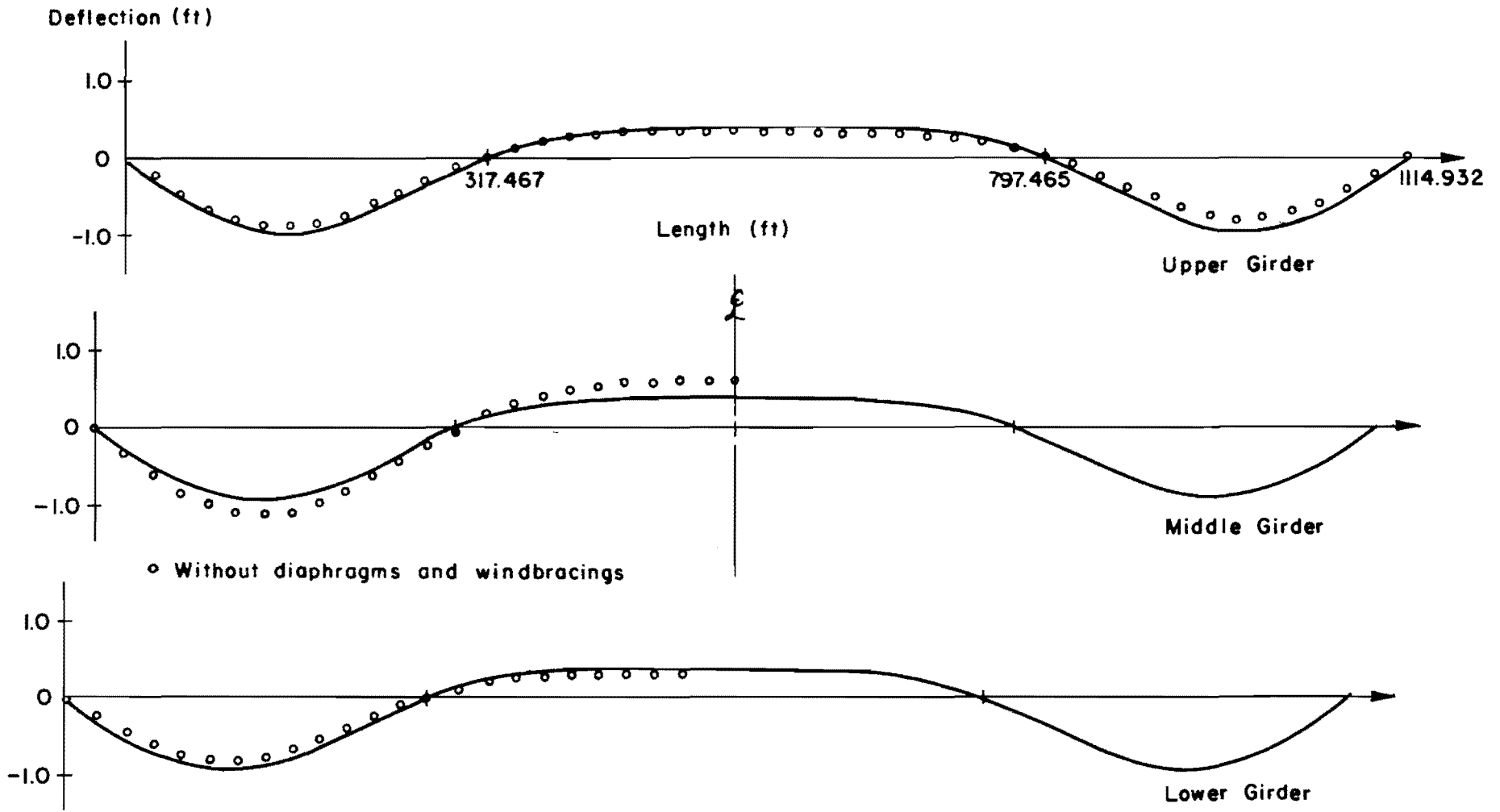


Fig 38. Vertical deflections along the bottom of girders under load case 1.

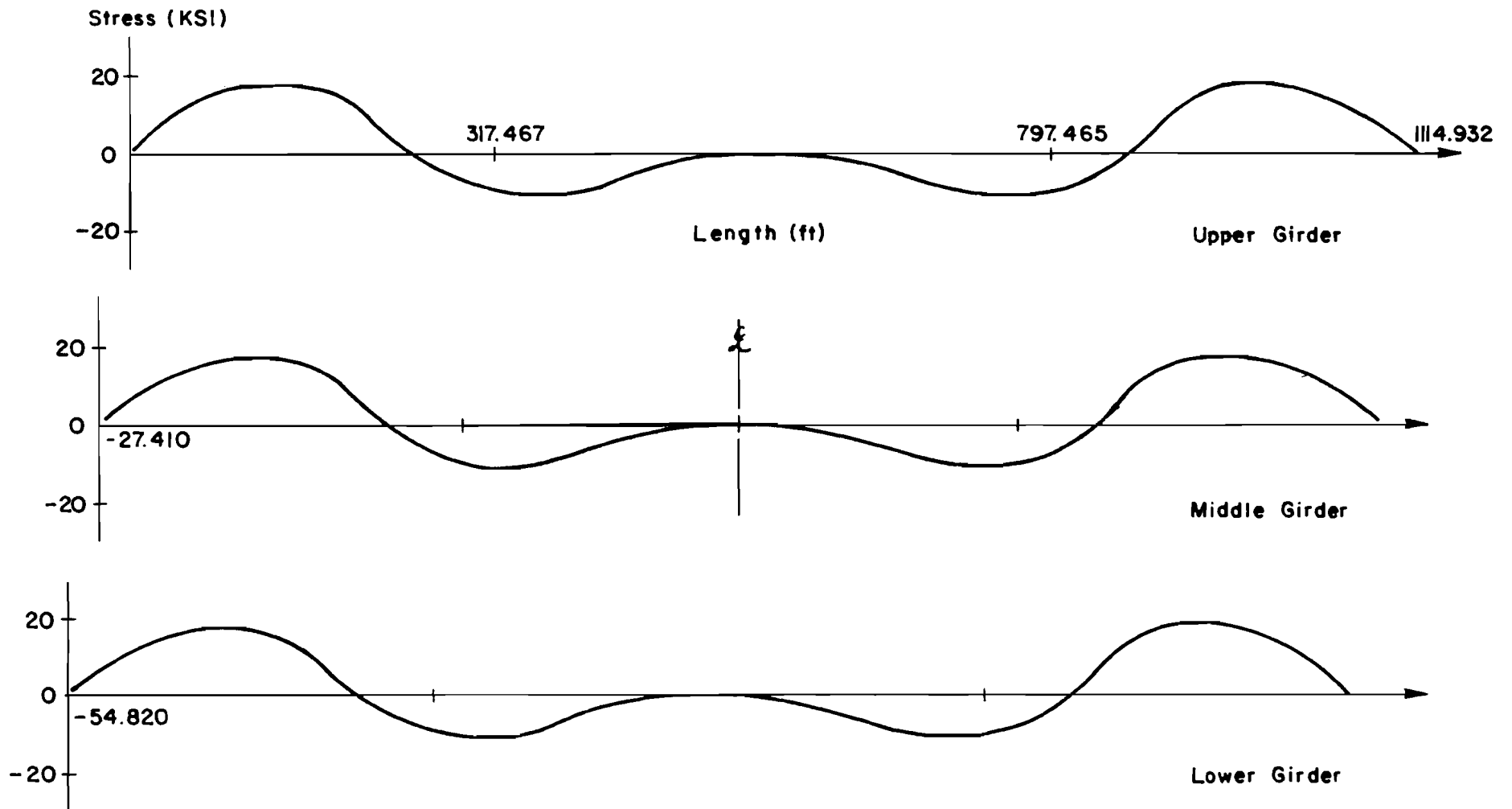


Fig 39. Longitudinal stresses along the bottom of girders under load case 1.

tensile and compressive stresses in the bottom wing of the girder were 18.5 and -10.2 ksi respectively. It is of interest to note that all three girders behave in the same manner and deflect almost the same amount. As a point of interest, another analysis was made without the diaphragms and wind bracing. The results are partially shown in Fig 38. The deflected shape of the middle girder is increased while the deflected shape of the exterior girders is decreased. This is due to the fact that without the diaphragms a larger portion of slab weight is transferred to the middle girder than to either of the exterior girders.

Load Case 2. This load case includes the loads of Load Case 1 plus the weight of the concrete of the second placing sequence (Fig 36b). Thus all dead loads are included in this load case. Deflections and stresses for Load Case 2 are plotted in Figs 40 and 41. As shown in Table 1, the maximum dead load deflection is 1.04 ft while the maximum tensile and compression stresses in the bottom wing of the girder are 15.1 and -20.4 ksi respectively.

Load Case 3. This analysis was made for live loads positioned for maximum positive moment in the central span as shown in Fig 37c. Key results for live load only are given in Table 1. Stresses and deflection are considerably less than those produced by dead load.

Load Case 4. For this load case the live loads were positioned for maximum negative moment at the first interior support as shown in Fig 37d. Refer to Table 1 for maximum deflections and stresses caused by this set of live loads.

Load Cases 5 and 6. Load Case 5 is a result of the assumed temperatures of Fig 4a while Load Case 6 is a result of the temperatures of Fig 4b. A plot of the vertical deflection resulting from Load Case 5 is shown in Fig 42 while a plot of longitudinal stresses in the bottom flanges of the girders is shown in Fig 43. From these plots three-dimensional behavior is evident. For example, the longitudinal stresses change from tension (upper girder) to compression (lower girder). The largest tensile stress in the bottom flange for this load case was 7.2 ksi which is approximately one-half of the corresponding stress due to dead load. For the uniform gradient in the transverse direction (Load Case 6) beam behavior predominated. Each of the bottom flanges were in tension over the entire bridge length with a maximum tensile stress of 8.5 ksi. Key results for Load Cases 5 and 6 are summarized in Table 1.

TABLE 1

Finite Element Analysis

NO.	LOAD CASE	MAX. VERTICAL DEFL. (FT.)		MAX. LONG. STRESSES (KSI.)*		
		Span A-B	Span B-C	Span A-B	Span B-C	Point B
1	Seq. No. 1	- 0.97	+ 0.38	+ 18.5	0	- 10.2
2	DL	- 0.53	- 1.04	+ 13.4	+ 15.1	- 20.4
3	LL. No. 1	+ 0.1	- 0.29	- 4.2	+ 4.3	- 3.0
4	LL. No. 2	- 0.04	- 0.22	+ 1.9	+ 3.8	- 4.2
5	Uneven Temperature Rise	+ 0.035	- 0.03	+ 7.2	+ 7.2	+ 5.1
6	Even Temperature Rise	+ 0.055	- 0.055	+ 8.0	+ 8.2	+ 5.1

* These are stresses along the bottom of the girder.

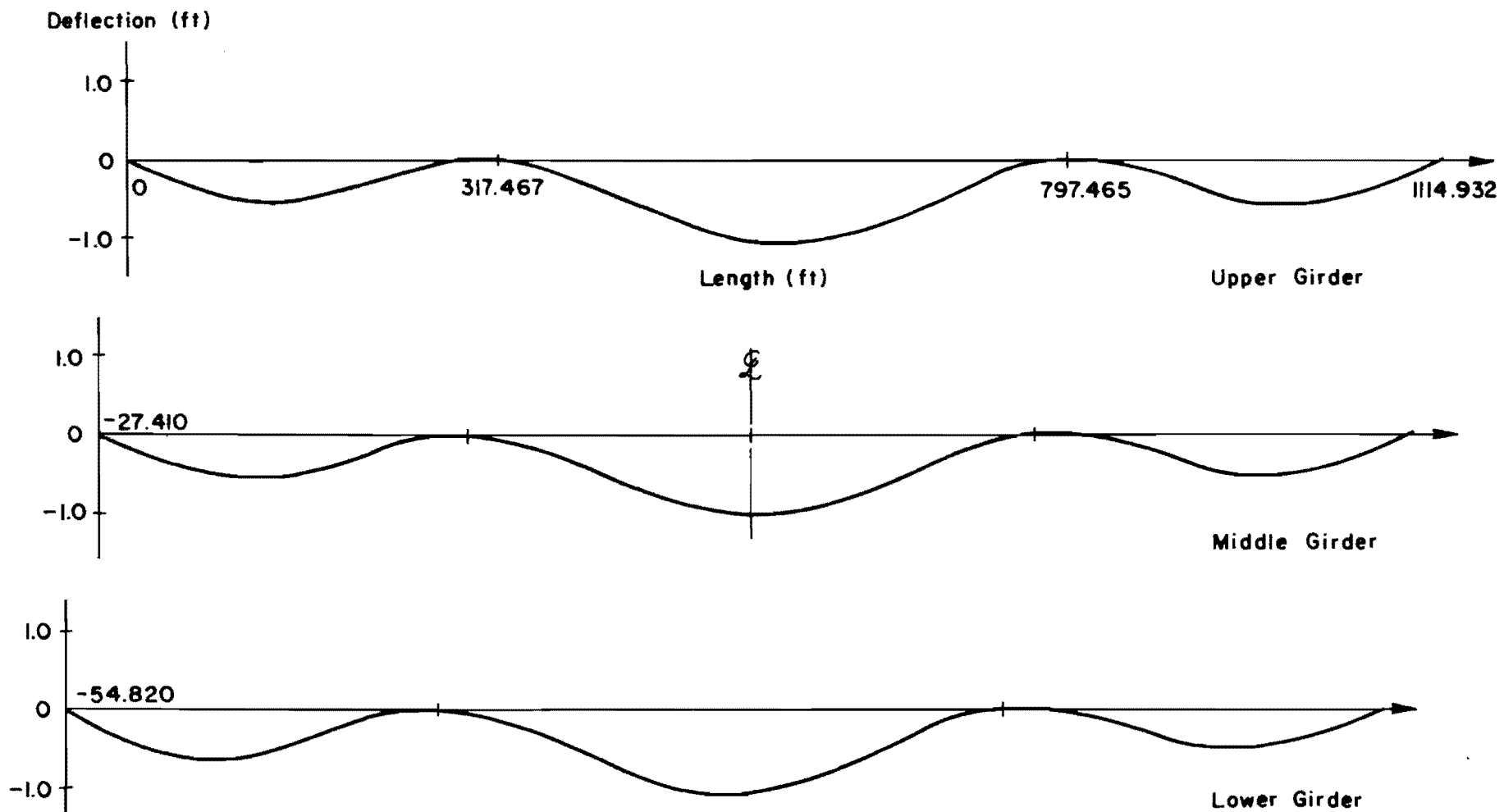


Fig 40. Vertical deflections along the bottom of girders under dead load.

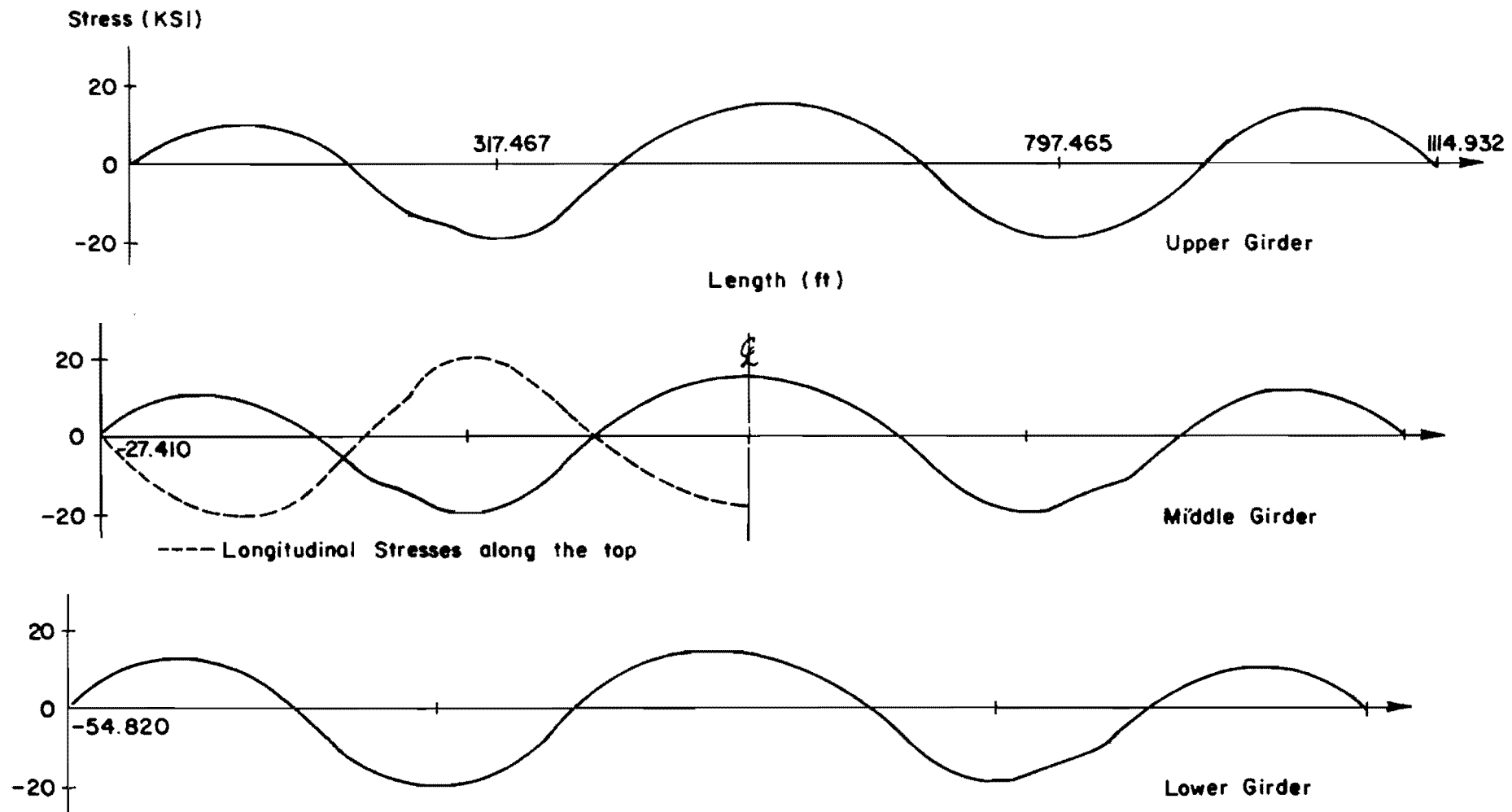


Fig 41. Longitudinal stresses along the bottom of girders under dead load.

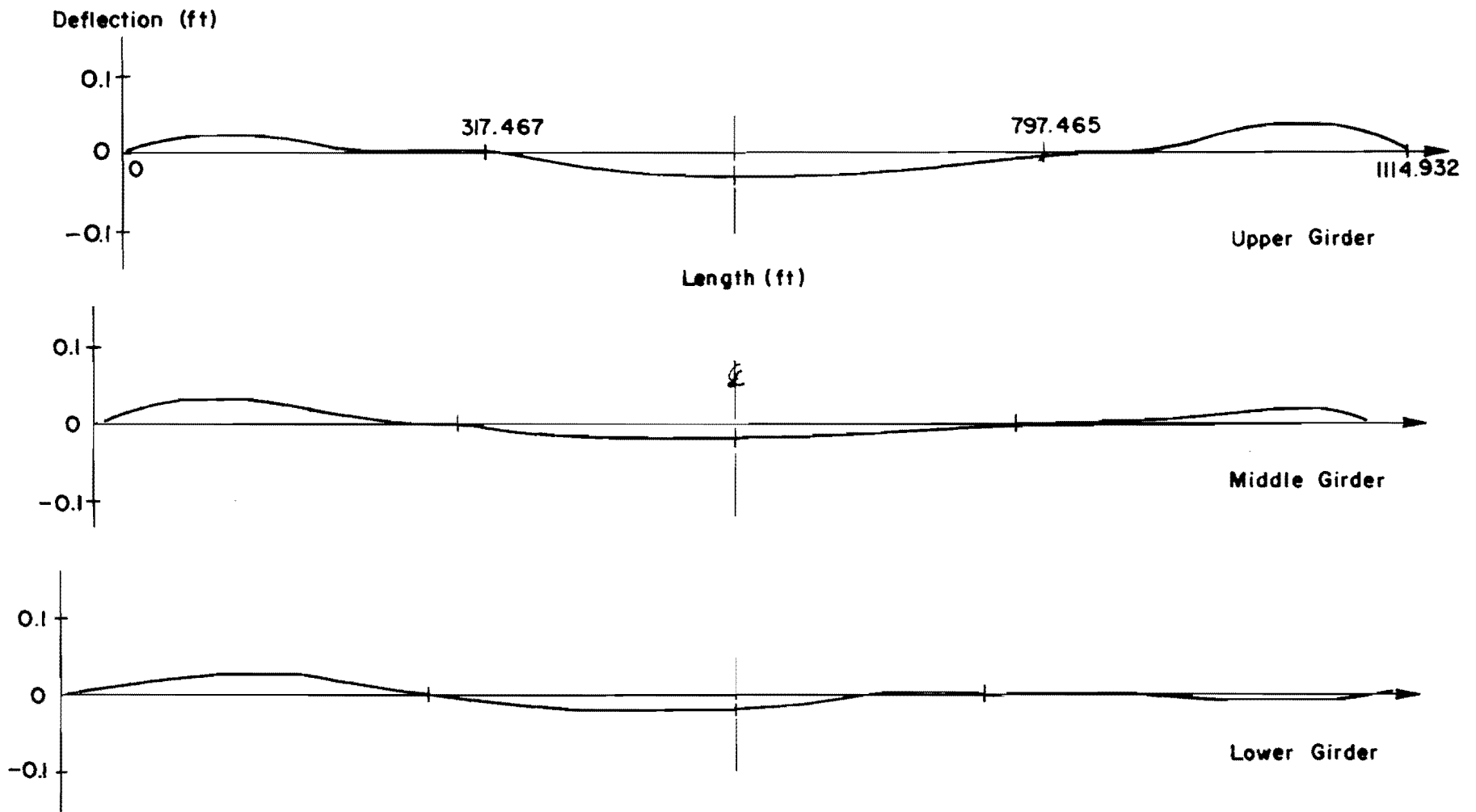


Fig 42. Vertical deflections along the bottom of girders under an approximate uneven temperature rise.

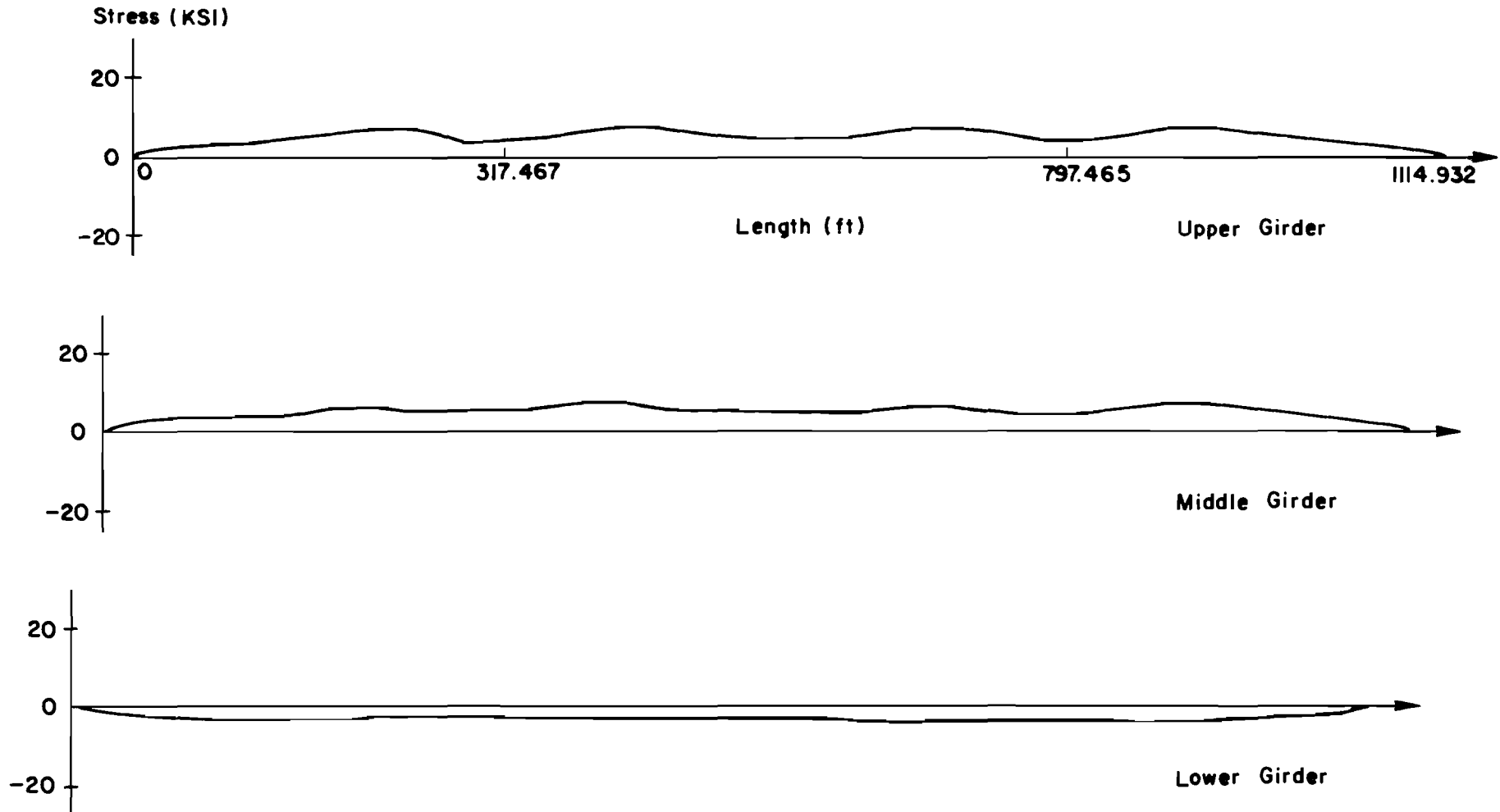
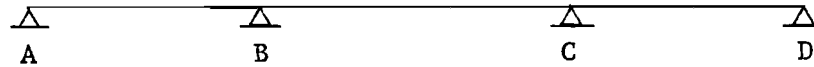


Fig 43. Longitudinal stresses along the bottom of girders under an approximate uneven temperature rise.

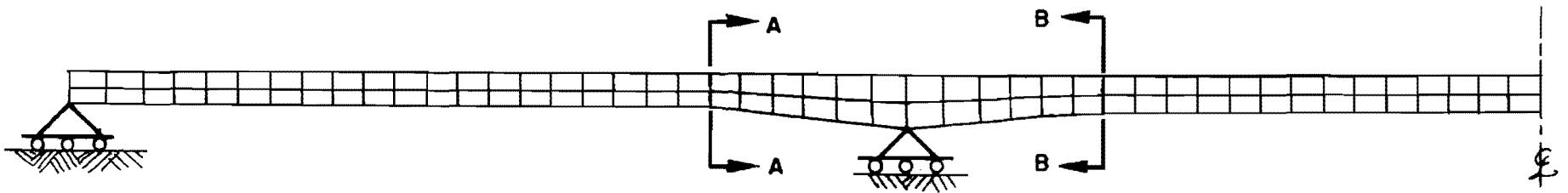
A Two-Dimensional Analysis of the Actual Placing Sequence. As previously stated the above results were obtained by considering only two placements as shown in Fig 36b. In an effort to evaluate the influence of this approximation, an independent analysis for dead load was made in which the central girder and a participating portion of the slab was idealized as a two-dimensional structure and analyzed by the procedure of Ref 14. The participating portion of the slab was adjusted so that the two-dimensional idealization had approximately one-third of the total moment of inertia of the actual cross section. Also one-third of the total load was used in the analysis. In this analysis, all six concrete placing sequences as shown in Fig 36a were considered step-by-step. In addition a comparative analysis was made for the sequence of Fig 36b. For comparison some results from the three analyses are listed in Table 2. Since the two-dimensional treatment is quite similar to considering the bridge as a three span beam, comparison of rows one and two (Table 2) is a relative indicator of the influence of the skewed supports. These results indicate that this influence is quite small since it is in the order of five to ten percent. As evidenced by the results of rows two and three, the simplified placing sequence of Fig 36b is reasonably accurate. The largest difference of the values of Table 2 takes place in the top portion at mid-span.

Buckling Analysis. The interior girder of the previously discussed three girder highway bridge was analyzed for buckling using the linear buckling program of Ref 14. A two-dimensional idealization as previously described was used which consisted of the girder and a participating portion of the slab. The slab was assumed to have gained its full stiffness and the concrete placing sequence was neglected. Since the two-dimensional idealization is symmetric about mid-span, it was possible to use only half of the bridge in the analysis as shown in Fig 44a. The two-dimensional idealization was first analyzed for total dead load. The top and bottom flanges were assumed to be fully braced laterally at the diaphragms with only the diaphragm stiffeners included in this analysis. This analysis predicted local web buckling in the haunch region near the interior support. The results indicated that this local buckling would occur at 83 percent of the dead load.

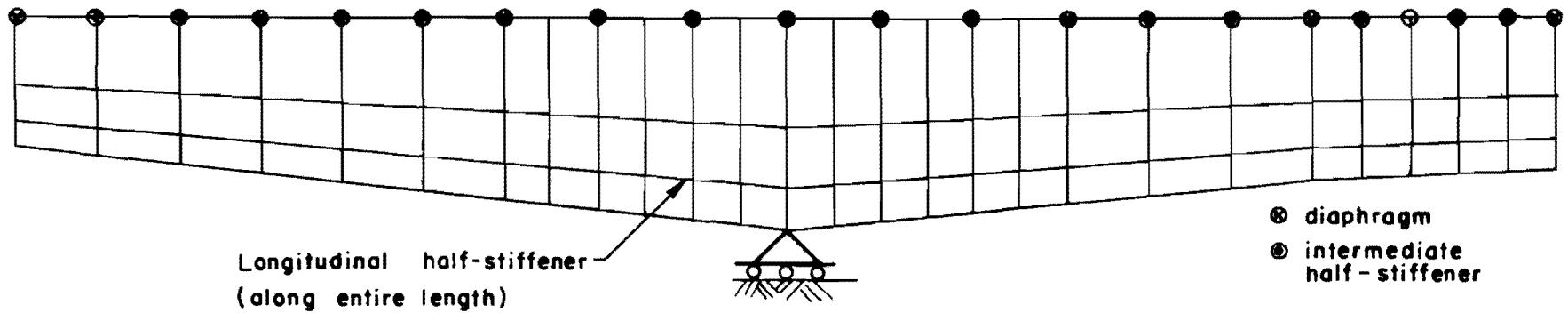
TABLE 2. Comparison of dead load analyses using two and three-dimensional idealizations.



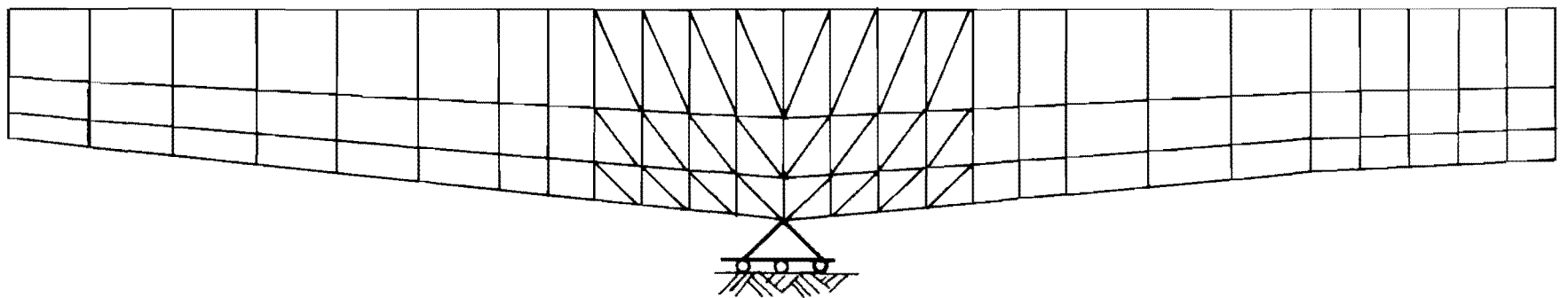
Source of analysis	Max. Vertical Defl.(ft)		Max. Long. Stresses (ksi) (top)			Max. Long. Stresses (ksi) (bottom)	
	Span A-B	Span B-C	Span A-B	Span B-C	Point B	Span B-C	Point B
Program SHELL (two placing sequences are used)	-0.53	-1.04	-20.6	-18.2	+19.2	+15.1	-20.4
Central Girder analysis (two placing sequences are used)	-0.59	-1.07	-21.6	-18.1	+21.5	+14.5	-21.7
Central Girder analysis (six placing sequences are used)	-0.52	-1.02	-22.2	-12.9	+20.6	+15.3	-20.2



a. Mesh for half of girder.



b. Haunch region section A - B . Mesh 1.



c. Haunch region section A - B . Mesh 2.

Fig 44. Partial elevation finite element mesh for buckling analyses.

Due to the localized nature of this buckling a more detailed analysis of the haunched portion of the girder was performed. Also, by isolating this region, an assessment of the roles of the intermediate and longitudinal stiffeners could be made. Two different meshes were used to study the haunch region as shown in Fig 44b and 44c. Displacements at the boundaries (sections A-A and B-B) for the static analyses were obtained from the results for the entire girder. Full lateral bracing was again assumed for the top and bottom wings at the diaphragms. The intermediate half-stiffeners were included in the first analysis using Mesh 1 (Fig 44b). Since the buckling program requires the stiffeners to be symmetric about the web, an equivalent width was used to produce symmetry and the same lateral inertia as the original half-stiffener. By including the intermediate stiffener, buckling occurred at 92 percent of the dead load. An analysis was then performed including both the intermediate and longitudinal half-stiffener. The width of the longitudinal stiffener was modified in the same manner as the intermediate stiffener. By including both stiffeners, it was predicted that buckling would occur at 1.74 times the dead load. This result clearly indicates the importance of the longitudinal stiffener. In both of the above results, local web buckling occurred near the support.

Mesh 2 as shown in Fig 44c was also used to study the haunch region. For this study, triangular elements were incorporated into the buckling program. These triangles can have from zero to three mid-side nodes and are useful for mesh grading to more carefully study critical regions. The results using this mesh with all stiffeners included indicated that buckling would occur at 1.63 times the dead load. The buckled mode shape plotted along the mid-depth of the web is shown in Fig 45. Also shown in this figure is the buckled cross section. Both plots illustrate the localized nature of the buckling.

The interior girder was also analyzed for dead load plus live load. A 10 percent impact factor was used with 1.57 lanes of live load going to the interior girder. The buckling load was computed to be 1.53 times the combined dead load plus live load. Again, the girder buckled locally in the same region.

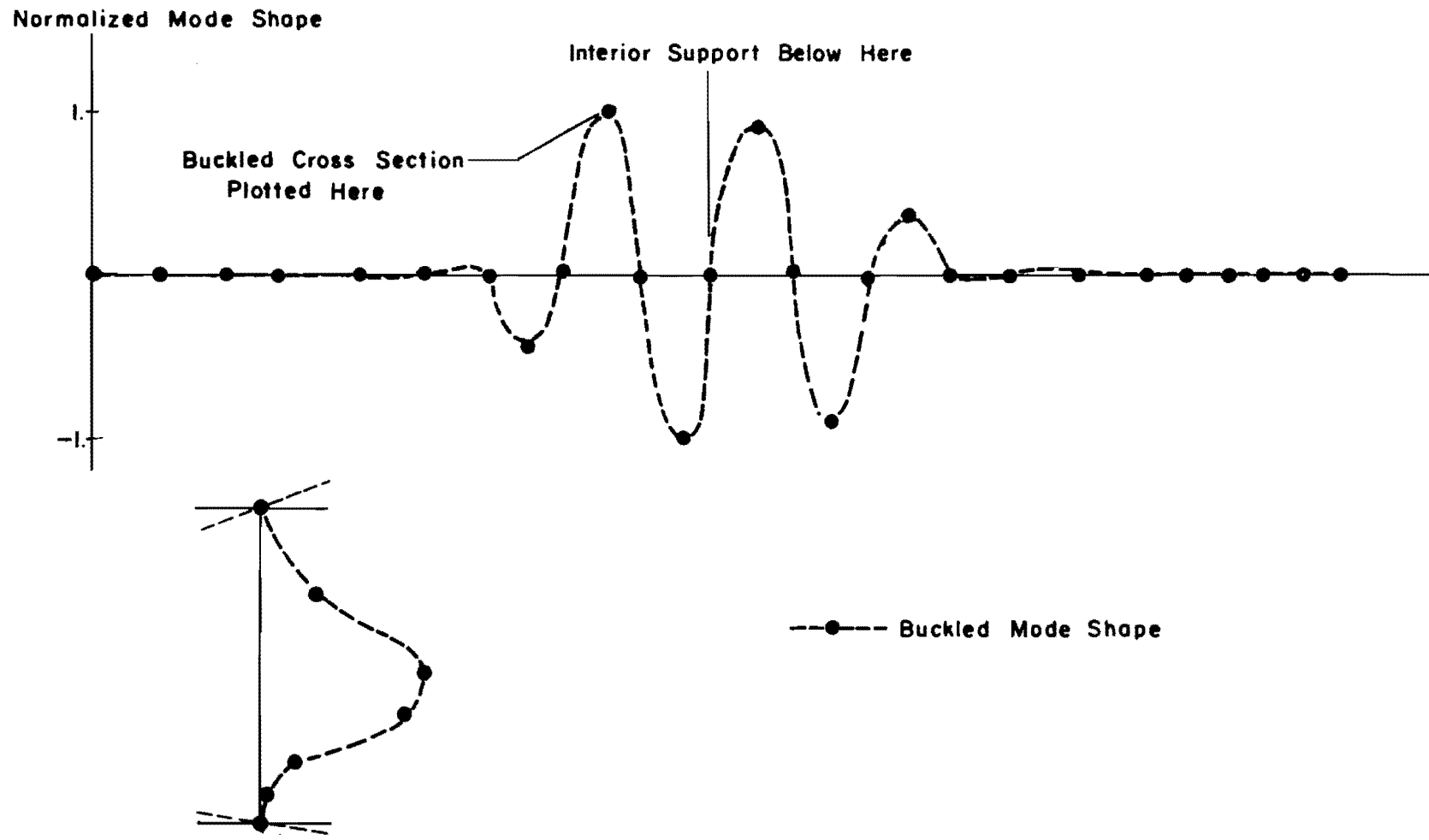


Fig 45. Buckled mode shape along web mid-depth and buckled cross section.

This page replaces an intentionally blank page in the original --- CTR Library Digitization Team

CHAPTER 6. CONCLUSIONS AND RECOMMENDATIONS

Program SHELL has been shown to be an effective tool for predicting structural response of complex highway bridges subjected to static loadings and prestressing forces. The program can be used to determine the effects of severely skewed supports, curvature along the bridge center-line, and the influence of the shape of the cross section. Demonstration analyses were performed on a gull-wing girder bridge and a three-girder bridge to illustrate the capabilities of the program. It was concluded that the severely skewed supports had considerable influence on the state of stress and displacement for the gull-winged girder bridge. This structure was generally stiffer than a similar straight structure with orthogonal supports. In contrast the effect of the skewed supports on the behavior of the three-girder bridge was quite small. This is attributed to the fact that this is a slender structure for which beam action is predominate. The influence of the transverse diaphragms and wind bracing on the overall response was found to be small.

In addition, program BASP was demonstrated to be useful in determining the buckling response of steel girders. This program can be used to determine the effect of stiffeners and lateral bracing on the buckling load. For the steel girder and the participating portion of the slab considered, local buckling of the web in the haunch region predominated. The longitudinal half-stiffener was the primary source for preventing web buckling under dead load.

Program SHELL was also used to study the effects of two assumed temperature distributions on the three-girder bridge. The temperature was assumed to be uniform through the thickness of the elements. Tensile stresses resulting from these assumed distributions were found to be approximately one-half of the corresponding stresses due to dead load. However, current research being performed under Research Project 3-5-74-23 has found that the distribution through the bridge slab thickness is non-uniform. Thus, the assumption used in this temperature study is not valid. It is recommended that the temperature option in program SHELL not be used for thick concrete

slabs or beams. The non-uniform temperature approximation has recently been incorporated into program PLS6DOF and is currently being evaluated. It is anticipated that this program will be adapted to the Texas Highway Department computer facilities at the end of Research Project 3-5-74-23.

REFERENCES

1. Powell, G. H., S. G. Bouwkamp, and I. G. Buckle, "Behavior of Skew Highway Bridges," SESM Report No. 69-9, University of California, Berkeley, 1969.
2. Vora, M. R., and Hudson Matlock, "A Discrete-Element Analysis for Anisotropic Skew Plates and Grids," Research Report No. 56-18, Center for Highway Research, The University of Texas at Austin, August 1970.
3. Scordelis, A. C., "Analysis of Continuous Box Girder Bridges," SESM Report No. 67-25, University of California, Berkeley, 1967.
4. Mehraïn, M., "Finite Element Analysis of Skew Composite Girder Bridges," SEL Report No. 67-28, University of California, Berkeley, 1967.
5. Willam, K. S., and A. C. Scordelis, "Computer Program for Cellular Structures of Arbitrary Plan Geometry," SESM Report No. 70-10, University of California, Berkeley, September 1970.
6. Clough, R. W., and C. P. Johnson, "A Finite Element Approximation for the Analysis of Thin Shells," International Journal of Solids and Structures, Vol 4, Pergamon Press, Great Britain, 1968.
7. Johnson, C. P., "The Analysis of Thin Shells by a Finite Element Procedure," SEL Report No. 67-22, University of California, Berkeley, 1967.
8. Johnson, C. P., and P. G. Smith, "A Computer Program for the Analysis of Thin Shells," Structural Engineering Laboratory Report No. 69-5, University of California, Berkeley, 1969.
9. Clough, R. W., and C. P. Johnson, "Finite Element Analysis of Arbitrary Thin Shells," American Concrete Institute Symposium on Concrete Thin Shells, April 1970.
10. Johnson, C. P., "Analysis of Thin Shells," a User's Manual, Department of Civil Engineering, The University of Texas, October 1970.
11. Johnson, C. P., "Lateral Buckling of Rigid Frames by Finite Element Procedures," CESM Report No. 72-1, The University of Texas at Austin, January, 1972.
12. Will, K. M., "Elastic Instability Analysis of Thin-Walled Structures by a Refined Finite Element Procedure," CESM Report No. 71-2, The University of Texas at Austin, December, 1971.

13. Johnson, C. P., and Kenneth M. Will, "Beam Buckling by Finite Element Procedure," Journal of the Structural Division, ASCE, Vol 100, No. ST3, March, 1974.
14. Akay, H. U., "Linear Buckling and Geometrically Nonlinear Analysis of Planar Plate-Stiffener Type Structures by the Finite Element Method," TICOM Report 74-1, Ph.D. Dissertation, Department of Civil Engineering, The University of Texas at Austin, January, 1974.
15. Abdelraouf, M. R. S., "Finite Element Analysis of Shell-Type Structures," thesis presented to the University of Texas at Austin, in partial fulfillment of the requirements for the degree of Doctor of Philosophy, 1971.
16. Clough, R. W., and J. L. Tocher, "Finite Element Stiffness Matrices for the Analysis of Plate Bending," Proceedings, First Conference on Matrix Methods in Structural Mechanics, Air Force Institute of Technology, Wright-Patterson Air Force Base, Ohio, 1965 (AFFDL-TR-66-60, Nov., 1966).
17. Felippa, C. A., "Refined Finite Element Analysis of Linear and Non-linear Two-Dimensional Structures," Structural Engineering Laboratory Report No. 66-22, University of California, Berkeley, California, 1966.
18. Doherty, W. P., E. L. Wilson, and R. L. Taylor, "Stress Analysis of Axisymmetric Solids Utilizing Higher-Order Quadrilateral Finite Elements," Structural Engineering Laboratory Report No. 69-3, University of California, Berkeley, California, January, 1969.
19. Zienkiewicz, O. C., C. J. Parekh, and I. P. King, "Arch Dams Analyzed by a Linear Finite Element Shell Solution Program," Proceedings, Symposium on Arch Dams, Institute of Civil Engineering, London, 1968.
20. Zienkiewicz, O. C., The Finite Element Method in Engineering Science McGraw-Hill Book Company, London, 1971, pp. 219-221.
21. Matlock, Hudson, and Thomas P. Taylor, "A Computer Program to Analyze Beam Columns under Movable Loads," Research Report 56-4, Center for Highway Research, The University of Texas, Austin, June, 1968.
22. Zuk, William, "Thermal Behavior of Composite Bridges - Insulated and Uninsulated," Highway Research Record No. 76, 1965.
23. Timoshenko, S., and S. Woinowsky-Krieger, Theory of Plates and Shells, McGraw-Hill Book Company, Inc., New York, 1959.

APPENDIX 1

An Example Problem for Input and Output

This page replaces an intentionally blank page in the original.

-- CTR Library Digitization Team

Appendix 1. An Example Problem for Input and Output

A simply supported square slab subjected to both uniform biaxial and vertical pressures as shown in Fig 46 was selected to illustrate the required input and the interpretation of output for program SHELL. The concrete slab was assumed to be isotropic with a modulus of elasticity of 4×10^6 psi and a Poisson's ratio of 0.15. By taking advantage of symmetry of the structure only one-fourth of the plate was used in the finite element idealization. This idealization which is depicted in Fig 47 included 16 elements and 25 nodal points. The 4×4 mesh was used since in this case it gives a sufficiently accurate solution. The vertical displacement at the center of the plate differed from the exact solution (23) by approximately 2.7% while the maximum resultant force (lb. in/in) differed by approximately 2.5%.

Two sets of input data were used as shown in Table 3. The only difference in the inputs appears on the second card (i.e. the value for ISIG of Sec. 2.2). The first set of input data of Table 3 used the option of membrane stress and bending resultants having the units of force and moment per unit length of mid-surface respectively. The second set of input data of Table 3 used the option to compute fiber stresses having the units of force per unit area. These stresses thus include the effects of both membrane and bending actions. Details of interpreting the stresses will be discussed later.

In preparing the input data it is advisable to use as many generation options as possible to minimize the coding time and reduce the coding errors. For example with regard to the nodal coordinate cards (the third card in each set of input data of Table 3), Sec. 3.1 of the data input guide was used to generate nodal point coordinates along the x-axis (Fig 47). Then, on the fourth card, Sec. 3.6 was used to generate all the remaining nodal point coordinates. With these mesh generation options the surface coordinates, ξ_1 and ξ_2 were set to coincide with the x and y-axes respectively (Fig 47). Therefore the surface coordinate direction cosine cards, Sec. 2.4, were not necessary. Again on the sixth card, only one data card was required to generate all 16 elements' nodal point number by following the description of Sec. 2.5 for a regular mesh.

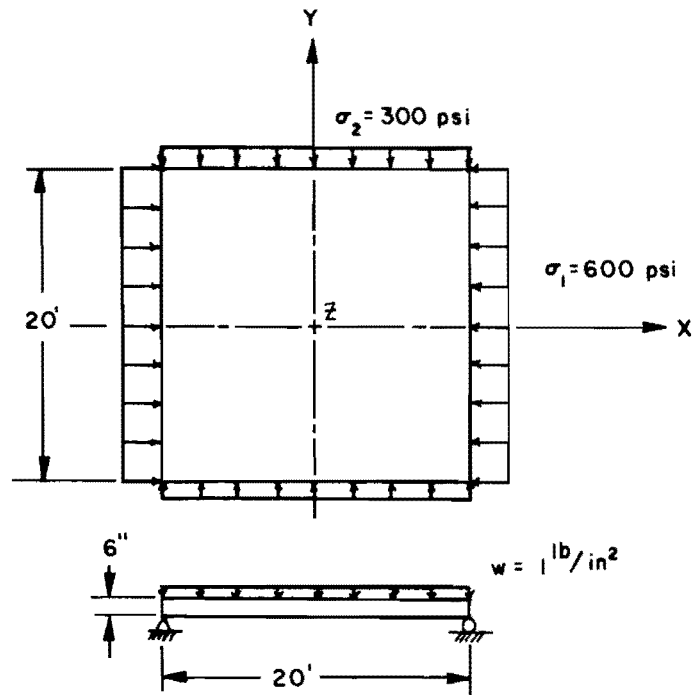


Fig 46. Simply supported square plate.

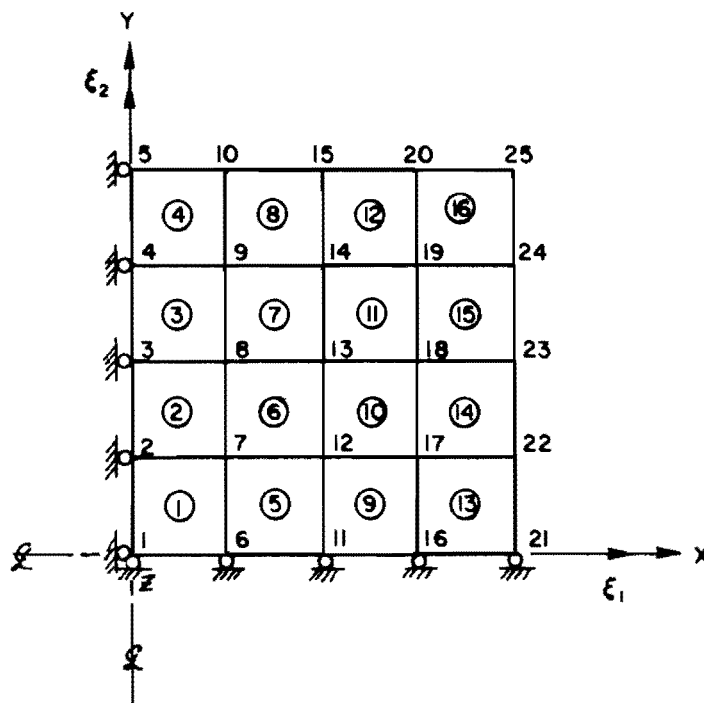


Fig 47. Mesh layout (one-fourth of the plate).

With regard to the boundary condition cards, Sec. 2.10, care must be exercised in specifying the correct boundary conditions since only one-fourth of the plate was used in the analysis. Referring to Fig 47 at nodal points 1, 2, 3, 4 and 5, because of the symmetry, the displacement in the x-direction, D1, and the rotation about ξ_2 , D5, are zero. Also at nodal points 1, 6, 11, 16 and 21 the displacement in the y-direction, D2, and the rotation about ξ_1 , D4, are zero. For nodal points 5, 10, 15, 20, 21, 22, 23, 24 and 25 which were on the top of the support the vertical displacement, D3, is zero. In addition the rotation about ξ_2 , D5, is zero at points 5, 10, 15, 20 and 25 while the rotations about ξ_1 , D4, is zero at points 21, 22, 23, 24 and 25. Lines 12 to 19 in each set of input data of Table 3 contain all these specified boundary conditions.

The uniform pressure along the boundary was input as concentrated forces applied at the nodal points as described in Secs. 2.13 and 2.14. For example, at nodal points 10, 15 and 20 the concentrated force in the y-direction, P_2 , was $-300 \times 6 \times 30 = -54000$ lb and was input as shown on line number 24 in the tables. Also at points 5 and 25 a concentrated force of -27,000 lb in the y-direction were used. Concentrated forces in the x-direction at points 21, 22, 23, 24 and 25 were computed and input in the same manner.

The output obtained by executing the first set of input data of Table 3 on the CDC 6600 at the University of Texas at Austin is contained in Tables 4 through 10. With regard to the second set of input data of Table 3, only the portion of the output relating to stresses is listed since the remaining output (except for ISIG) would be identical to the first set of input data. This portion of output is contained in Tables 11 and 12. Each section of input data is generally echo printed for check purposes followed by a complete listing in tabular form. For example, in Table 4 three lines were used to echo print the input required to define the coordinates of the twenty-five nodal points while the complete listing of the twenty-five nodal point coordinates are printed in the lower portion of Table 4. All echo and complete listings are contained in Tables 4 through 6.

Nodal point displacements are listed in Table 7. At each node five displacements are given. They consist of three translations (D1, D2 and D3) and two rotations (D4 and D5). The three translations (D1, D2 and D3) are

in the global (x, y and z) directions since IFLAG = 0 was used on the control card of Sec. 2.2 in the data input guide. The two rotations (D4 and D5) are about the surface coordinates (ξ_1 and ξ_2) respectively as shown in Fig 47. For example at node 1 the only nonzero displacement was the vertical translation (D3) which has a magnitude of -0.177251 inch.

Nodal forces including reactions are also listed in Table 7. Translational forces (R1, R2 and R3) are in the direction of D1, D2 and D3 respectively. The nodal point moments (R4 and R5) share the same sign convention as D4 and D5. For example at node 25, the vertical reaction, R3, is -3652.0 lbs. The minus sign indicates that this reaction is in the opposite direction of the global z-axis.

As mentioned previously, there are two options available to the user in program SHELL for printing out the stresses, i.e.,

- a) stress resultants (force and moment per unit length of mid-surface)
- b) stresses and principal stresses (force per unit area)

A) Stress Resultants

At a typical point the output stress resultants are as shown in Fig 48 and they are in the form of the two in-plane axial forces (N1,N2), the in-plane shearing force (S), the two bending moment components (M1,M2) and the twisting moment (M12). Stress resultants are referenced to element coordinates (η_1 , η_2 and η_3). Positive directions are shown in Fig 48.

B) Stresses and Principal Stresses

At a typical point the output stresses are as shown in Fig 49 and are in the form of the two in-plane normal stresses (σ_1 , σ_2), and an in-plane shearing stress (τ). These stresses are also referenced to the element coordinates (η_1 , η_2 and η_3) with positive directions shown in Fig 49. These stresses are printed at the top (upper surface in the η_3 direction) and bottom fiber of the element as shown in Tables 11 and 12. Principal stresses are computed only at the central interior node of the quadrilateral element and printed as shown in

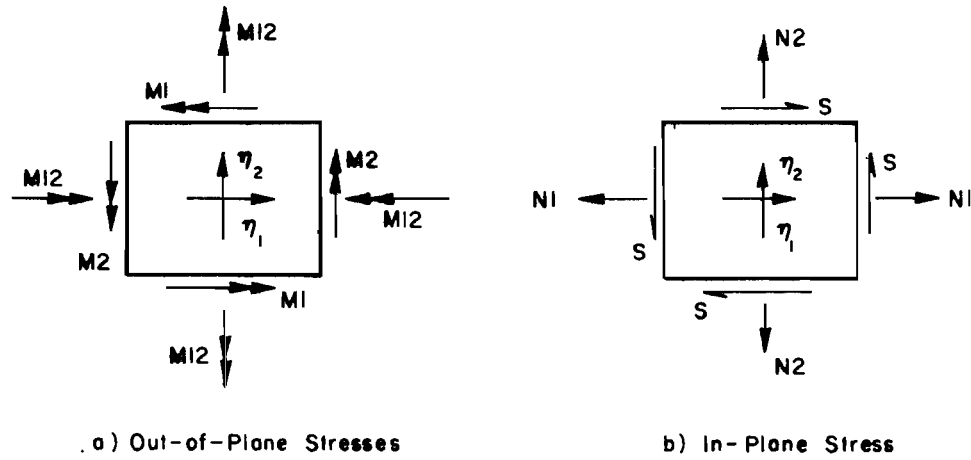


Fig 48. Positive direction of stress resultants.

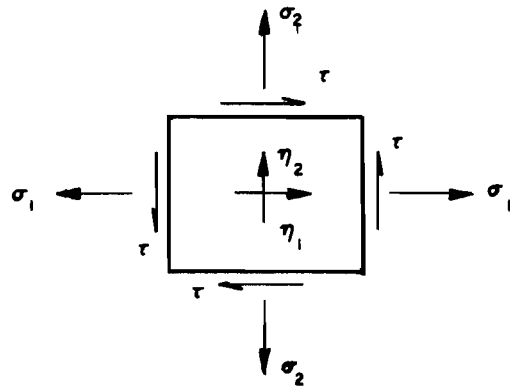


Fig 49. Positive direction of stresses.

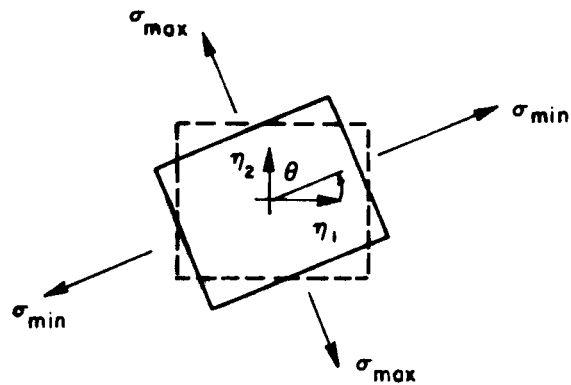


Fig 50. Positive direction of principal stresses.

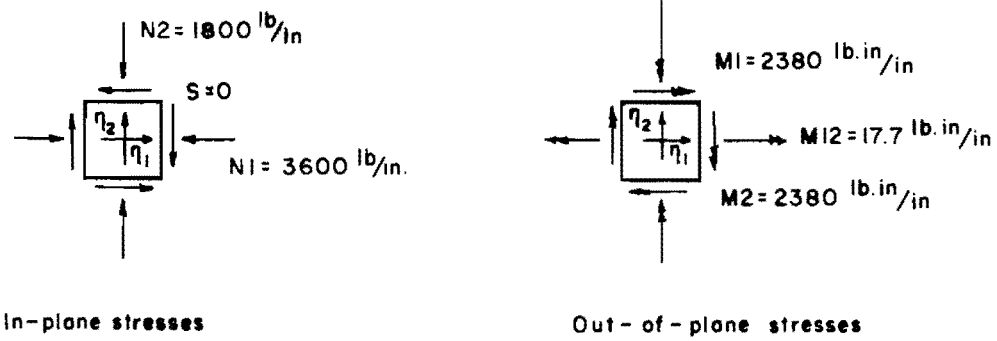
Table 12. This orientation is given in terms of the angle between the minimum stress and η_1 -direction, as shown in Fig 50.

Stress resultants in the computer output (Tables 6, 7 and 8) using the first set of input data from Table 3 are forces and moments per unit length at the locations defined by the nodal point numbers since ISIG = 0 was used on the control card (Sec. 2.2 in the data input guide). Two sets of stress resultants are given. The first set (Table 5 and 6 represent stress resultants printed element by element. Node 0 defines the location at the centroid of the element. The second set (Table 9) represents the average value of nodal stress resultants. It should be noted that they are referenced to surface coordinates (ξ_1 and ξ_2). For example at nodal point 1, the magnitude of the average stress resultants and their directions are shown in Fig 51a.

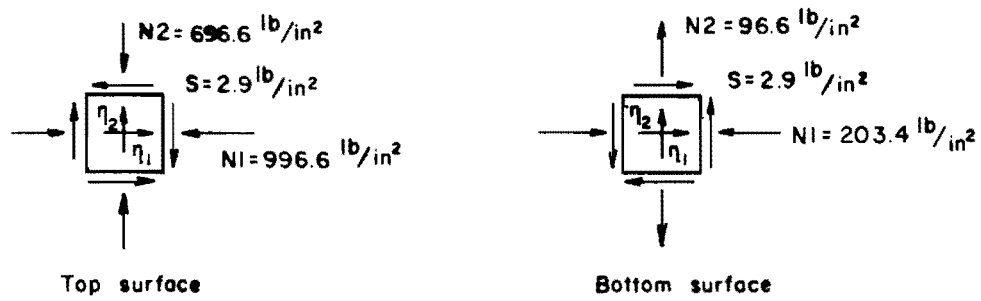
With regard to the second set of input data of Table 3 (ISIG = 1), output stresses have the unit of forces per unit area. Two sets of stresses are given. The first set (Tables 11 and 12) represent stresses acting at the top and bottom surfaces printed element by element. Stresses at nodal point 1 are shown on Fig 51b. The second set (lower portion of Table 12) represent principal stresses computed at the centroid of each element at both the top and bottom surfaces. Principal stresses and their directions at the bottom surface of element 1 are shown on Fig 51c.

To demonstrate the relationships between stress resultants, stresses and principal stresses the following calculations are presented. At the centroid of element 1, the stress resultants are

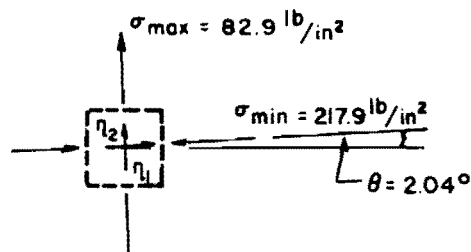
$$\begin{aligned}
 M2 &= -2295 && \text{lb in/in} \\
 M1 &= -2295 && \text{lb in/in} \\
 M12 &= 64.2 && \text{lb in/in} \\
 N1 &= -3600 && \text{lb/in} \\
 N2 &= -1800 && \text{lb/in} \\
 S &= 0 && \text{lb/in}
 \end{aligned}$$



a) Stress Resultants at Node 1.



b) Stresses at Node 1.



c) Principal stresses at bottom surface at centroid of element 1.

Fig 51. Stresses and principal stresses.

For a cross section of unit width and a thickness of 6 inches, the section properties were as follows

$$\text{Cross-sectional area (A)} = 1.0 \times 6.0 = 6 \text{ in}^2$$

$$\text{Section Modulus (S)} = \frac{1}{6} \times 1.0 \times (6.0)^2 = 6 \text{ in}^3$$

Therefore,

$$\text{Due to } M2, M1, \sigma_m = \frac{M2}{S} = \mp \frac{2295}{6} = \mp 382.5 \text{ lb/in}^2$$

$$\text{Due to } N1, \sigma_{n1} = \frac{N1}{A} = - \frac{3600}{6} = - 600 \text{ lb/in}^2$$

$$\text{Due to } N2, \sigma_{n2} = \frac{N2}{A} = - \frac{1800}{6} = - 300 \text{ lb/in}^2$$

$$\text{Due to } M12, \tau_m = \frac{M12}{S} = \frac{64.2}{6} = \pm 10.7 \text{ lb/in}^2$$

Finally, by combining both the out-of-plane and in-plane stresses, we have

$$\text{top surface } N1 = \sigma_m + \sigma_{n1} = -382.5 + (-600) = -982.5 \text{ lb/in}^2$$

$$N2 = \sigma_m + \sigma_{n2} = -382.5 + (-300) = -682.5 \text{ lb/in}^2$$

$$S = \tau_m + \tau_n = 10.7 + (0) = 10.7 \text{ lb/in}^2$$

$$\text{bottom surface } N1 = \sigma_m + \sigma_{n1} = 382.5 + (-600) = -217.5 \text{ lb/in}^2$$

$$N2 = \sigma_m + \sigma_{n2} = 382.5 + (-300) = 82.5 \text{ lb/in}^2$$

$$S = \tau_m + \tau_n = -10.7 + (0) = -10.7 \text{ lb/in}^2$$

These values should be compared with element 1 (node 0) of Table 12.

Now the principal stresses were calculated by using

$$\sigma_p = \frac{\sigma_x + \sigma_y}{2} \pm \sqrt{\left(\frac{\sigma_x - \sigma_y}{2}\right)^2 + \tau^2}$$

$$\tan 2\theta = \frac{2\tau}{\sigma_x - \sigma_y}$$

$$\tau_{\max} = \sqrt{\left(\frac{\sigma_x - \sigma_y}{2}\right)^2 + \tau^2}$$

For example, at the bottom surface of the mid-node inside element 1,

$$\begin{aligned}\sigma_p &= \frac{-217.5 + 82.5}{2} \pm \sqrt{\left(\frac{-217.5 - 82.5}{2}\right)^2 + (-10.7)^2} \\ &= -67.5 \pm 150.4\end{aligned}$$

Therefore,

$$\begin{aligned}\sigma_{\max} &= 82.9 \quad 1b/in^2 \\ \sigma_{\min} &= -217.9 \quad 1b/in^2 \\ \tau_{\max} &= 150.4 \quad 1b/in^2 \\ 2\theta &= \tan^{-1} \left(\frac{-2 \times 10.7}{-300} \right) \\ &= \tan^{-1} 0.0713 \\ &= 4.08^\circ \\ \theta &= 2.04^\circ\end{aligned}$$

The magnitudes and directions of these stresses are shown on Fig 51c.

TABLE 3

SAMPLE PROBLEM * SQUARE PLATF * (LR=IN) CODED BY T.THEPCHATRI 7/18/74

16	25	1A	7	5	0	1	0	0	1	0	2	0
1	21	5	1	0.	0.	0.	120.	0.	0.			
2	22	5	-4	0.	30.	0.						

1	1	6	7	2	4	4						
1		4000000.	1.		0.15	0.15						
1	1	1A	1	0	6.	6.	6.	6.				
1	1A	1		0.	-1.	-1.	-1.	-1.				
1	25	1		0.								

1	11011											
2	10001	4	1									
5	10101											
6	01010	16	5									
10	00101	20	5									
21	01110											
22	00110	24	1									
25	00111											

1	9											
5												
10	20	5										
25												
22	24	1										
21												

SAMPLE PROBLEM * SQUARE PLATF * (LR=IN) CODED BY T.THEPCHATRI 7/18/74

16	25	1A	7	5	0	1	0	0	1	0	2	1
1	21	5	1	0.	0.	0.	120.	0.	0.			
2	22	5	-4	0.	30.	0.						

1	1	6	7	2	4	4						
1		4000000.	1.		0.15	0.15						
1	1	1A	1	0	6.	6.	6.	6.				
1	1A	1		0.	-1.	-1.	-1.	-1.				
1	25	1		0.								

1	11011											
2	10001	4	1									
5	10101											
6	01010	16	5									
10	00101	20	5									
21	01110											
22	00110	24	1									
25	00111											

1	9											
5												
10	20	5										
25												
22	24	1										
21												

TABLE 4

SAMPLE PROBLEM * SQUARE PLATF * (LR=IN) CODED BY T.THEPCHATRI 7/18/74

NUMEL = 16
 NUPTS = 25
 NURPTS = 16
 IBANDP = 7
 NDFRE = 5
 IFLAG = 0
 NUMAT = 1
 ISHEAR = 0
 NRED = 0
 IRECT = 1
 LPROR = 0
 IGEN = 2
 ISIG = 0

DUPLICATION OF INPUT NODAL COORDINATE CARDS.

1	21	5	1	0.	0.	0.						
2	22	5	-4	0.	1.20000E+02	0.	0.	0.				

DUPLICATION OF INPUT SURFACE DIRECTION COSTNE CARDS.

-0	-0	-0	-0.	0.00000	-0.00000	-0.00000	-0.00000	-0.00000	-0.00000	-0.00000	-0.00000	-0.00000
----	----	----	-----	---------	----------	----------	----------	----------	----------	----------	----------	----------

DUPLICATION OF ELEMENT NODAL POINT NUMBER CARDS.

1	1	6	7	2	4	4	-0					
---	---	---	---	---	---	---	----	--	--	--	--	--

DUPLICATION OF ELEMENT MATERIAL TABLE.

1	4.00000E+06	1.00000E+00	1.50000E-01	1.50000E-01	-0.	-0.						
---	-------------	-------------	-------------	-------------	-----	-----	--	--	--	--	--	--

DUPLICATION OF ELEMENT PROPERTY CARDS.

1	1	16	1	0	6.00000E+00	6.00000E+00	6.00000E+00	6.00000E+00	6.00000E+00	6.00000E+00	6.00000E+00	6.00000E+00
---	---	----	---	---	-------------	-------------	-------------	-------------	-------------	-------------	-------------	-------------

ELEMENT DISTRIBUTED LOADS.

1	16	1	0.	-1.0000E+00	-1.0000E+00	-1.0000E+00	-1.0000E+00	-1.0000E+00	-1.0000E+00	-1.0000E+00	-1.0000E+00	-1.0000E+00
---	----	---	----	-------------	-------------	-------------	-------------	-------------	-------------	-------------	-------------	-------------

DUPLICATION OF INPUT NODAL TEMP. DIFFERENCES.

1	25	1	0.									
---	----	---	----	--	--	--	--	--	--	--	--	--

NODAL COORDINATES AND TEMPERATURE DIFFERENCES.

PT.	X	Y	Z	TEMP.
1	0.	0.	0.	0.
2	0.	3.00000E+01	0.	0.
3	0.	6.00000E+01	0.	0.
4	0.	9.00000E+01	0.	0.
5	0.	1.20000E+02	0.	0.
6	3.00000E+01	0.	0.	0.
7	6.00000E+01	3.00000E+01	0.	0.
8	9.00000E+01	6.00000E+01	0.	0.
9	3.00000E+01	9.00000E+01	0.	0.
10	6.00000E+01	1.20000E+02	0.	0.
11	6.00000E+01	0.	0.	0.
12	6.00000E+01	3.00000E+01	0.	0.
13	6.00000E+01	6.00000E+01	0.	0.
14	6.00000E+01	9.00000E+01	0.	0.
15	6.00000E+01	1.20000E+02	0.	0.
16	9.00000E+01	0.	0.	0.
17	9.00000E+01	3.00000E+01	0.	0.
18	9.00000E+01	6.00000E+01	0.	0.
19	9.00000E+01	9.00000E+01	0.	0.
20	9.00000E+01	1.20000E+02	0.	0.
21	1.20000E+02	0.	0.	0.
22	1.20000E+02	3.00000E+01	0.	0.
23	1.20000E+02	6.00000E+01	0.	0.
24	1.20000E+02	9.00000E+01	0.	0.
25	1.20000E+02	1.20000E+02	0.	0.

TABLE 5

SURFACE DIRECTIONS COSINES.

PT.	F1X	F1Y	F1Z	F2X	F2Y	F2Z
1	1.00000	0.00000	0.00000	-0.00000	1.00000	0.00000
2	1.00000	0.00000	0.00000	-0.00000	1.00000	0.00000
3	1.00000	0.00000	0.00000	-0.00000	1.00000	0.00000
4	1.00000	0.00000	0.00000	-0.00000	1.00000	0.00000
5	1.00000	0.00000	0.00000	-0.00000	1.00000	0.00000
6	1.00000	0.00000	0.00000	-0.00000	1.00000	0.00000
7	1.00000	0.00000	0.00000	-0.00000	1.00000	0.00000
8	1.00000	0.00000	0.00000	-0.00000	1.00000	0.00000
9	1.00000	0.00000	0.00000	-0.00000	1.00000	0.00000
10	1.00000	0.00000	0.00000	-0.00000	1.00000	0.00000
11	1.00000	0.00000	0.00000	-0.00000	1.00000	0.00000
12	1.00000	0.00000	0.00000	-0.00000	1.00000	0.00000
13	1.00000	0.00000	0.00000	-0.00000	1.00000	0.00000
14	1.00000	0.00000	0.00000	-0.00000	1.00000	0.00000
15	1.00000	0.00000	0.00000	-0.00000	1.00000	0.00000
16	1.00000	0.00000	0.00000	-0.00000	1.00000	0.00000
17	1.00000	0.00000	0.00000	-0.00000	1.00000	0.00000
18	1.00000	0.00000	0.00000	-0.00000	1.00000	0.00000
19	1.00000	0.00000	0.00000	-0.00000	1.00000	0.00000
20	1.00000	0.00000	0.00000	-0.00000	1.00000	0.00000
21	1.00000	0.00000	0.00000	-0.00000	1.00000	0.00000
22	1.00000	0.00000	0.00000	-0.00000	1.00000	0.00000
23	1.00000	0.00000	0.00000	-0.00000	1.00000	0.00000
24	1.00000	0.00000	0.00000	-0.00000	1.00000	0.00000
25	1.00000	0.00000	0.00000	-0.00000	1.00000	0.00000

EL. NO.	EL. NO.	EL. NO.	MATL.	TYPE=T	EL.	TYPE=F	EL.	THICKNESS	ANG.	THER.	COEF.
EL.	I	J	K	L	T	TJ	TK	TL	ANG	ALPHA	
1	1	6	7	2	1	0	6.000E+00	6.000E+00	6.000E+00	6.000E+00	-0.0-0.0
2	2	7	8	3	1	0	6.000E+00	6.000E+00	6.000E+00	6.000E+00	-0.0-0.0
3	3	8	9	4	1	0	6.000E+00	6.000E+00	6.000E+00	6.000E+00	-0.0-0.0
4	4	9	10	5	1	0	6.000E+00	6.000E+00	6.000E+00	6.000E+00	-0.0-0.0
5	5	10	11	6	1	0	6.000E+00	6.000E+00	6.000E+00	6.000E+00	-0.0-0.0
6	6	11	12	7	1	0	6.000E+00	6.000E+00	6.000E+00	6.000E+00	-0.0-0.0
7	7	12	13	8	1	0	6.000E+00	6.000E+00	6.000E+00	6.000E+00	-0.0-0.0
8	8	13	14	9	1	0	6.000E+00	6.000E+00	6.000E+00	6.000E+00	-0.0-0.0
9	9	14	15	10	1	0	6.000E+00	6.000E+00	6.000E+00	6.000E+00	-0.0-0.0
10	10	15	16	11	1	0	6.000E+00	6.000E+00	6.000E+00	6.000E+00	-0.0-0.0
11	11	16	17	12	1	0	6.000E+00	6.000E+00	6.000E+00	6.000E+00	-0.0-0.0
12	12	17	18	13	1	0	6.000E+00	6.000E+00	6.000E+00	6.000E+00	-0.0-0.0
13	13	18	19	14	1	0	6.000E+00	6.000E+00	6.000E+00	6.000E+00	-0.0-0.0
14	14	19	20	15	1	0	6.000E+00	6.000E+00	6.000E+00	6.000E+00	-0.0-0.0
15	15	20	21	16	1	0	6.000E+00	6.000E+00	6.000E+00	6.000E+00	-0.0-0.0
16	16	21	22	17	1	0	6.000E+00	6.000E+00	6.000E+00	6.000E+00	-0.0-0.0
17	17	22	23	18	1	0	6.000E+00	6.000E+00	6.000E+00	6.000E+00	-0.0-0.0
18	18	23	24	19	1	0	6.000E+00	6.000E+00	6.000E+00	6.000E+00	-0.0-0.0
19	19	24	25	20	1	0	6.000E+00	6.000E+00	6.000E+00	6.000E+00	-0.0-0.0

DUPLICATION OF INPUT BOUNDARY CONDITION CARDS.
 D1,D2 AND D3 ARE TRANSLATIONS IN BASE COORDINATES.
 D4 AND D5 ARE ROTATIONS IN SURFACE COORDINATES.
 PT. 12345 LIM MOD D1 D2 D3 D4 D5
 1 11011 -0 -0 -0.0 -0.0 -0.0 -0.0 -0.0
 2 10001 4 1 -0.0 -0.0 -0.0 -0.0 -0.0
 5 10101 -0 -0 -0.0 -0.0 -0.0 -0.0 -0.0
 6 01010 16 5 -0.0 -0.0 -0.0 -0.0 -0.0
 10 00101 20 5 -0.0 -0.0 -0.0 -0.0 -0.0
 21 01110 -0 -0 -0.0 -0.0 -0.0 -0.0 -0.0
 22 00110 24 1 -0.0 -0.0 -0.0 -0.0 -0.0
 25 00111 -0 -0 -0.0 -0.0 -0.0 -0.0 -0.0

TABLE 6

BOUNDARY CONDITIONS OF POINTS HAVING SPECIFIED DISPLS.

PT.	1	2	3	4	5	D1	D2	D3	D4	D5
1	1	1	0	1	1	-0.	-0.	-0.	-0.	-0.
2	1	0	0	0	1	-0.	-0.	-0.	-0.	-0.
3	1	0	0	0	1	-0.	-0.	-0.	-0.	-0.
4	1	0	0	0	1	-0.	-0.	-0.	-0.	-0.
5	1	0	0	0	1	-0.	-0.	-0.	-0.	-0.
6	0	1	0	1	0	-0.	-0.	-0.	-0.	-0.
11	0	1	0	1	0	-0.	-0.	-0.	-0.	-0.
16	0	1	0	1	0	-0.	-0.	-0.	-0.	-0.
18	0	0	1	0	1	-0.	-0.	-0.	-0.	-0.
15	0	0	1	0	1	-0.	-0.	-0.	-0.	-0.
20	0	0	1	0	1	-0.	-0.	-0.	-0.	-0.
21	0	1	1	1	0	-0.	-0.	-0.	-0.	-0.
22	0	0	1	1	0	-0.	-0.	-0.	-0.	-0.
23	0	0	1	1	0	-0.	-0.	-0.	-0.	-0.
24	0	0	1	1	0	-0.	-0.	-0.	-0.	-0.
25	0	0	1	1	0	-0.	-0.	-0.	-0.	-0.

NUMBER OF INDEPENDENT LOAD CASES = 1
 NUMBER OF LOADED NODES FOR LOAD CASE 1 = 9
 NUMBER OF LOADED NODES FOR LOAD CASE 2 = -0
 NUMBER OF LOADED NODES FOR LOAD CASE 3 = -0
 UNIFORM VERTICAL LOAD = -0.
 -0 -0

DUPLICATION OF INPUT NODAL FORCES, LOAD CASE NO. 1

PT.	LIM	MOD	P1	P2	P3	P4	P5
5	-0	-0	-0.	-2.7000E+04	-0.	-0.	-0.
10	20	5	-0.	-5.4000E+04	-0.	-0.	-0.
25	-0	-0	-0.	-5.4000E+04	-2.7000E+04	-0.	-0.
22	24	1	-1.0000E+05	-0.	-0.	-0.	-0.
21	-0	-0	-0.	-5.4000E+04	-0.	-0.	-0.

TOTAL APPLIED NODAL POINT FORCES, LOAD CASE 1

PT.	LIM	MOD	P1	P2	P3	P4	P5
1	0.	0.	0.	0.	-2.7000E+02	0.	0.
2	0.	0.	0.	0.	-4.5000E+02	0.	0.
3	0.	0.	0.	0.	-4.5000E+02	0.	0.
4	0.	0.	0.	0.	-4.5000E+02	0.	0.
5	0.	0.	0.	-2.7000E+04	0.	0.	0.
6	0.	0.	0.	0.	-4.5000E+02	0.	0.
7	0.	0.	0.	0.	-9.0000E+02	0.	0.
8	0.	0.	0.	0.	-9.0000E+02	0.	0.
9	0.	0.	0.	0.	-9.0000E+02	0.	0.
10	0.	0.	0.	-5.4000E+04	0.	0.	0.
11	0.	0.	0.	0.	-4.5000E+02	0.	0.
12	0.	0.	0.	0.	-9.0000E+02	0.	0.
13	0.	0.	0.	0.	-9.0000E+02	0.	0.
14	0.	0.	0.	0.	-9.0000E+02	0.	0.
15	0.	0.	0.	-5.4000E+04	0.	0.	0.
16	0.	0.	0.	0.	-4.5000E+02	0.	0.
17	0.	0.	0.	0.	-9.0000E+02	0.	0.
18	0.	0.	0.	0.	-9.0000E+02	0.	0.
19	0.	0.	0.	0.	-9.0000E+02	0.	0.
20	0.	0.	0.	-5.4000E+04	0.	0.	0.
21	-5.4000E+04	0.	0.	0.	0.	0.	0.
22	-1.0000E+05	0.	0.	0.	0.	0.	0.
23	-1.0000E+05	0.	0.	0.	0.	0.	0.
24	-1.0000E+05	0.	0.	0.	0.	0.	0.
25	-5.4000E+04	-2.7000E+04	0.	0.	0.	0.	0.

TABLE 7

DISPLACEMENTS FOR LOAD CASE 1 INITIAL SOLUTION

NODE	D1	D2	D3	D4	D5
1	0.	0.	-1.77251E-01	0.	0.
2	0.	-1.57500E-03	-1.64673E-01	8.40635E-04	0.
3	0.	-3.15000E-03	-1.27907E-01	1.61375E-03	0.
4	0.	-4.72500E-03	-7.04284E-02	2.21285E-03	0.
5	0.	-6.30000E-03	0.	2.45190E-03	0.
6	-4.16250E-03	0.	-1.64673E-01	0.	-8.40635E-04
7	-4.16250E-03	-1.57500E-03	-1.53016E-01	7.79363E-04	-7.79363E-04
8	-4.16250E-03	-3.15000E-03	-1.18914E-01	1.49793E-03	-6.01723E-04
9	-4.16250E-03	-4.72500E-03	-6.55214E-02	2.05785E-03	-3.28642E-04
10	-4.16250E-03	-6.30000E-03	0.	2.28238E-03	0.
11	-8.32500E-03	0.	-1.27907E-01	0.	-1.61375E-03
12	-8.32500E-03	-1.57500E-03	-1.18914E-01	6.01723E-04	-1.49793E-03
13	-8.32500E-03	-3.15000E-03	-9.25516E-02	1.16040E-03	-1.16040E-03
14	-8.32500E-03	-4.72500E-03	-5.11018E-02	1.60300E-03	-6.36312E-04
15	-8.32500E-03	-6.30000E-03	0.	1.78324E-03	0.
16	-1.24875E-02	0.	-7.04284E-02	0.	-2.21285E-03
17	-1.24875E-02	-1.57500E-03	-6.55214E-02	2.28642E-04	-2.05785E-03
18	-1.24875E-02	-3.15000E-03	-5.11018E-02	4.36312E-04	-1.60300E-03
19	-1.24875E-02	-4.72500E-03	-2.83078E-02	8.85638E-04	-8.85638E-04
20	-1.24875E-02	-6.30000E-03	0.	9.89420E-04	0.
21	-1.66500E-02	0.	0.	0.	-2.45190E-03
22	-1.66500E-02	-1.57500E-03	0.	0.	-2.28238E-03
23	-1.66500E-02	-3.15000E-03	0.	0.	-1.78324E-03
24	-1.66500E-02	-4.72500E-03	0.	0.	-9.89420E-04
25	-1.66500E-02	-6.30000E-03	0.	0.	0.

NODAL FORCES INCLUDING REACTIONS LOAD CASE 1

PT.	R1	R2	R3	R4	R5
1	5.40000E+04	2.70000E+04	-2.25000E+02	-3.69740E+04	3.69740E+04
2	1.08000E+05	6.79310E+04	-4.50000E+02	1.57290E+04	6.89570E+04
3	1.08000E+05	1.32000E+04	-4.50000E+02	5.75240E+04	5.42530E+04
4	1.08000E+05	2.94810E+04	-4.50000E+02	2.99130E+04	3.08110E+04
5	5.40000E+04	-2.70000E+04	1.32720E+03	-5.94310E+04	-4.23090E+03
6	2.81960E+09	5.40000E+04	-4.50000E+02	-6.89570E+04	3.28870E+08
7	4.43450E+09	8.30300E+10	-9.00000E+02	1.09050E+08	4.28180E+08
8	4.17500E+09	1.81870E+09	-9.00000E+02	2.55020E+10	4.40330E+08
9	2.35620E+09	4.05060E+09	-9.00000E+02	-3.11430E+09	-1.17990E+08
10	1.14870E+09	-5.40000E+04	2.53700E+03	2.93730E+09	1.25550E+03
11	5.20340E+09	5.40000E+04	-4.50000E+02	-5.42530E+04	-7.64880E+08
12	7.48290E+09	5.60700E+10	-9.00000E+02	2.86260E+09	8.40920E+08
13	9.69690E+09	1.77880E+09	-9.00000E+02	1.91400E+08	5.73730E+08
14	7.10230E+09	4.92560E+09	-9.00000E+02	1.08150E+08	-2.63520E+08
15	4.67130E+09	-5.40000E+04	2.14630E+03	1.18430E+09	2.79560E+03
16	5.52250E+09	5.40000E+04	-4.50000E+02	-3.08110E+04	-8.56730E+09
17	7.81130E+09	1.06980E+09	-9.00000E+02	6.70830E+09	-1.04020E+08
18	7.68420E+09	2.34370E+09	-9.00000E+02	-2.71920E+10	-3.34760E+08
19	8.92500E+09	3.10830E+09	-9.00000E+02	4.07640E+09	-1.01420E+08
20	8.28890E+10	-5.40000E+04	1.32800E+03	1.99790E+09	5.40840E+03
21	-5.40000E+04	2.70000E+04	1.32720E+03	4.23090E+03	3.12450E+09
22	-1.08000E+05	-3.77520E+10	2.53700E+03	-2.5550E+03	1.40050E+09
23	-1.08000E+05	4.83590E+10	2.14630E+03	-2.79560E+03	-1.05970E+09
24	-1.08000E+05	1.10170E+09	1.32800E+03	-5.40840E+03	-1.45710E+09
25	5.40000E+04	-2.70000E+04	-3.65200E+03	-3.56830E+03	3.56830E+03

TABLE 8

ELEMENT STRESS RESULTS FOR LOAD CASE 1

ELEMENT NO.	M2	M1	M12	N1	N2	S	NODF
1	-2.380E+03	-2.380E+03	-1.774E+01	-3.600E+03	-1.800E+03	-2.263E-12	1
2	-2.294E+03	-2.267E+03	5.911E+01	-3.600E+03	-1.800E+03	4.073E-11	6
3	-2.183E+03	-2.183E+03	1.544E+02	-3.600E+03	-1.800E+03	-3.620E-11	7
4	-2.267E+03	-2.294E+03	5.931E+01	-3.600E+03	-1.800E+03	-9.051E-12	2
5	-2.295E+03	-2.295E+03	6.422E+01	-3.600E+03	-1.800E+03	4.356E-11	0
6	-2.164E+03	-2.272E+03	2.722E+01	-3.600E+03	-1.800E+03	-9.051E-12	2
7	-2.091E+03	-2.170E+03	2.659E+02	-3.600E+03	-1.800E+03	-7.755E-25	7
8	-1.765E+03	-1.890E+03	3.522E+02	-3.600E+03	-1.800E+03	-3.620E-11	8
9	-1.835E+03	-1.986E+03	9.502E+01	-3.600E+03	-1.800E+03	-9.051E-12	3
10	-1.978E+03	-2.094E+03	1.859E+02	-3.600E+03	-1.800E+03	-2.036E-11	0
11	-1.630E+03	-1.913E+03	7.422E+01	-3.600E+03	-1.800E+03	-9.051E-11	3
12	-1.583E+03	-1.833E+03	4.377E+02	-3.600E+03	-1.800E+03	3.620E-11	8
13	-1.068E+03	-1.271E+03	5.076E+02	-3.600E+03	-1.800E+03	-1.267E-10	9
14	-1.178E+03	-1.334E+03	1.205E+02	-3.600E+03	-1.800E+03	-5.430E-11	4
15	-1.364E+03	-1.603E+03	2.851E+02	-3.600E+03	-1.800E+03	5.430E-11	0
16	-8.113E+02	-1.148E+03	1.207E+02	-3.600E+03	-1.800E+03	-8.146E-11	4
17	-7.983E+02	-1.109E+03	5.402E+02	-3.600E+03	-1.800E+03	7.241E-11	9
18	-1.499E+02	-1.120E+02	5.701E+02	-3.600E+03	-1.800E+03	-7.755E-25	10
19	-1.707E+02	-1.250E+02	1.371E+02	-3.600E+03	-1.800E+03	-9.051E-12	5
20	-4.972E+02	-6.380E+02	3.425E+02	-3.600E+03	-1.800E+03	3.168E-11	0
21	-2.272E+03	-2.164E+03	2.722E+01	-3.600E+03	-1.800E+03	5.204E-11	6
22	-1.986E+03	-1.835E+03	9.502E+01	-3.600E+03	-1.800E+03	1.041E-10	11
23	-1.890E+03	-1.765E+03	2.522E+02	-3.600E+03	-1.800E+03	-1.539E-10	12
24	-2.170E+03	-2.091E+03	2.659E+02	-3.600E+03	-1.800E+03	-8.146E-11	7
25	-2.094E+03	-1.978E+03	1.859E+02	-3.600E+03	-1.800E+03	1.188E-10	0
26	-2.068E+03	-2.068E+03	3.182E+02	-3.600E+03	-1.800E+03	9.051E-11	7
27	-1.820E+03	-1.767E+03	5.329E+02	-3.600E+03	-1.800E+03	5.430E-11	12
28	-1.533E+03	-1.533E+03	7.662E+02	-3.600E+03	-1.800E+03	-5.430E-11	13
29	-1.767E+03	-1.820E+03	5.329E+02	-3.600E+03	-1.800E+03	-3.620E-11	8
30	-1.812E+03	-1.812E+03	5.402E+02	-3.600E+03	-1.800E+03	-9.051E-11	0
31	-1.559E+03	-1.749E+03	5.791E+02	-3.600E+03	-1.800E+03	-3.620E-11	8
32	-1.395E+03	-1.512E+03	9.144E+02	-3.600E+03	-1.800E+03	-3.102E-24	13
33	-9.265E+02	-1.041E+03	1.089E+03	-3.600E+03	-1.800E+03	-2.172E-10	14
34	-1.087E+03	-1.234E+03	7.350E+02	-3.600E+03	-1.800E+03	-1.087E-10	9
35	-1.256E+03	-1.399E+03	8.337E+02	-3.600E+03	-1.800E+03	3.620E-11	0
36	-7.712E+02	-1.058E+03	7.725E+02	-3.600E+03	-1.800E+03	7.241E-11	9
37	-7.208E+02	-9.397E+02	1.167E+03	-3.600E+03	-1.800E+03	1.810E-10	14
38	-1.134E+02	-7.464E+01	1.239E+03	-3.600E+03	-1.800E+03	3.620E-11	15
39	-1.178E+02	-1.169E+02	8.259E+02	-3.600E+03	-1.800E+03	-7.241E-11	10
40	-4.606E+02	-5.619E+02	1.087E+03	-3.600E+03	-1.800E+03	1.177E-10	0
41	-1.913E+03	-1.630E+03	7.422E+01	-3.600E+03	-1.800E+03	1.946E-10	11
42	-1.334E+03	-1.117E+03	1.205E+02	-3.600E+03	-1.800E+03	2.172E-10	14
43	-1.271E+03	-1.068E+03	5.076E+02	-3.600E+03	-1.800E+03	-1.810E-11	17
44	-1.833E+03	-1.583E+03	4.377E+02	-3.600E+03	-1.800E+03	-2.082E-10	12
45	-1.603E+03	-1.364E+03	2.851E+02	-3.600E+03	-1.800E+03	1.103E-10	0
46	-1.749E+03	-1.559E+03	5.791E+02	-3.600E+03	-1.800E+03	2.534E-10	12
47	-1.234E+03	-1.087E+03	7.350E+02	-3.600E+03	-1.800E+03	1.810E-10	17
48	-1.041E+03	-9.265E+02	1.089E+03	-3.600E+03	-1.800E+03	-1.810E-10	18

TABLE 9

-1.512E+03	-1.795E+03	9.144E+02	-3.600E+03	-1.800E+03	-1.448E-10	13
-1.399E+03	-1.256E+03	4.337E+02	-3.600E+03	-1.800E+03	-1.312E-10	0
ELEMENT NO. 11 NODE						
-1.332E+03	-1.332E+03	1.033E+03	-3.600E+03	-1.800E+03	1.810E-11	13
-9.685E+02	-9.633E+02	1.291E+03	-3.600E+03	-1.800E+03	1.086E-10	18
-6.286E+02	-6.284E+02	1.548E+03	-3.600E+03	-1.800E+03	-2.896E-10	19
-9.333E+02	-9.685E+02	1.291E+03	-3.600E+03	-1.800E+03	-2.534E-10	14
-9.852E+02	-9.852E+02	1.303E+03	-3.600E+03	-1.800E+03	-1.041E-10	0
ELEMENT NO. 12 NODE						
-6.584E+02	-8.257E+02	1.369E+03	-3.600E+03	-1.800E+03	2.172E-10	14
-5.285E+02	-6.372E+02	1.690E+03	-3.600E+03	-1.800E+03	3.620E-11	19
-4.905E+01	1.926E+00	1.805E+03	-3.600E+03	-1.800E+03	-2.172E-10	20
-1.725E+02	-9.129E+01	1.466E+03	-3.600E+03	-1.800E+03	-1.086E-10	15
-3.667E+02	-4.029E+02	1.592E+03	-3.600E+03	-1.800E+03	1.810E-10	0
ELEMENT NO. 13 NODE						
-1.148E+03	-8.113E+02	1.207E+02	-3.600E+03	-1.800E+03	1.086E-10	16
-1.250E+02	-1.707E+02	1.321E+02	-3.600E+03	-1.800E+03	2.941E-10	21
-1.120E+02	-1.499E+02	5.701E+02	-3.600E+03	-1.800E+03	-1.991E-10	22
-1.108E+03	-7.983E+02	5.407E+02	-3.600E+03	-1.800E+03	-2.715E-11	17
-6.380E+02	-4.972E+02	3.475E+02	-3.600E+03	-1.800E+03	2.727E-10	0
ELEMENT NO. 14 NODE						
-1.058E+03	-7.712E+02	7.725E+02	-3.600E+03	-1.800E+03	1.267E-10	17
-1.169E+02	-1.786E+02	8.259E+02	-3.600E+03	-1.800E+03	-5.430E-11	22
-7.464E+01	-1.134E+02	1.239E+03	-3.600E+03	-1.800E+03	-6.154E-10	23
-9.393E+02	-7.202E+02	1.167E+03	-3.600E+03	-1.800E+03	-5.430E-11	18
-5.619E+02	-4.606E+02	1.007E+03	-3.600E+03	-1.800E+03	-9.051E-12	0
ELEMENT NO. 15 NODE						
-8.267E+02	-6.584E+02	1.349E+03	-3.600E+03	-1.800E+03	-3.620E-11	18
-9.129E+01	-1.725E+02	1.466E+03	-3.600E+03	-1.800E+03	-9.051E-11	23
1.926E+00	-4.905E+01	1.805E+03	-3.600E+03	-1.800E+03	-5.068E-10	24
-6.372E+02	-5.285E+02	1.690E+03	-3.600E+03	-1.800E+03	-1.086E-10	19
-4.029E+02	-3.667E+02	1.592E+03	-3.600E+03	-1.800E+03	1.855E-10	0
ELEMENT NO. 16 NODE						
-4.297E+02	-4.297E+02	1.823E+03	-3.600E+03	-1.800E+03	1.810E-10	19
-5.091E+01	-1.269E+02	1.952E+03	-3.600E+03	-1.800E+03	2.172E-10	24
4.647E+01	4.647E+01	2.099E+03	-3.600E+03	-1.800E+03	-2.172E-10	25
-1.269E+02	-5.091E+01	1.952E+03	-3.600E+03	-1.800E+03	-1.086E-10	20
-1.549E+02	-1.549E+02	1.995E+03	-3.600E+03	-1.800E+03	-5.430E-11	0

TABLE 10

AVERAGED NODAL STRESS RESULTS, W.W.T., SURFACE COORDINATES, LOAD CASE 1

NODE	M2	M1	M12	N1	N2	S
1	-2.380E+03	-2.380E+03	-1.774E+01	-3.600E+03	-1.800E+03	-2.263E-12
2	-2.215E+03	-2.283E+03	4.376E+01	-3.600E+03	-1.800E+03	-9.051E-12
3	-1.733E+03	-1.949E+03	8.462E+01	-3.600E+03	-1.800E+03	-4.978E-11
4	-9.639E+02	-1.241E+03	1.206E+02	-3.600E+03	-1.800E+03	-6.788E-11
5	-1.707E+02	-1.250E+02	1.321E+02	-3.600E+03	-1.800E+03	-9.051E-12
6	-2.283E+03	-2.215E+03	4.376E+01	-3.600E+03	-1.800E+03	4.638E-11
7	-2.128E+03	-2.128E+03	2.512E+02	-3.600E+03	-1.800E+03	-6.788E-12
8	-1.668E+03	-1.823E+03	4.755E+02	-3.600E+03	-1.800E+03	-1.810E-11
9	-9.311E+02	-1.168E+03	6.376E+02	-3.600E+03	-1.800E+03	-2.263E-11
10	-1.643E+02	-1.145E+02	6.980E+02	-3.600E+03	-1.800E+03	-3.620E-11
11	-1.949E+03	-1.733E+03	8.462E+01	-3.600E+03	-1.800E+03	1.493E-10
12	-1.823E+03	-1.668E+03	4.755E+02	-3.600E+03	-1.800E+03	-1.358E-11
13	-1.443E+03	-1.443E+03	9.069E+02	-3.600E+03	-1.800E+03	-4.525E-11
14	-8.147E+02	-9.439E+02	1.229E+03	-3.600E+03	-1.800E+03	-1.810E-11
15	-1.429E+02	-8.296E+01	1.353E+03	-3.600E+03	-1.800E+03	-3.620E-11
16	-1.241E+03	-9.639E+02	1.206E+02	-3.600E+03	-1.800E+03	1.629E-10
17	-1.145E+03	-9.311E+02	6.376E+02	-3.600E+03	-1.800E+03	6.562E-11
18	-9.439E+02	-8.147E+02	1.229E+03	-3.600E+03	-1.800E+03	-4.073E-11
19	-5.560E+02	-5.560E+02	1.693E+03	-3.600E+03	-1.800E+03	-4.525E-11
20	-8.795E+01	-2.449E+01	1.879E+03	-3.600E+03	-1.800E+03	-1.629E-10
21	-1.250E+02	-1.707E+02	1.321E+02	-3.600E+03	-1.800E+03	2.941E-10
22	-1.145E+02	-1.643E+02	6.980E+02	-3.600E+03	-1.800E+03	-1.267E-10
23	-8.296E+01	-1.429E+02	1.353E+03	-3.600E+03	-1.800E+03	-3.530E-10
24	-2.449E+01	-8.795E+01	1.879E+03	-3.600E+03	-1.800E+03	-1.448E-10
25	4.647E+01	4.647E+01	2.099E+03	-3.600E+03	-1.800E+03	-2.172E-10
	7.8630					
	6.7940					
	4.5710					
	2.7270					

APPENDIX 2

A Listing of the IBM Version

This page replaces an intentionally blank page in the original.

-- CTR Library Digitization Team

DISCLAIMER

Although the authors have personally tested the program listed in Appendix 2, no warranty, expressed or implied, is made by the authors or any representatives of The University of Texas as to the accuracy, completeness, reliability, usability, or suitability of the computer program and its associated data and documentation. No responsibility is assumed by the authors or any representatives of The University of Texas for incorrect results or damages resulting from the use of the program.

This page replaces an intentionally blank page in the original.

-- CTR Library Digitization Team


```

CNUL PROGRAM MAIN ( INPUT,OUTPUT,TAPE1,TAPE2,TAPE3,TAPE4,TAPE8,TAPE9) LMB 6/29
C.....THIS VERSION OF THE SHELL PROGRAM HAS BEEN MODIFIED TO RUN ON THE LMB 7/10
C IBM 360 AT THE TEXAS HIGHWAY DEPARTMENT. ALL REAL VARIABLES ARE LMB 7/10
C DOUBLE LENGTH AND INTEGER VARIABLES STANDARD LENGTH. BOTH SEQUEN-LMB 7/10
C TIAL AND DIRECT ACCESS DATA SETS ARE UTILIZED. LMB 7/10
C.....THE LATEST REVISION DATE FOR THIS VERSION IS 8 AUG 1973 ...
IMPLICIT REAL*8 (A-H,O-Z) LMB 7/09
C DEFINE FILE 8(5,8000,L,NAV1), 9(5,800,L,NAV2) LMB JJP
C DEFINE FILE 8(50,8000,L,NAV1), 9(50,800,L,NAV2) LMB JJP
C.....DEFINE FILE 8( N2 ,M2,L,NAV1), 9(NBLOC,ML,L,NAV2)... LMB
C WHERE NBLOC = NUPTS/IBANDP ( ALWAYS ROUND UP )
C N2 = NBLOC*MBAND
C M2 = 8*MBAND
C ML = 8*MBAND*LVECT LMB 7/09
C MBAND = IBANDP*NDFRE LMB 7/09
C LVECT = NO. OF LOAD CASES LMB 7/09
COMMON NWORDS(26600) LMB 7/03
COMMON/CV/NUMEL,NUPTS,NUBPTS,IBANDP,MBAND,NBLOC,NDFRE,IFLAG,NUMAT
COMMON/SS/IGEN,ISHEAR,JSHEAR,NRED,IREACT,NTRUSS,ISIG
COMMON /BTAPE/ LCPJ(100),MCPJ(100) LMB
DIMENSION ITITLE(20),C(5)
EQUIVALENCE (ISHEAR,N1) , (NRED,N2), (IREACT,N3)
CALL ERRSET (208,256,-1,I) LMB
1 READ 1002,ITITLE LMB 7/03
PRINT 1003,ITITLE LMB 7/03
DO 50 I=1,100 LMB
LCPJ(I) = I LMB
50 MCPJ(I) = I LMB
1002 FORMAT (20A4) LMB
1003 FORMAT (2H1 ,20A4) LMB
READ 30,NUMEL,NUPTS,NUBPTS,IBANDP,NDFRE,IFLAG,NUMAT,N1,N2,N3,N4,
, IGEN,ISIG
, JSHEAR = N1
PRINT 31,NUMEL,NUPTS,NUBPTS,IBANDP,NDFRE,IFLAG,NUMAT,N1,N2,N3,N4,
, IGEN,ISIG
, MBAND=IBANDP*NDFRE
NBLOC = (NUPTS*NDFRE)/MBAND
IF ((MBAND*NBLOC-NUPTS*NDFRE).NE.0) NBLOC=NBLOC+1
REWIND 1 LMB 6/26
REWIND 2 LMB 6/26
REWIND 3 LMB 6/26
REWIND 4 LMB 6/26
CALL OVER1 LMB 7/09
CALL OVER2 LMB 7/09
CALL OVER3 LMB 7/09
IF (IGEN.GT.3) GO TO 3
CALL OVER4 LMB 7/09
3 CONTINUE LMB 7/09
30 FORMAT (13I4)
31 FORMAT ( 9H NUMEL =,I5/9H NUPTS =,I5/9H NUBPTS =,I5/9H IBANDP =,
.I5/ 9H NDFRE =,I5/9H IFLAG =,I5/9H NUMAT =,I5/9H ISHEAR =,
.I5/ 9H NRED =,I5/9H IRECT =,I5/9H LPROB =,I5/9H IGEN =,
.I5/ 9H ISIG =,I5)
90 FDRMAT ( F13.4 )
IF ( N4.GT.0 ) 80 TO 1
2 STOP
END

```

```

SUBROUTINE QTAPE ( MQ,NTAPE,P,Q,ICHOL )
IMPLICIT REAL*8 (A-H,O-Z) LMB 7/09
COMMON/CV/NUMEL,NUPTS,NUBPTS,IBANDP,MBAND,NBLOC,NDFRE,IFLAG,LVECT
COMMON/BTAPE/ LCPJ(100),MCPJ(100)
DIMENSION P(1),Q(1)
NWORDS=MBAND*LVECT
IF ( IABS(MQ).GT.1 ) GO TO 5
1 DO 4 N=1,NBLOC
IF ( MQ.EQ.-1 ) READ (NTAPE) (Q(I),I=1,NWORDS) LMB 6/26
IN=0
IF ( MQ.EQ. 1 ) K=(N-1)*MBAND+1
IF ( MQ.EQ.-1 ) K=(NBLOC-N)*MBAND+1
L=K*MBAND-1
DO 3 I=1,LVECT
DO 2 J=K,L
IN=IN+1
IF ( MQ.GT.0 ) Q(IN)=P(J)
IF ( MQ.LT.0 ) P( J)=Q(IN)
2 CONTINUE
K=K+250
3 L=K*MBAND-1
IF ( MQ.EQ.1 ) WRITE (NTAPE) (Q(I),I=1,NWORDS) LMB 6/26
4 CONTINUE
GO TO 8
5 IF ( MQ.EQ.-2 ) READ (NTAPE) (Q(I),I=1,NWORDS) LMB 6/26
IF ( MQ.EQ.-3 ) CALL IOBIN (7HREADSKP,NTAPE,Q,NWORDS,MCPJ(ICHOL))
IF (MQ.EQ.-3) READ (NTAPE:MCPJ(ICHOL)) (Q(I),I=1,NWORDS)- 3MK+
IN=0
K=1
L = MBAND
DO 7 I=1,LVECT
DO 6 J=K,L
IN=IN+1
IF ( MQ.GT.0 ) Q(IN)=P( J)
IF ( MQ.LT.0 ) P( J)=Q(IN)
6 CONTINUE
K=K+100
7 L=K*MBAND-1
IF ( MQ.EQ.2 ) WRITE (NTAPE) (Q(I),I=1,NWORDS) LMB 6/26
IF ( MQ.EQ. 3 ) CALL IOBIN ( 6HWRITER,NTAPE,Q,NWROS,MCPJ(ICHOL))
IF (MQ.EQ. 3) WRITE (NTAPE:MCPJ(ICHOL)) (Q(I),I=1,NWORDS) LMB
8 RETURN
END

```

```

SUBROUTINE RLOAD ( MQ,NTAPE,R,L1,L2,IDIM )
IMPLICIT REAL*8 (A-H,O-Z)
COMMON/CV/NUMEL,NUPTS,NUBPTS,IBANDP,MBAND,NBLOC,NDFRE,IFLAG,LVECT
DIMENSION R(1)
N=NUPTS*NDFRE
DO 1 LV=L1,L2
I=(LV-1)*IDIM*5+1
IPN = 1 * N - 1
IF (MQ.GT.0) WRITE (NTAPE) (R(I),II=I,IPN)
1 IF (MQ.LT.0) READ (NTAPE) (R(I),II=I,IPN)
IF (MQ.GT.0) CALL WIND (NTAPE,2)
RETURN
END

```

LMB 7/09
LMB 6/26
LMB 6/26
LMB 6/26

```

SUBROUTINE WIND (NTAPE,IREC)
2 REWIND NTAPE
6 RETURN
END

```

LMB 6/26

```

SUBROUTINE DVER1
IMPLICIT REAL*8 (A-H,O-Z)
COMMON/CV/NUMEL,NUPTS,NUBPTS,IBANDP,MBAND,NBLOC,NDFRE,IFLAG,NUMAT
COMMON/SS/IGEN,ISHEAR,JSHEAR,NRED,IREACT,NTRUSS,ISIG
COMMON KQ(4),NODES,QUADT,SMAT(7,30),EM,RM,VM,GM,01,02,
1 XQ(3,800),DIR(6,801),U(9),S(201),T(3,3),E1(3),
2 E2(3),TH(5),TPC(6),X(4),Y(4),Z(4),D11,D12,D22,D33,G1,G2,
3 D1(3,4),D2(3,4),ELOAD(5),IB(801),IDUMMY,TEMP(800)
DIMENSION DMAT(6)
DIMENSION IQ(4,2000),ITYPE(2000),QTYPE(2000),
1 TMAT(5,2000),DISTLD(5,2000)
DIMENSION TH58(58)
CNULLEQUIVALENCE (TH,TH58)
EQUIVALENCE (TH(1), TH58(1) )
EQUIVALENCE (SMAT(1),IQ(1)),(XQ(1),ITYPE(1),DISTLD(1))
1 ,(XQ(2001),QTYPE(1)),(DIR(1601),TMAT(1))
CNULLEQUIVALENCE (EM,DMAT),
EQUIVALENCE (EM, DMAT(1) ),
1 (U(1),XI),(U(2),YI),(U(3),ZI),(U(4),XJ),(U(5),YJ),(U(6),ZJ),
2 (U(7),XK),(U(8),YK),(U(9),ZK),(U(1),X0),(U(2),Y0),(U(3),Z0),
3 (U(4),BI),(U(5),BJ),(U(7),W),(U(6),A),(U(7),B),(U(8),O)
LOGICAL TEST1,TEST2
INTEGER QTYPE,QUADT
DO 80 I=1,801
80 DIR(6,I)=0.
PI=3.1415926535898
C.....GENERATE NODAL COORDINATES AND DIRECTION COSINES.
PRINT 900
1 READ 90,II,JJ,IJ,I60,U
IF ( I60.LE.0 ) PRINT 30,II,JJ,IJ,I60,(U(I),I=1,3)
IF ( I60.EQ.1 ) PRINT 31,II,JJ,IJ,I60,(U(I),I=1,6)
IF ( I60.GT.1 ) PRINT 91,II,JJ,IJ,I60,U
IF (I60.LT.0) GOTO 17
I60=I60+1
IF (IJ .GT.0) XINC = (JJ-II)/IJ
GOTO ( 2, 4, 8,10,12),I60
2 DO 3 I=1,3
3 XQ(I,II)=U(I)
IF (II-NUPTS) 1,51,51
C.....STRAIGHT LINE.
4 XJ=XJ-XI
YJ=YJ-YI
ZJ=ZJ-ZI
XL=DSQRT(XJ**2+YJ**2+ZJ**2)
XD=XJ/XINC
YD=YJ/XINC
ZD=ZJ/XINC
DO 5 I=II,JJ,IJ

```

LMB 7/09
LMB 7/09
LMB 6/27
LMB 6/26
LMB 6/26
LMB
JJP
LMB
JJP
LMB 7/02
LMB 7/02
22MAR75

```

XINC=(1-I)/IJ
XQ(1,1)=X1+XD*XINC
XQ(2,1)=Y1+YD*XINC
5 XQ(3,1)=Z1+ZD*XINC
SQ=DSQRT(XJ*XJ+YJ*YJ)
DO 7 I=1, JJ, IJ
DIR(1,1)=XJ/XL
DIR(2,1)=YJ/XL
DIR(3,1)=ZJ/XL
IF(SQ.EQ..0) GOTO 6
DIR(4,1)=-YJ/SQ
DIR(5,1)= XJ/SQ
GOTO 7
6 DIR(4,1)=0.
DIR(5,1)=1.
7 CONTINUE
GOTO 19
C.....CIRCULAR CURVE.
8 DIJ=DSQRT((X1-XJ)**2+(Y1-YJ)**2+(Z1-ZJ)**2)
DIL=DSQRT((X1-XK)**2+(Y1-YK)**2+(Z1-ZK)**2)/2.
DJL=DSQRT(DIJ**2-DIL**2)
DEL=PI -2.*DATAN(DIL/DJL)
XL=(X1+XK)/2.
YL=(Y1+YK)/2.
ZL=(Z1+ZK)/2.
R= DIJ/DSIN(DEL/2.)
T(1,1)=(XK-XL)/DIL
T(2,1)=(YK-YL)/DIL
T(3,1)=(ZK-ZL)/DIL
T(1,2)=(XJ-XL)/DJL
T(2,2)=(YJ-YL)/DJL
T(3,2)=(ZJ-ZL)/DJL
T(1,3)= T(2,1)*T(3,2)-T(2,2)*T(3,1)
T(2,3)=-T(1,1)*T(3,2)+T(1,2)*T(3,1)
T(3,3)= T(1,1)*T(2,2)-T(1,2)*T(2,1)
CONST=DSQRT(T(1,3)**2+T(2,3)**2+T(3,3)**2)
AINC=DEL/XINC
DO 9 I=1, JJ, IJ
XINC=(1-I)/IJ
ANG=AINC*XINC
DX=R*DSIN(ANG)*DCOS(DEL-ANG)
DY=R*DSIN(ANG)*DSIN(DEL-ANG)
XQ(1,1)=X1+T(1,1)*DX+T(1,2)*DY
XQ(2,1)=Y1+T(2,1)*DX+T(2,2)*DY
XQ(3,1)=Z1+T(3,1)*DX+T(3,2)*DY
C=DCOS(DEL-2.*ANG)
D=DSIN(DEL-2.*ANG)
DIR(1,1)=T(1,1)*C+T(1,2)*D
DIR(2,1)=T(2,1)*C+T(2,2)*D
DIR(3,1)=T(3,1)*C+T(3,2)*D
DIR(4,1)=-T(1,3)/CONST
DIR(5,1)=-T(2,3)/CONST
9 DIR(6,1)=-T(3,3)/CONST
GOTO 19
C.....PARABOLA.
10 IF(DABS(BI).GT.DABS(BJ)) CONST=ZJ/BI**2
IF(DABS(BJ).GE.DABS(BI)) CONST=ZJ/BJ**2
DIJ=DABS(BI)+DABS(BJ)
W=PI/180.
CW=DCOS(W)
SW=DSIN(W)
DINC=DIJ/XINC
DO 11 I=1, JJ, IJ

```

```

XINC=(1-I)/IJ
DX=BI+DINC*XINC
XQ(1,1)=X0+DX*CW
XQ(2,1)=Y0+DX*SW
XQ(3,1)=Z0+CONST*DX*DX
ANG=DATAN(2.*CONST*DX)
DIR(1,1)=CW*DCOS(ANG)
DIR(2,1)=SW*DCOS(ANG)
DIR(3,1)=DSIN(ANG)
DIR(4,1)=-SW
11 DIR(5,1)= CW
GOTO 19
C.....ELLIPSE.
12 A2=A*A
B2=B*B
AB=A/B
BA=B/A
ATB=A*B
W=D*PI/180.
SW=DSIN(W)
CW=DCOS(W)
IFAC=200
FAC=IFAC
XK=B2/DSQRT(A2+B2)
Z1=AB*DSQRT(B2-BI*BI)
ZJ=AB*DSQRT(B2-BJ*BJ)
WI=-PI/2.
WJ= PI/2.
IF(Z1.GT..0) WI=DATAN(BI/Z1)
IF(ZJ.GT..0) WJ=DATAN(BJ/ZJ)
DW=(WJ-WI)/FAC
WC=PI/2. -WI-DW
S(1)=0.
DO 13 I=1, IFAC
SWC=DSIN(WC)
CWC=DCOS(WC)
R= ATB/DSQRT(B2*SWC*SWC+A2*CWC*CWC)
DX=R*CWC-BI
DZ=R*SWC-Z1
S(I+1)=S(I)+DSQRT(DX*DX+DZ*DZ)
BI=BI+DX
Z1=Z1+DZ
13 WC=WC-DW
DS=S(IFAC+1)/XINC
ST=0.
WC=PI/2. -WI
14 DO 15 K=1, IFAC
J=K+1
IF(S(J).GE.ST) GOTO 16
15 CONTINUE
16 AINC=J-2
AINC=AINC*DW
ANG=WC-AINC-((S(J)-S(J-1))/(S(J)-S(J-1))) *DW
SS=DSIN(ANG)
CC=DCOS(ANG)
R= ATB/DSQRT(B2*SS*SS+A2*CC*CC)
XR=DABS(R*CC)
ZR=DABS(R*SS)
Q = DABS(CC)
IF(XR.LE.XK) ANG=-Q*DATAN((AB*XR)/DSQRT(B2-XR*XR))
IF(XR.GT.XK) ANG=-Q*(PI/2. -DATAN(BA*ZH/DSQRT(A2-ZH*ZR)))
SA = DABS(A)
XQ(1,1)=X0+XR*CW*Q

```

LMB

LMB

```

XQ(2,II)=Y0+XR*SW*Q
XQ(3,II)=Z0+ZR*SA
DIR(1,II)=DCOS(ANGT)*CW*SA
DIR(2,II)=DCOS(ANGT)*SW*SA
DIR(3,II)=DSIN(ANGT)*SA
DIR(4,II)=-SW
D.R(5,II)=CW
IF(II.EQ.JJ) GOTO 19
II=II+IJ
ST=ST+DS
GOTO 14
C.....REPEATED NODAL COORDINATES,AND E1 COSINES.
17 IGO=IABS(IG0)
IF ( IJ.LE.1 ) I=IABS(IJ)
IF ( IJ.LE.1 ) IJ=1
IF ( IJ.GT.1 ) I=1
JI=0
20 DO 18 J=II,JJ+IJ
DO 18 L=1,3
DIR(L ,J)=DIR(L ,J-I)
DIR(L+3,J)=DIR(L+3,J-I)
18 XQ(L,J)=XQ(L,J-I)+U(L)
JI=JI+1
IF ( JI.GE.IG0 ) GO TO 19
II=II+I
JJ=JJ+I
GOTO 20
19 IF((JJ.LT.NUPTS).AND.(II.LT.NUPTS))GOTO 1
C.....INPUT DIRECTION COSINES FOR ARBITRARY NODAL POINTS.
51 PRINT 901
53 READ 95,M,LIM,MOP,E1,E2
PRINT 33,M,LIM,MOP,E1,E2
IF ( M.LE.0 ) GOTO 57
TEST1=DABS(E1(1))+DABS(E1(2))+DABS(E1(3)).GT..0
TEST2=DABS(E2(1))+DABS(E2(2))+DABS(E2(3)).GT..0
IF (MOP.LE.0) LIM=M
IF (MOP.LE.0) MOP=1
DO 52 L=M,LIM,MOP
DO 52 K=1,3
IF (TEST1) DIR(K , L)=E1(K)
IF (TEST2) DIR(K+3, L)=E2(K)
GOTO 53
57 L = 3 * NUPTS
WRITE (3) XQ
WRITE (3) DIR
C.....INPUT MESH.
PRINT 902
59 READ 93,JJ, (IQ(I,JJ),I=1,4),MODL,NLAY,LASTEL
PRINT 193,JJ, (IQ(I,JJ),I=1,4),MODL,NLAY,LASTEL
193 FORMAT (8(1X,I4))
IF ( JJ .EQ. NUMEL ) GOTO 66
IF ( NLAY .EQ. 0 ) GO TO 59
62 II=JJ
IF ( MODL ) 69,60,64
60 IF (II.EQ.NUMEL) GOTO 66
READ 93,JJ,(IQ(I,JJ),I=1,4),MODL,NLAY,LASTEL
PRINT 193,JJ,(IQ(I,JJ),I=1,4),MODL,NLAY,LASTEL
IF(II+1.EQ.JJ) GOTO 62
JK=JJ-2
DO 63 J=II,JK
DO 63 K=1,4
63 IQ(K,J+1)=IQ(K,J)+1
IF (JJ -NUMEL) 62,66,66

```

LMB 6/26
LMB 6/26

```

64 IFAC=IQ(1,II)-1
DO 65 I=1,NLAY
M=(MODL+1)*(I-1)
DO 65 J=1,MODL
IQ(1,II)=M+J+IFAC
IQ(4,II)=IQ(1,II)+1
IQ(2,II)=IQ(4,II)+MODL
IQ(3,II)=IQ(2,II)+1
65 II=II+1
IF(II-1 - NUMEL) 59,66,66
69 II=JJ+NLAY
DO 72 J=II,LASTEL,NLAY
L=J-NLAY
DO 70 K=1,4
70 IQ(K,J)=IQ(K,L)-MODL
IF ( IQ(3,L).LE.0 ) IQ(3,J)=0
IF ( IQ(4,L).LE.0 ) IQ(4,J)=0
72 CONTINUE
IF(LASTEL.LT.NUMEL) GOTO 59
66 PRINT 903
DO 1100 I = 1, NUMEL
DO 1000 J = 1, 4
1000 KQ(J) = IQ(J,I)
1100 WRITE (1) KQ
C.....INPUT MATERIAL TABLE.
DO 67 II=1,NUMAT
READ 100,I,(SMAT(J,I),J=1,7)
67 PRINT 96,I,(SMAT(J,I),J=1,7)
C.....INPUT ELEMENT PROPERTY CARDS.
PRINT 906
75 READ 97,II,JJ,LIM,MODL,KK,(DMAT(I),I=1,5)
PRINT 98,II,JJ,LIM,MODL,KK,(DMAT(I),I=1,5)
IF (LIM.LE.0) LIM=II
IF (MODL.LE.0) MODL=1
DO 71 I=II,LIM,MODL
ITYPE(I) = JJ
QTYPE(I) = KK
DO 71 J=1,5
71 TMAT(J,I)=DMAT(J)
IF (LIM.LT.NUMEL) GOTO 75
DO 2200 I = 1, NUMEL
MTYPE = ITYPE(I)
QUADT = QTYPE(I)
WRITE (2) MTYPE,QUADT
DO 2000 J = 1, 5
2000 DMAT(J) = TMAT(J,I)
2200 WRITE (2) (DMAT(J),J=1,5)
C.....INPUT DISTRIBUTED LOADS ON ELEMENTS.
PRINT 35
40 READ 36,II, LIM,MODL,(DMAT(I),I=1,5)
PRINT 37,II, LIM,MODL,(DMAT(I),I=1,5)
IF (LIM.LE.0) LIM=II
IF (MODL.LE.0) MODL=1
DO 41 I=II,LIM,MODL
DO 41 J=1,5
41 DISTLD(J,I)=DMAT(J)
IF (LIM.LT.NUMEL) GOTO 40
DO 4400 I = 1, NUMEL
DO 4000 J = 1, 5
4000 DMAT(J) = DISTLD(J,I)
4400 WRITE (4) (DMAT(J),J=1,5)
CALL WIND(3,3)
CALL WIND(1,3)

```

LMB 6/26

LMB 7/02
LMB 7/02

LMB 6/26

LMB 6/26

LMB 6/26

```

CALL WIND(2,3)
CALL WIND(4,3)
L = 3 * NUPTS
READ (3) XQ
READ (3) DIR
CALL WIND(3,1)
DO 5000 I = 1, 801
5000 IB(I) = 0
C.....INPUT TEMPERATURE CHANGES
PRINT 300
301 READ 302,M,LIM,MOP,TEM
IF (M.LE.0) GOTO 777
PRINT 303,M,LIM,MOP,TEM
IF (MOP.LE.0) LIM=M
IF (MOP.LE.0) MOP=1
OD 304 L = M,LIM,MOP
304 TEMP(L)=TEM
GO TO 301
777 IF (IGEN .GT. 2) GO TO 77
73 PRINT 904
PRINT 700
DO 74 I=1,NUPTS
PRINT 92,I,(XQ(J,I),J=1,3),TEMP(I)
PRINT 701
PRINT 702
DO 76 I=1,NUPTS
76 PRINT 32,I,(DIR(J,I),J=1,6)
PRINT 905
PRINT 703
77 DO 83 M=1,NUMEL
READ (1) KQ
READ (2) MTYPE,QUADT
DO 85 I=1,4
85 DMAT(I)=SMAT(I,MTYPE)
G1 = SMAT(5,MTYPE)
G2 = SMAT(6,MTYPE)
TPC(5)=(SMAT(7,MTYPE)*EM)/(24.*(1.-VM))
TPC(6)=SMAT(7,MTYPE)
READ (2) TH
READ (4) ELOAD
NODES=4
IF (KQ(4).LE.0) NODES=3
IF (KQ(3).LE.0.AND.KQ(4).LE.0) NODES = 2
DO 82 J=1,NODES
K=KQ(J)
IF (NODES.EQ.2) GO TO 600
C1=DSQRT ( DIR(1,K)**2+DIR(2,K)**2+DIR(3,K)**2 )
C2=DSQRT ( DIR(4,K)**2+DIR(5,K)**2+DIR(6,K)**2 )
DO 81 L=1,3
D1(L,J)=DIR(L,K)/C1
81 D2(L,J)=DIR(L,3,K)/C2
600 X(J)=XQ(1,K)
Y(J)=XQ(2,K)
Z(J)=XQ(3,K)
TPC(J)=TEMP(K)
82 IR(K)=IB(K)+1
IF (IGEN .GT.2) GO TO 78
PRINT 94,M,KQ,MTYPE,QUADT,TH,TPC(6)
78 IF (NODES.GT.2) GO TO 610
TH(2) = EM
GO TO 620
610 TH(5)=TH(5)*PI/180.
D=EM/(1.-VM*VM)

```

LMB 6/26
LMB 6/26

22MAR75
LMB 7/02
LMB 7/02

LMB 7/02
LMB 7/02

LMB 7/02
LMB 7/02

LMB 6/26
LMB 6/26

LMB 6/26
LMB 6/26

22MAR75

```

D11=D*DSQRT(RM)
D22=D/DSQRT(RM)
D33=D*(1.-VM*VM)*.5/(1.-GM)
D12=D*VM
620 WRITE (3) KQ,NODES,QUADT
83 WRITE (3) TH58
CALL WIND(1,1)
CALL WIND(2,1)
CALL WIND(4,1)
CALL WIND ( 3,3 )
IF (IGEN.GT.1) GO TO 79
PRINT 84,(IB(I),I=1,NUPTS)
79 CONTINUE
WRITE (2) IB
CALL WIND ( 2,3 )
CALL SEARCH
84 FORMAT (1H0,60I2)
90 FORMAT ( 4I4,1X,9F7.3 )
91 FORMAT ( 4I4,2X,1P3E12.4/18X,1P3E12.4/18X,1P3E12.4 )
92 FORMAT ( I4,2X,1P4E12.4 )
93 FORMAT(8I4)
94 FORMAT (1X,5I4,2I2,1P4E10.3,F6.1,1PE10.3 )
95 FORMAT ( 3I4,5X,6F7.5 )
96 FORMAT ( I4,2X,1P7E12.4 )
97 FORMAT(5I4,5F10.0)
98 FORMAT (1X,5I4,2X,1P5E12.4 )
100 FORMAT ( I4,6X,7F10.0 )
900 FORMAT (46H0 DUPLICATION OF INPUT NODAL COORDINATE CARDS. )
901 FORMAT (/53H DUPLICATION OF INPUT SURFACE DIRECTION COSINE CARDS.)
902 FORMAT (/49H DUPLICATION OF ELEMENT NODAL PDINT NUMBER CARDS. )
903 FORMAT (40H0DUPLICATION OF ELEMENT MATERIAL TABLE. )
904 FORMAT (47H0NODAL COORDINATES AND TEMPERATURE DIFFERENCES. )
700 FORMAT(4H PT.,3X,1HX,11X,1HY,11X,1HZ,11X,5HTEMP.)
701 FORMAT (28H0SURFACE DIRECTIONS COSINES. )
702 FORMAT ( 4H PT.,6X,3HE1X,6X,3HE1Y,6X,3HE1Z
.
6X,3HE2X,6X,3HE2Y,6X,3HE2Z )
905 FORMAT(64H0EL. NO.,EL. NODE NOS.,MATL. TYPE=T,EL. TYPE=E,EL.THICKN22MAR75
,ESS,ANG. 10HTHER,COEF.) 22MAR75
703 FORMAT(1X,4H EL.,3X,1HI,3X,1HJ,3X,1HK,3X,5HL T E,3X,2HTI,8X,2HTJ, 22MAR75
8X,2HTK,8X,2HTL,8X,11HANG ALPHA )
906 FORMAT(39H0DUPLICATION OF ELEMENT PROPERTY CARDS.)
30 FORMAT ( 4I4,2X,1P3E12.4 )
31 FORMAT ( 4I4,2X,1P3E12.4,/,18X,1P3E12.4 )
32 FORMAT ( I4,2X,6F9.5 )
33 FORMAT ( 3I4,4X,6F9.5 )
35 FORMAT (27H0ELEMENT DISTRIBUTED LOADS. )
36 FORMAT ( 3I4,8X,5F10.0 )
37 FORMAT (1X,3I4,10X,1P5E12.4 )
303 FORMAT(1X,3I4,2X,1PE12.4)
300 FORMAT(47H0DUPLICATION OF INPUT NODAL TEMP. DIFFERENCES. )
302 FORMAT(3I4,3X,F10.0)
RETURN
END

```

LMB 6/26
LMB 6/26

LMB 6/26

```

SUBROUTINE SEARCH
IMPLICIT REAL*8 (A-H,O-Z)
COMMON/SS/IGEN,ISHEAR,JSHEAR,NRED,IREACT,NTRUSS,ISIG
COMMON/CV/NUMEL,NUPTS,NUBPTS,IBANDP,MBAND,NBLDC,NDFRE,IFLAG,NUMAT
COMMON IQ(4), IB(801),IDUMMY, LLJQ(800), Q(20,41)
DIMENSION INTEG(2426)
EQUIVALENCE (INTEG,IQ)
INTEGER Q
00 30 I=1,2426
30 INTEG(I) = 0
READ (2) IB
IK = 1
00 50 LZ = 1, NUMEL
READ (1) IQ
NDOES = 4
      IF (IQ(4).LE.0) NDOES = 3
IF (IQ(3).LE.0) NDOES = 2
DD 4 I = 1, NDOES
I = IQ(I)
IB(I) = IB(I) - 1
DO 4 JJ = 1, NDOES
J = IQ(JJ) - IK + 1
IF (IQ(JJ).GT.I) GOTO 4
DO 1 LL = 1, IBANDP
IF (Q(LL,J).EQ.0) Q(LL,J) = I
IF (Q(LL,J).EQ.I) GOTO 4
1 CONTINUE
4 CONTINUE
IF (IB(IK).GT.0) GOTO 50
10 DO 8 I = 1, IBANDP
IF (Q(I,1).EQ.0) GOTO 9
8 IT = I
9 IF (IK.EQ.1) LLJQ(IK) = IT
IF (IK.GT.1) LLJQ(IK) = LLJQ(IK-1) + IT
C PRINT 91, LLJQ(IK)
C IF (IGEN.GT.1) GO TO 7
C PRINT 91,IK,(Q(I,1),I=1,IT)
7 IF (IK.EQ.NUPTS) GO TO 50
IF (IK.EQ.NUPTS) GO TO 50
DO 5 I = 1, 40
DD 5 J = 1, IBANDP
5 Q(J,I) = Q(J,I+1)
IK = IK + 1
IF (IB(IK).EQ.0) GOTO 10
50 CONTINUE
CALL WIND ( 1,1 )
CALL WIND ( 2,1 )
READ (2) IB
WRITE (1) IB
WRITE (1) LLJQ
CALL WIND ( 1,3 )
CALL WIND ( 2,1 )
91 FORMAT (10I6 )
RETURN
END

```

LMB 7/09

LMB 6/27

LMB 6/25

LMB 6/25

LMB 6/25

LMB 6/25

LMB 6/26

LMB 7/02

LMB 7/02

LMB 6/26

LMB 7/02

LMB 7/02

LMB 6/25

LMB 6/28

LMB 6/28

LMB 6/28

LMB 6/28

LMB 6/28

LMB 6/25

LMB 6/25

LMB 6/26

LMB 6/26

LMB 6/26

LMB 6/26

LMB 6/26

LMB 6/26

LMB 6/26

LMB 6/26

LMB 6/26

LMB 6/26

LMB 6/26

LMB 6/26

LMB 6/26

LMB 6/26

LMB 6/26

LMB 6/26

LMB 6/26

LMB 6/26

LMB 6/26

LMB 6/26

LMB 6/26

LMB 6/26

```

SUBROUTINE OVER2
IMPLICIT REAL*8 (A-H,O-Z)
COMMON/CV/NUMEL,NUPTS,NUBPTS,IBANDP,MBAND,NBLDC,NDFRE,IFLAG,LVECT
COMMON/SS/IGEN,ISHEAR,JSHEAR,NRED,IREACT,NTRUSS,ISIG
COMMON LLJQ(800)
COMMON IB(801),IQ(4),NODES,QUADT,IX1,IBO(200,6),IBC(800),Q(240),
IBC(200,5),PX1(7971),THQ(4),ANG,TPC(6),X(4),Y(4),Z(4),D11,
2 D12, D22, D33, G1, G2, C(3,4), E(3,4), GM, QP(4),
3 PX2(1109), TG(3,3,4), PX3(96),SPRING(5,50),ISPRNG(50)
DIMENSION P(5,850,3),R(5),DX(5,5),LOADS(3),CQ1(12750)
INTEGER Q,QUADT
EQUIVALENCE (LLJQ,P),(P,CQ1)
EQUIVALENCE (THQ,TH58)
C D(NDFRE**2,6,25),IBD(NUBPTS,NDFRE+1),BC(NUBPTS,NDFRE),IBC(NUPTS)
C IB(NUPTS),P(NUPTS,NDFRE),R(NDFRE),IQ,X,Y,Z(NODES),
DATA DX/1.,4*0.,0.,1.,3*0.,2*0.,1.,2*0.,3*0.,1.,0.,4*0.,1./
C.....INITIALIZE BLANK COMMON (EXCEPT IB).
DO 1 I=1,3848
1 LLJQ(I) = 0
00 2 I=1,5
DO 2 J=1,200
2 BC(J,I) = 0.0
DD 4 I=1,9520
4 PX1(I) = 0.0
DD 3 I=1,50
3 ISPRNG(I) = 0
READ (1) IB
READ (1) LLJQ
CALL WIND ( 1,1 )
IK=1
PRINT 82
PRINT 83
L=0
7 L=L+1
READ 80,(IBD(L,K),K=1,6),LIM,MOP,(BC(L,K),K=1,5)
PRINT 81,(IRD(L,K),K=1,6),LIM,MOP,(BC(L,K),K=1,5)
IF(L.FQ.NUBPTS) GOTO 74
IF(MOP) 7,7,8
8 K=IRD(L,1)+MOP
DO 70 I=K,LIM,MOP
L=L+1
IBD(L,1)=I
DO 70 J=1,5
IBD(L,J+1)=IBD(L-1,J+1)
70 BC(L,J)=BC(L-1,J)
IF(L.LT.NURPTS) GOTO 7
74 IF (IGEN .GT. 2) GO TO 155
PRINT 90
PRINT 91
DO 79 L=1,NURPTS
79 PRINT 89,(IRD(L,K),K=1,6),(BC(L,K),K=1,5)
155 READ 80,NSPRNG
IF (NSPRNG.LE. 0) GOTO 15
PRINT 29
L=0
21 L=L+1
READ 22, ISPRNG(L),LIM,MOP,(SPRING(K,L),K=1,5)
PRINT 23,ISPRNG(L),LIM,MOP,(SPRING(K,L),K=1,5)
IF (L.EQ.NSPRNG) GOTO 15
IF (MOP) 21,21,24
24 K=ISPRNG(L)+MOP
DO 25 I = K,LIM,MOP

```

LMB 7/09

LMB 7/09

LMB 6/25

LMB 6/25

LMB 6/25

LMB 6/25

LMB 6/25

LMB 6/26

LMB 6/26

LMB 6/26

LMB 6/26

LMB 6/26

LMB 6/26

LMB 6/25

LMB 6/28

LMB 6/28

LMB 6/28

LMB 6/28

LMB 6/28

LMB 6/28

LMB 6/25

LMB 6/25

LMB 6/26

LMB 6/26

LMB 6/26

L=0

L=L+1

L=L+1

L=L+1

L=L+1

L=L+1

L=L+1

L=L+1

L=L+1

L=L+1

L=L+1

L=L+1

L=L+1

L=L+1

L=L+1

L=L+1

L=L+1

L=L+1

L=L+1

L=L+1

L=L+1

L=L+1

L=L+1

L=L+1

L=L+1

```

25 SPRING(J,L)=SPRING(J,L-1)
IF(L.LT.NSPRNG) GOTO 21
IF (IGEN.GT.0) GOTO 15
PRINT 26
PRINT 27
DO 28 L = 1,NSPRNG
28 PRINT 35,ISPRNG(L), (SPRING(K,L),K=1,5)
15 READ 50,LVECT,LOAOS,UPL
PRINT 51,LVECT,LOAOS,UPL
50 FORMAT ( 4I4,4X,F10.3 )
51 FORMAT (/41H NUMBER OF INDEPENDENT LOAD CASES      = 15/
.           41H NUMBER OF LOADED NODES FOR LOAD CASE 1 = 15/
.           41H NUMBER OF LOADED NODES FOR LOAD CASE 2 = 15/
.           41H NUMBER OF LOADED NODES FOR LOAD CASE 3 = 15/
.           24H UNIFORM VERTICAL LOAD = 1PE12.4 )
DO 9 I=1,NUBPTS
J=IBO(I,1)
9 IBC(J)=1
READ 85,ISKIP,JSKIP
PRINT 85,ISKIP,JSKIP
IF(IGEN.LT.2) PRINT 87
NTRUSS=0
NQBLOC = 0
DO 10 LZ=1,NUMEL
READ (3) IQ,NODES,QUADT
READ (3) TH58
IF ( NODES.EQ.2 ) NTRUSS=NTRUSS+1
IF(NODES.EQ.2) GO TO 600
DO 20 I=1,NODES
TG(1,1,I)=C(1,I)
TG(1,2,I)=C(2,I)
TG(1,3,I)=C(3,I)
TG(3,1,I)= C(2,I)*E(3,I)-C(3,I)*E(2,I)
TG(3,2,I)=-C(1,I)*E(3,I)+C(3,I)*E(1,I)
TG(3,3,I)= C(1,I)*E(2,I)-C(2,I)*E(1,I)
CONST=DSORT(TG(3,1,I)**2+TG(3,2,I)**2+TG(3,3,I)**2)
TG(3,1,I)=TG(3,1,I)/CONST
TG(3,2,I)=TG(3,2,I)/CONST
TG(3,3,I)=TG(3,3,I)/CONST
TG(2,1,I)= TG(1,3,I)*TG(3,2,I)-TG(1,2,I)*TG(3,3,I)
TG(2,2,I)=-TG(1,3,I)*TG(3,1,I)+TG(1,1,I)*TG(3,3,I)
20 TG(2,3,I)= TG(1,2,I)*TG(3,1,I)-TG(1,1,I)*TG(3,2,I)
600 CALL QDSHEL ( ISHEAR,JSHEAR,LZ,ISKIP,JSKIP )
10 CALL SUBSPR (IK,NSPRNG,NQBLOC)
CALL WIND ( 1,2 )
CALL WIND ( 3,1 )
CALL WIND ( 4,3 )
CALL RLOAD ( 1,3,P,1,LVECT,850 )
JK=NQBLOC*IBANOP
IF(IK.GT.JK) GOTO 31
K=1
IK=IK+1
DO 30 I=IK,JK
Q(1) = I
WRITE (2) K,I
WRITE (2) DX
WRITE (2) OX
30 .....INITIALIZE ENTIRE BLANK COMMON.( EXCEPT LOADS(3) ).
31 DO 36 I=1,12750
36 CQ1(I) = 0.0
DO 11 L=1,NUPTS
I=(L-1)*NDFRE+1
J=I+8500

```

LMB 6/26
LMB 6/26

LMB 7/05
LMB 7/05

```

JN = J+NDFRE-1
READ (4) (CQ1(K),K=J,JN)
JN = I+NDFRE-1
11 READ (4) (CQ1(K),K=I,JN)
41 DO 40 I=1,NUPTS
DO 40 J=1,NDFRE
DO 40 K=1,2
40 P(J,I,K) = P(J,I,3) + P(J,I,K)
DO 73 I=1,LVECT
II=1
IF(LOADS(I).LE.0) GOTO 73
PRINT 84,1
PRINT 86
71 READ 1000,M,LIM,MOP,R
PRINT 85,M,LIM,MOP,R
IF(MOP.LE.0) LIM=M
IF(MOP.LE.0) MOP=1
DO 72 L=M,LIM,MOP
II=II+1
DO 72 K=1,5
72 P(K,L,I) = P(K,L,I) + R(K)
IF(II.LE.LOADS(II)) GOTO 71
73 CONTINUE
CALL RLOAD ( 1,2,P,1,LVECT,850 )
DO 14 LV=1,LVECT
IF(IGEN.GT.2) GO TO 14
PRINT 92,LV
PRINT 86
PRINT 88,(L,(P(J,L,LV),J=1,NDFRE),L=1,NUPTS)
14 CONTINUE
CALL WIND ( 2,3 )
CALL WIND ( 4,1 )
CALL QTAPE ( 1,4,P,PIX2,0 )
80 FORMAT ( 14,2X,5I1,1X,2I4,5F10.0 )
81 FORMAT ( 14,1X,5I1,1X,2I4,1X,1P5E10.3 )
82 FORMAT (47H00DUPLICATION OF INPUT BOUNDARY CONDITION CARDS./
. 51H D1,D2 AND D3 ARE TRANSLATIONS IN BASE COORDINATES./
. 48H 04 AND 05 ARE ROTATIONS IN SURFACE COORDINATES. )
83 FORMAT(23H PT. 12345 LIM MOD D1 ,8X2HD2,8X2HD3,8X2HD4,8X2HD5)
84 FORMAT(48H00DUPLICATION OF INPUT NODAL FORCES,LOAD CASE NO.15)
85 FORMAT ( 314,3X,1P5E11.4 )
86 FORMAT (12H PT. LIM MOD,4X,2HP1,9X2HP2,9X2HP3,9X2HP4,9X2HP5 )
87 FORMAT(50H00POINTS CONTAINED IN EQUIL.EQS.,RIGHT OF DIAGONAL./
. 7H EQ. )
1000 FORMAT ( 314,8X,5F10.0 )
88 FORMAT(14,11X,1P5E11.4)
89 FORMAT ( 14,5I2,1X,1P5E11.4 )
90 FORMAT(55H00BOUNDARY CONDITIONS OF POINTS HAVING SPECIFIED DISPLS.)
91 FORMAT (16H PT. 1 2 3 4 5 2HD1,9X2HD2,9X2HD3,9X2HD4,9X2HD5 )
92 FORMAT(43H0TOTAL APPLIED NODAL POINT FORCES,LOAD CASE,17)
26 FORMAT(54H00BOUNDARY CONDITIONS OF POINTS HAVING SPECIFIED SPRING
.11H CONSTANTS. )
27 FORMAT(4H PT.,5X2HD1,9X2HD2,9X2HD3,9X2HD4,9X2HD5 )
29 FORMAT(39H00DUPLICATION OF INPUT SPRING CONSTANTS. /
.17H PT. LIM MOD D1,8X2HD2,8X2HD3,8X2HD4,8X2HD5 )
22 FORMAT (314,8X,5F10.0)
23 FORMAT (14,1X,2I4,1X,1P5E10.3)
35 FORMAT (14,4X,1P5E11.4)
RETURN
END

```

LMB 6/26
LMB 6/26
LMB 6/26
LMB 6/26

```

SUBROUTINE SUHSPR (IK,NSPRNG,NQBLOC)
IMPLICIT REAL*8 (A-H,O-Z)
COMMON/CV/NUMEL,NUPTS,NUBPTS,IBANDP,MBAND,NBLOC,NDFRE,IFLAG,LVECT
COMMON/SS/IGEN,ISHEAR,JSHEAR,NRED,IReact,NTRUSS,ISIG
COMMON LLJQ(800)
COMMON IH(801), IQ(4), NODES, IX1(2002), Q(240), PX1(1000),
1 D(25,240), PX2(125), PM(5,25), S(37,37), PT(37),
2 PX3(1614),SPRING(5,50),ISPRNG(50)
INTEGER Q
DO 4 II=1,NODES
I=IQ(II)
L=(II-1)*5
K=I-IK+1
PM(1,K)=PT(L+1)+PM(1,K)
PM(2,K)=PT(L+2)+PM(2,K)
PM(3,K)=PT(L+3)+PM(3,K)
IB(I)=IB(I)-1
DO 4 JJ=1,NODES
J=IQ(JJ)
IF(J.GT.I) GOTD 4
NB=LLJQ(J)
IF(J.GT.1) NB=NB-LLJQ(J-1)
LLCJ=0
IF(J.GT.1) LLCJ=LLJQ(J-1)-NQBLOC
DO 1 LL=1,NB
IF ( Q(LLCJ+LL).EQ.0 ) Q(LLCJ+LL) = 1
IF ( Q(LLCJ+LL).EQ.I ) GOTD 2
1 CONTINUE
2 IS=(II-1)*NDFRE
JS=(JJ-1)*NDFRE
DO 3 IC=1,NDFRE
N=IC+JS
MN=(IC-1)*NDFRE
DO 3 IR=1,NDFRE
M=IR+IS
MN=MN+1
3 D(MN+LLCJ+LL) = D(MN+LLCJ+LL) + S(M,N)
4 CONTINUE
IF(IB(IK).GT.0) GOTD 6
10 IT=LLJQ(IK)-NQBLOC
IF (IGEN.GT.1) GO TO 7
PRINT 91,IK,(Q(I),I=1,IT)
7 CALL BLAYER (IK,NSPRNG,IT)
IF ( IK.EQ.NUPTS ) GO TO 6
IS = IT + 1
DO 5 I = IS, 240
Q(I-IT) = Q(I)
DO 5 K=1,25
5 D(K,I-IT) = D(K,I)
NQBLOC=LLJQ(IK)
IK=IK+1
IF ( IB(IK).EQ.0 ) GOTD 10
91 FORMAT(7I7)
6 RETURN
END

```

LMB 7/09
LMB 6/25

```

SUBROUTINE BLAYER (J,NSPRNG,IT)
IMPLICIT REAL*8 (A-H,O-Z)
COMMON/CV/NUMEL,NUPTS,NUBPTS,IBANDP,MBAND,NBLOC,NDFRE,IFLAG,LVECT
COMMON IX1(1608),IBD(200,6), IBC(800), QQ(240), BC(200,5),
1 DD(5,5,240),P(5,25), PM(5,25), PX1(1369), PT(37),
2 PX2(1614),SPRING(5,50),ISPRNG(50)
INTEGER QQ,X,Y,Z
DO 40 II = 1,IT
I=QQ(II)
IF ( I.EQ.0 ) GOTD 40
IF (I.NE.J.OR.NSPRNG.LE.0) GOTD 40
DO 32 L = 1,NSPRNG
IF (ISPRNG(L).NE. J) GOTD 32
DO 33 M = 1,NDFRE
33 DD(M,M,II) = DD(M,M,II)+SPRING(M,L)
32 CONTINUE
40 CONTINUE
LT=25*IT
WRITE (2) IT,(QQ(II),II=1,IT)
WRITE (2) (((DD(II,L,M),II=1,5),L=1,5),M=1,IT)
1 DD 10 II=1,IT
I=QQ(II)
IF(I.EQ.0) GOTD 10
X=IBC(I)
Y=IBC(J)
Z=I-J+1
C.....
IF (I.EQ.J.OR.X.EQ.0) GOTD 4
C.....MODIFY LOAD VECTOR FOR B.C. ON UPPER BLOCKS.....
DO 3 L=1,NDFRE
IF (IBD(X,L+1).EQ.0) GOTD 3
DO 2 M=1,NDFRE
2 P(M,L)=P(M,L) - DD(L,M,II)*BC(X,L)
3 CONTINUE
C.....
4 IF(Y.EQ.0) GOTD 7
C.....MODIFY LOAD VECTOR FOR B.C. ON LOWER BLOCKS.....
DO 6 L=1,NDFRE
IF (IBD(Y,L+1).EQ.0) GOTD 6
DO 5 M=1,NDFRE
P(M,Z)=P(M,Z)-DD(M,L,II)*BC(Y,L)
5 DD(M,L,II)=0.
6 CONTINUE
C.....
7 IF(X.EQ.0) GOTD 10
DO 9 L=1,NDFRE
IF (IBD(X,L+1).EQ.0) GOTD 9
DO 8 M=1,NDFRE
DD(L,M,II)=0.
8 IF (I.EQ.J.AND.L.EQ.M) DD(M,L,II)=1.
9 CONTINUE
C.....
10 CONTINUE
ZERO=0.001
DO 990 K = 1,IT
IF (QQ(K).NE.J) GO TO 990
DO 900 I = 1,NDFRE
IF (DD(I,I,K).LE.ZERO) DD(I,I,K)=1.0
900 CONTINUE
990 CONTINUE
WRITE (2) (((DD(II,L,M),II=1,5),L=1,5),M=1,IT)
IF(Y.EQ.0) GOTD 14

```

LMB 7/09
LMB 6/25
LMB 6/26
LMB 6/26
LMB 6/26


```

DO 11 K=1,NDFRE
IF(I8D(Y,K+1).EQ.1) PM(K,1)=0.
11 IF(I8D(Y,K+1).EQ.1) P(K,1) = RC(Y,K)
14 WRITE (4) (P(I,1),I=1,5)
WRITE (4) (PM(I,1),I=1,5)
DO 12 I=1,24
DD 12 K=1,NDFRE
PM(K,1)=PM(K,I+1)
12 P(K,I)=P(K,I+1)
RETURN
END

```

LMB 6/26
LMB 6/26

```

SUBROUTINE QDSMEL ( ISHEAR,JSHEAR,LZ,ISKIP,JSKIP )
IMPLICIT REAL*8 (A-H,O-Z)
COMMON/ CV/NUMEL,NUPTS,NUBPTS,IBANOP,MBAND,NBLOC,NDFRE,IFLAG,LVECT
COMMON LLJQ(800)
COMMON IX1(801), IQ(4),NODES,QUADT, NTRI, IX2(2240), PX1(7250),
1 S(37,37), PT(37), TH(3), AD(3,4), BD(3,4),
2 TD(3,36), TR(3,36), T(3,3,4), XMQ(3,3,4), THQ(4),ANG,
3 TPC(6), X(4), Y(4), Z(4), D11, D12, D22, D33, G1, G2, PX3(24),
4 GM, QR(4), AREA, B(3), A(3), XM(3,3), ST(15,15), PX4(504),
5 XS(2,2), SCOND(15,6,4), TG(3,3,4), T0(3,3), TDIS(3,3,3),
6 TRDT(3,3,3), X1, Y1, Z1, X2, Y2, Z2, X3, Y3, Z3,
7 PE(3,5), P1, P2, P3, D1, D2, D3, Q1, Q2, Q3, PX5(300)
C.....
DIMENSION LOCS(10),TX(3,3),IPERM(4),LOCB(15,4),LOCQ(3,5,4),
1 LOCN(5),TP(9),TEMP(3)
DIMENSION TH23(23),TH324(324),S481(481)
EQUIVALENCE (THQ,TH23),(TH(3),TH324),(S(1,21),S481)
EQUIVALENCE (X1,TX),(P1,TP)
DATA LOCQ /
1 1, 2, 3, 6, 7, 8,21,22,23,28,29,35,26,27,34,
2 6, 7, 8,11,12,13,21,22,23,30,31,36,28,29,35,
3 11,12,13,16,17,18,21,22,23,32,33,37,30,31,36,
4 16,17,18, 1, 2, 3,21,22,23,26,27,34,32,33,37 /
DATA LOCB / 1, 2, 3, 4, 5, 6, 7, 8, 9,10,21,22,23,24,25,
1 6, 7, 8, 9,10,11,12,13,14,15,21,22,23,24,25,
2 11,12,13,14,15,16,17,18,19,20,21,22,23,24,25,
3 16,17,18,19,20, 1, 2, 3, 4, 5,21,22,23,24,25 /
DATA LOCS / 1,2,6,7,11,12,16,17,21,22 /
DATA LOCN/1,3,5,7,9/, IPERM /2,3,4,1/
REAL*8 NU,NORM
INTEGER QUADT
C.....TRANSFORMATION MATRICES.....
C.....T(3,3,4).....FROM Z TO ZBAR.....
C.....T(3,3).....FROM Z TO Z0.....
C.....TG(3,3,4).....FROM Z TO Z'.....
C.....TROT(3,3,3).....FROM Z' TO ZBAR.....
C.....TDIS(3,3,3).....FROM ZB TO ZBAR.....
C.....T(3,3,4).....FROM ZB TO Z0.....
C.....COMPUTE INTERNAL MID POINT COORDINATES IF QUAD.....
DO 160 I =1,37
PT(I)=0.
DO 160 J =1,37
160 S(I,J) = 0.
IF ( NODES.GT.2 ) GOTO 500
CALL TRUSS ( IQ,X,Y,Z,THQ(1),THQ(2),S,PT,GM,TPC )
WRITE (1) IQ,NODES,QUADT,NTRI
WRITE (1) TH23
GOTO 1001
500 NTRI=4
IF (IQ(4).LT.1) NTRI=1
IF (NTRI.EQ.1) IADD=10
IF (NTRI.EQ.4) IADD=20
IF (NTRI.EQ.1) TEMP(3)=TPC(3)
IF (NTRI.EQ.4) TEMP(3)=0.25*(TPC(1)+TPC(2)+TPC(3)+TPC(4))
IF (NTRI.EQ.1) TH(3)=THQ(3)
IF (NTRI.EQ.4) TH(3)=(THQ(1)+THQ(2)+THQ(3)+THQ(4))/4.
DO 10 I=1,3
10 LOCQ(I,3,1)=IADD*1
DO 11 I=1,5
11 LOCB(I+10,1)=IADD*I
IF ( D11 .GE. .000001 ) GO TO 1100
XMQ(1,1,1) = 0.0
LMB 7/09
LMB 7/02
LMB 6/26
LMB 6/26

```

```

      XMQ(2,2,1) = 0.0
      GO TO 1000
1100  XC=X(3)
      YC=Y(3)
      ZC=Z(3)
      TP(3)=QP(3)
      IF(NTRI.EQ.1) GOTO 700
      XC = 0.25*(X(1)+X(2)+X(3)+X(4))
      YC = 0.25*(Y(1)+Y(2)+Y(3)+Y(4))
      ZC = 0.25*(Z(1)+Z(2)+Z(3)+Z(4))
      TP(3)=.25*(QP(1)+QP(2)+QP(3)+QP(4))
C.....COMPUTE ELEMENT DIRECTION COSINES, T(I,J,4).....
700  DO 130 N = 1,NTRI
      M = IPERM(N)
      X1 = X(M)-X(N)
      Y1 = Y(M)-Y(N)
      Z1 = Z(M)-Z(N)
      X2 = XC - X(N)
      Y2 = YC - Y(N)
      Z2 = ZC - Z(N)
      S11 = X1*X1+Y1*Y1+Z1*Z1
      S12 = X1*X2+Y1*Y2+Z1*Z2
      S22 = X2*X2+Y2*Y2+Z2*Z2
      COS12 = -S12/S11
      X2 = X2 + X1*COS12
      Y2 = Y2 + Y1*COS12
      Z2 = Z2 + Z1*COS12
      S1 = DSQRT(S11)
      S2 = DSQRT(X2*X2+Y2*Y2+Z2*Z2)
      T(1,1,N) = X1/S1
      T(1,2,N) = Y1/S1
      T(1,3,N) = Z1/S1
      T(2,1,N) = X2/S2
      T(2,2,N) = Y2/S2
      T(2,3,N) = Z2/S2
      T(3,1,N) = T(1,2,N)*T(2,3,N) - T(1,3,N)*T(2,2,N)
      T(3,2,N) = T(1,3,N)*T(2,1,N) - T(1,1,N)*T(2,3,N)
      T(3,3,N) = T(1,1,N)*T(2,2,N) - T(1,2,N)*T(2,1,N)
C.....COMPUTE A'S AND B'S.....
      AD(2,N) = S1*COS12
      AD(3,N) = S1
      AD(1,N) = -AD(3,N)-AD(2,N)
      BD(1,N) = -(S22*COS12*S12)/S2
      BD(2,N) = -BD(1,N)
130  BD(3,N) = 0.
C.....DIRECTION COSINES FOR MID POINT IF ELEMENT IS A TRI.....
      DO 900 I=1,3
      DO 900 J=1,3
      XM(I,J)=0.
      T0(I,J)=TG(I,J,3)
900  TDIS(I,J,3)= T(I,J,1)
      IF(NTRI.EQ.1) GOTO 701
C.....COMPUTE DIRECTION COSINES OF N1,N2 PLANE.....
      CALL QDCOS ( 4,X,Y,Z,T0 )
C.....SUM OVER 4 TRIS. IF QUAD OR 1 TRI. IF ELEMENT IS A TRI.....
701  DO 301 NT = 1,NTRI
      N1 = NT
      N2 = IPERM(N1)
      TH(1)=THQ(N1)
      TH(2)=THQ(N2)
      TEMP(1)=TPC(N1)
      TEMP(2)=TPC(N2)
      TP(1)=QP(N1)

```

```

      TP(2)=QP(N2)
C.....COMPUTE TRANSFORMATIONS FOR EACH POINT OF TRIANGLE.....
      DO 200 I = 1,3
      TP(1+3)=TH(I)*GM
      TP(1+6)=T(I,3,NT)
      A(I) = AD(I,NT)
      B(I) = BD(I,NT)
      T1 = T(I,1,NT)
      T2 = T(I,2,NT)
      T3 = T(I,3,NT)
      DO 200 J = 1,3
      TROT(I,J,1) = T1*TG(J,1,N1) + T2*TG(J,2,N1) + T3*TG(J,3,N1)
      TROT(I,J,2) = T1*TG(J,1,N2) + T2*TG(J,2,N2) + T3*TG(J,3,N2)
      TROT(I,J,3) = T1*T0(J,1) + T2*T0(J,2) + T3*T0(J,3)
      IF(NTRI.EQ.4.OR.IFLAG.EQ.1) TDIS(I,J,3)=TROT(I,J,3)
      IF (IFLAG.EQ.0) GO TO 180
      TDIS(I,J,1) = TROT(I,J,1)
      TDIS(I,J,2) = TROT(I,J,2)
      GO TO 200
180  TDIS(I,J,1) = T(I,J,NT)
      TDIS(I,J,2) = T(I,J,NT)
200  CONTINUE
C.....STORE BASE TRANSFORMATION MATRICES.....
      C=DCOS ( ANG )
      R=DSIN ( ANG )
      IF(NTRI.EQ.1) GOTO 201
      CC=TDIS(1,1,3)
      RR=TDIS(1,2,3)
      CS=DSQRT(CC*CC+RR*RR)
      CC=CC/CS
      RR=RR/CS
      C= CC*DCOS(ANG)-RR*DSIN(ANG)
      R= CC*DSIN(ANG)+RR*DCOS(ANG)
201  CALL SSTQM5 ( C,R,D11,D12,D22,D33,XM )
      XS(1,1)=G1
      XS(2,2)=G2
      XS(1,2)=0.
      XS(2,1)=0.
      KK=(NT-1)*9
      DO 1 K=1,3
      L=KK+(K-1)*3
      DO 1 J=1,3
      XMQ(K,J,NT)=XM(K,J)
      JL=J+L
      DO 1 I=1,3
      TD(I,JL)=TDIS(I,J,K)
1  TR(I,JL)=TROT(I,J,K)
C.....ADJUST TDIS FOR TRANSFORMING TO N COORDINATES.....
      IF(NTRI.EQ.1) GOTO 3
      DO 2 I=1,3
      DO 2 J=1,3
      TDIS(I,J,1)=TDIS(I,J,3)
2  TDIS(I,J,2)=TDIS(I,J,3)
C.....COMPUTE AREA OF TRIANGLE.....
3  AREA = A(3)*B(2) - A(2)*B(3)
C.....FORM AND TRANSFORM MEMBRANE STIFFNESS TO BASE SYSTEM IF A TRI.....
C.....FORM AND TRANSFORM MEMBRANE STIFFNESS TO Z0 SYSTEM IF A QUAD....
      IF ( QUADT.GT.0 ) GOTO 5000
      IF(NTRI.EQ.1) CALL CLST10 (3,3)
      IF(NTRI.EQ.4) CALL CLST10 (5,1)
      IEND=3
      IF(NTRI.EQ.4) IEND=5
      DO 27 II=1,IEND

```

```

I=LOCM(II)
IF(II.LT.4) IL=II
DO 27 JJ=I,II
J=LOCM(JJ)
IF(JJ.LT.4) JL=JJ
LS=1
DO 27 K=1,J
N=LOCQ(K,JJ,NT)
M1=ST(I ,J)*TDIS(1,K,JL)+ST(I ,J+1)*TDIS(2,K,JL)
M2=ST(I+1,J)*TDIS(1,K,JL)+ST(I+1,J+1)*TDIS(2,K,JL)
IF(I.EQ.J) LS=K
DO 27 L=LS,3
M=LOCQ(L,II,NT)
S(M,N)=S(M,N)+TDIS(1,L,IL)*M1+TDIS(2,L,IL)*M2
27 S(N,M)=S(M,N)
C.....FORM AND TRANSFORM PLATE STIFFNESS TO BASE SYSTEM IF A TRI.....
C.....FORM AND TRANSFORM PLATE STIFFNESS TO Z0 SYSTEM IF A QUAD.....
5000 IF ( LZ.LT.ISKIP .OR. LZ.GT.JSKIP ) GOTD 6002
GOTO 301
6002 CALL SLCTT ( 9,ISHEAR,NT )
DO 300 II = 1,3
K = 3*II - 2
KK = 5*(II-1)
DO 300 JJ = II,3
L = 3*JJ - 2
LL = 5*(JJ-1)
DO 300 M = 1,5
J = LL + M
JS = LOCB(J,NT)
IF (M.GT.3) GO TO 270
T3 = TDIS(3,M,JJ)
M1 = ST(K, L)*T3
M2 = ST(K+1,L)*T3
M3 = ST(K+2,L)*T3
GO TO 280
270 T1 = TROT(1,M-3,JJ)
T2 = TRDT(2,M-3,JJ)
M1 = ST(K, L+1)*T1 + ST(K, L+2)*T2
M2 = ST(K+1,L+1)*T1 + ST(K+1,L+2)*T2
M3 = ST(K+2,L+1)*T1 + ST(K+2,L+2)*T2
280 DO 300 N = 1,5
I = KK + N
IF (I.GT.J) GO TO 300
IS = LOCB(I,NT)
IF (N.GT.3) GO TO 290
S(IS,JS) = S(IS,JS) + M1*TDIS(3,N,II)
GO TO 295
290 S(IS,JS) = S(IS,JS) + M2*TROT(1,N-3,II) + M3*TROT(2,N-3,II)
295 S(JS,IS) = S(IS,JS)
300 CONTINUE
CALL NLOAD (Q1,Q2,Q3,P1,P2,P3,D1,D2,D3,PE,AREA,A,B,TEMP,TPC(5),TH)
DO 800 I=1,3
K=I
IF(NTRI.EQ.4) K=3
Q1=PE(1,I)
Q2=PE(2,I)
Q3=PE(3,I)
DO 800 J=1,3
L=LOCQ(J,I,NT)
800 PT(L)=PT(L)+TDIS(1,J,K)*Q1+TDIS(2,J,K)*Q2+TDIS(3,J,K)*Q3
301 CONTINUE
IF(NTRI.EQ.1) GOTD 1000
IF ( QUADT.GT.0 ) GOTD 5001

```

```

C.....ELIMINATE TRANSL. COMPONENTS NORMAL TO N1,N2 PLANE OF MIDSIDE NODE
DO 34 I=1,37
S(I, 3)=S(I, 3)+S(I,34)/2.
S(I, 8)=S(I, 8)+S(I,35)/2.
S(I,13)=S(I,13)+S(I,36)/2.
S(I,18)=S(I,18)+S(I,37)/2.
34 S(I,23)=S(I,23)+(S(I,34)+S(I,35)+S(I,36)+S(I,37))/2.
DO 35 J=1,37
S( 3,J)=S( 3,J)+S(34,J)/2.
S( 8,J)=S( 8,J)+S(35,J)/2.
S(13,J)=S(13,J)+S(36,J)/2.
S(18,J)=S(18,J)+S(37,J)/2.
35 S(23,J)=S(23,J)+(S(34,J)+S(35,J)+S(36,J)+S(37,J))/2.
GOTO 5004
5001 DO 5002 I=1,4
Q1 = X(I)
Q2 = Y(I)
Q3 = Z(I)
X(I)=T0(1,1)*Q1+T0(1,2)*Q2+T0(1,3)*Q3
5002 Y(I)=T0(2,1)*Q1+T0(2,2)*Q2+T0(2,3)*Q3
CALL SSTQMS (DCOS(ANG),DSIN(ANG),D11,D12,D22,D33,XM )
DO 5005 I=1,3
DO 5005 J=1,3
5005 XM(I,J)=XMQ(I,J,1)*TH(3)
CALL QMSSTF ( X,Y,XM,ST )
DO 5003 I=1,10
II=LOC5(I)
DO 5003 J=1,10
JJ=LOC5(J)
5003 S(II,JJ)=S(II,JJ)+ST(II,J)
DO 5500 I = 1, 16, 5
PT(I) = PT(I) + PT(21)/4.
5500 PT(I+1) = PT(I+1) + PT(22)/4.
PT(21) = 0.0
PT(22) = 0.0
C.....CONDENSE INTERNAL DEGREES OF FREEDOM.....
5004 IF ( LZ.LT.ISKIP.OR.LZ.GT.JSKIP ) GOTD 6001
DO 6000 J=23,25
DO 6000 I= 1,33
S(I,J)=0.
S(J,I)=0.
IF ( I.EQ.J ) S(I,J)=1.
6000 CONTINUE
6001 NDOFQ = 33
IF ( QUADT.GT.0 ) NDOFQ=25
NDOFC = 13
IF (QUADT.GT.0) NDOFC = 5
DO 400 N =1,NDOFC
K=NDOFQ-N
L = K + 1
PIVOT = S(L,L)
DO 400 I = 1,K
C = S(I,L)/PIVOT
PT(I)=PT(I)-C*PT(L)
S(I,L) = C
DO 400 J = I,K
S(I,J) = S(I,J) - C*S(L,J)
400 S(J,I) = S(I,J)
C.....ESTABLISH TRANSFORMATION FROM BASE COORDS. TO N1,N2 PLANE.....
IF(IFLAG.EQ.1) GOTD 39
DO 38 L=1,4
DO 38 I=1,3
DO 38 J=1,3

```

LMB 7/02
LMB 7/02
LMB 7/02

LMB 7/02
LMB 7/02
LMB 7/02
LMB 7/02

```

38 T(I,J,L)=T0(I,J)
GOTO 41
39 DO 40 L=1,4
DO 40 I=1,3
DO 40 J=1,3
T(I,J,L)=0.
DO 40 K=1,3
40 T(1,J,L)=T(I,J,L)+T0(I,K)*TG(J,K,L)
C.....TRANSFORM THE 4 EXTERIOR NODES TO THE BASE SYSTEM.....
41 K=0
DO 43 II=1,16,5
K=K+1
DO 42 I=1,3
DO 42 J=1,3
42 TX(I,J)=T(I,J,K)
Q1=PT(II )
Q2=PT(II+1)
Q3=PT(II+2)
PT(II )=X1*Q1+Y1*Q2+Z1*Q3
PT(II+1)=X2*Q1+Y2*Q2+Z2*Q3
PT(II+2)=X3*Q1+Y3*Q2+Z3*Q3
DO 43 I=II,20
F=S(I,II )
G=S(I,II+1)
H=S(I,II+2)
S(I,II )=F*X1+G*Y1+H*Z1
S(I,II+1)=F*X2+G*Y2+H*Z2
43 S(I,II+2)=F*X3+G*Y3+H*Z3
K=0
DO 45 II=3,18,5
K=K+1
DO 44 I=1,3
DO 44 J=1,3
44 TX(J,I)=T(I,J,K)
DO 45 J=1,II
F=S(II-2,J)
G=S(II-1,J)
H=S(II ,J)
S(II-2,J)=X1*F+X2*G+X3*H
S(II-1,J)=Y1*F+Y2*G+Y3*H
45 S(II ,J)=Z1*F+Z2*G+Z3*H
DO 46 J=1,20
DO 46 I=J,20
46 S(J,I)=S(I,J)
1000 WRITE (1) IQ,NODES,QUAOT,NTRI LMB 6/26
TPC(5)=TEMP(3) LMB 6/26
WRITE (1) TH324 LMB 6/26
IF(QUAOT.GT.0) WRITE (1) X,Y LMB 6/26
IF(JSHEAR.EQ.6) WRITE (1) SCONO LMB 6/26
IF(NODES.EQ.4) WRITE (1) S4B1 LMB 6/26
IF(NODES.EQ.4) WRITE (1) (PT(I),I=21,33) LMB 6/26
1001 RETURN
END

```

```

SUBROUTINE TRUSS(IQ,X,Y,Z,AREA,E,S,PT,GM,TEMP)
IMPLICIT REAL*8 (A-H,O-Z)
DIMENSION IQ(4), X(4), Y(4), Z(4), S(37,37),PT(37)
DIMENSION A(3,3), LQ(6), TEMP(6)
DATA LQ / 3*0,3*2 /
EQUIVALENCE (A(1,1),X1),(A(2,1),Y1),(A(3,1),Z1),
1 (A(1,2),X2),(A(2,2),Y2),(A(3,2),Z2),
2 (A(1,3),X3),(A(2,3),Y3),(A(3,3),Z3)
REAL*8 L,L1,L2,L3,IY,IZ
DO 1 I=1,37
DO 1 J=1,37
1 S(I,J)=0.
L=DSQRT((X(1)-X(2))**2+(Y(1)-Y(2))**2+(Z(1)-Z(2))**2)
L1=E/L
L2=E/L**2
L3=E/L**3
S( 1, 1)=AREA*L1
S( 6, 1)=-AREA*L1
S( 1, 6)=S( 6, 1)
S( 6, 6)=AREA*L1
L1=X(2)-X(1)
L2=Y(2)-Y(1)
L3=Z(2)-Z(1)
M1=DSQRT(L1**2+L2**2)
C1=1.
S1=0.
IF(M1.GT..000001) C1=L1/M1
IF(M1.GT..000001) S1=L2/M1
C2=M1/L
S2=-L3/L
A(1,1)=L1/L
A(1,2)=L2/L
A(1,3)=L3/L
A(2,1)=-S1
A(2,2)= C1
A(2,3)= 0.
A(3,1)=C1*S2
A(3,2)= S1*S2
A(3,3)=C2
DO 4 II=1, 6,3
N = II + LQ(II)
DO 4 I=II, 6
M = I + LQ(II)
F=S(M, N )
G=S(M, N+1)
H=S(M, N+2)
S(M, N )=F*X1+G*Y1+H*Z1
S(M, N+1)=F*X2+G*Y2+H*Z2
4 S(M, N+2)=F*X3+G*Y3+H*Z3
DO 5 II=3, 6,3
M = II + LQ(II)
DO 5 J=1,II
N = J + LQ(J)
F=S( M-2,N)
G=S( M-1,N)
H=S( M ,N)
S( M-2,N)=F*X1+G*Y1+H*Z1
S( M-1,N)=F*X2+G*Y2+H*Z2
5 S( M ,N)=F*X3+G*Y3+H*Z3
DO 6 J=1,10
DO 6 I=J,10
6 S(J,I)=S(I,J)

```

LMB 7/09

22MAR75
22MAR75

LMB 7/09

```

AVTP = 0.5*(TEMP(1)+TEMP(2))
PP= E*TEMP(6)*AREA*AVTP
OO 10 I=1,6,5
PP=-PP
PT(I)=PP*C2*C1
PT(I+1)=PP*C2*S1
10 PT(I+2)= (PP*S2)+GM*L*AREA*0.5
7 RETURN
END

```

```

SUBROUTINE SSTQMS ( C,R,D11,D12,D22,D33,XM )
IMPLICIT REAL*8 (A-M,O-Z)
DIMENSION XM(3,3)
201 S4=R**4
C4=C**4
S2C2=R*R*C*C
SC3=R*C**3
S3C=R**3*C
XM(1,1)=C4*D11+S4*D22+S2C2*(2.*D12+4.*D33)
XM(2,1)=(S4+C4)*D12+S2C2*(D11+D22-4.*D33)
XM(3,1)=SC3*(-D11+D12+2.*D33)+S3C*(-D12+D22-2.*D33)
XM(2,2)=S4*D11+C4*D22+S2C2*(2.*D12+4.*D33)
XM(3,2)=SC3*(-D12+D22-2.*D33)+S3C*(-D11+D12+2.*D33)
XM(3,3)=(C4+S4)*D33+S2C2*(D11-2.*D12+D22-2.*D33)
XM(1,2)=XM(2,1)
XM(1,3)=XM(3,1)
XM(2,3)=XM(3,2)
RETURN
END

```

```

22MAR75
22MAR75
22MAR75
22MAR75
22MAR75
22MAR75
22MAR75

```

LMB 7/09

```

SUBROUTINE QMSSTF ( X,Y,DD,QQ )
IMPLICIT REAL*8 (A-M,O-Z)
C
C..... QM5 MEMBRANE STIFFNESS MATRIX FOR A GENERAL QUAD
C
DIMENSION X(4),Y(4),DD(3,3),QQ(15,15)
DIMENSION QC(3,10),SS(4),TT(4)
DATA SS /-1.,1.,1.,-1./, TT /-1.,-1.,1.,1./
DO 6 I=1,15
DO 6 J=1,15
6 QQ(I,J) = 0.0
R12 = X(1) - X(2)
R13 = X(1) - X(3)
R14 = X(1) - X(4)
R23 = X(2) - X(3)
R24 = X(2) - X(4)
R34 = X(3) - X(4)
Z12 = Y(1) - Y(2)
Z13 = Y(1) - Y(3)
Z14 = Y(1) - Y(4)
Z23 = Y(2) - Y(3)
Z24 = Y(2) - Y(4)
Z34 = Y(3) - Y(4)
VOL=R13*Z24-R24*Z13
CALL QM5C2 ( R13,R24,Z13,Z24,VOL,X5,X6,X7,X8,Y5,Y6,Y7,Y8 )
DO 30 I=1,4
S=SS(I)*0.577350269189626
T=TT(I)*0.577350269189626
CALL QM5C1 ( S,T,R12,R13,R14,R23,R24,R34,Z12,Z13,Z14,Z23,Z24,Z34,
* VOL,X1,X2,X3,X4,XC,Y1,Y2,Y3,Y4,YC,XJAC,X(1),X(2),
* X(3),X(4),Y(1),Y(2),Y(3),Y(4) )
C..... FORM STIFFNESS QQ
DO 10 I = 1, 3
D1 = DD(I,1)*XJAC
D2 = DD(I,2)*XJAC
D4 = DD(I,3)*XJAC
QC(I,1)= D1*Y1+D4*X5
QC(I,3)= D1*Y2+D4*X6
QC(I,5)= D1*Y3+D4*X7
QC(I,7)= D1*Y4+D4*X8
QC(I,9)= D1*YC
QC(I,2)= D2*X1+D4*Y5
QC(I,4)= D2*X2+D4*Y6
QC(I,6)= D2*X3+D4*Y7
QC(I,8)= D2*X4+D4*Y8
QC(I,10)= D2*XC
10 CONTINUE
DO 20 I=1,10
D1=QC(1,I)
D2=QC(2,I)
D4=QC(3,I)
QQ(1,I)=QQ(1,I)+D1*Y1+D4*X5
QQ(3,I)=QQ(3,I)+D1*Y2+D4*X6
QQ(5,I)=QQ(5,I)+D1*Y3+D4*X7
QQ(7,I)=QQ(7,I)+D1*Y4+D4*X8
QQ(9,I)=QQ(9,I)+D1*YC
QQ(2,I)=QQ(2,I)+D2*X1+D4*Y5
QQ(4,I)=QQ(4,I)+D2*X2+D4*Y6
QQ(6,I)=QQ(6,I)+D2*X3+D4*Y7
QQ(8,I)=QQ(8,I)+D2*X4+D4*Y8
QQ(10,I)=QQ(10,I)+D2*XC
20 CONTINUE
C
30 CONTINUE
RETURN
END

```

LMB 7/09

LMB 6/25
LMB 6/25
LMB 6/25

```

SUBROUTINE QM5C1 ( S,T,R12,R13,R14,R23,R24,R34,Z12,Z13,Z14,Z23,
.      Z24,Z34,VOL,X1,X2,X3,X4,XC,Y1,Y2,Y3,Y4,YC,XJAC,R1,R2,
.      R3,R4,Z1,Z2,Z3,Z4 )
C..... THIS ROUTINE IS CALLED BY QM5 STIFFNESS AND STRESS ROUTINES
IMPLICIT REAL*8 (A-H,O-Z)
XJ =VOL*S*(R34*Z12-R12*Z34)+T*(R23*Z14-R14*Z23)
XJAC=XJ/8.0
SM=1.0-S
SP=1.0-S
TM=1.0-T
TP=1.0-T
X1=(-R24+R34*S+R23*T)/XJ
X2=( R13-R34*S-R14*T)/XJ
X3=( R24-R12*S+R14*T)/XJ
X4=(-R13+R12*S-R23*T)/XJ
Y1=( Z24-Z34*S-Z23*T)/XJ
Y2=(-Z13+Z34*S+Z14*T)/XJ
Y3=(-Z24+Z12*S-Z14*T)/XJ
Y4=( Z13-Z12*S+Z23*T)/XJ
RS=0.25*(-TM*R1+TM*R2+TP*R3-TP*R4)
ZS=0.25*(-TM*Z1+TM*Z2+TP*Z3-TP*Z4)
RT=0.25*(-SM*R1-SP*R2+SP*R3+SM*R4)
ZT=0.25*(-SM*Z1-SP*Z2+SP*Z3+SM*Z4)
XC=-2.0*(T*SM*SP*RS-S*TM*TP*RT)/XJAC
YC= 2.0*(T*SM*SP*ZS-S*TM*TP*ZT)/XJAC
RETURN
END

```

LMB 7/09

```

SUBROUTINE QM5C2 ( R13,R24,Z13,Z24,VOL,X5,X6,X7,X8,Y5,Y6,Y7,Y8 )
IMPLICIT REAL*8 (A-H,O-Z)
C..... THIS ROUTINE IS CALLED BY QM5 STIFFNESS AND STRESS ROUTINES
Y5 = Z24/VOL
X6 = R13/VOL
X7 = R24/VOL
Y8 = Z13/VOL
X5 =-X7
Y6 =-Y8
Y7 =-Y5
X8 =-X6
RETURN
END

```

LMB 7/09

```

SUBROUTINE CLST10 (LNODES,LSIDES)
IMPLICIT REAL*8 (A-H,O-Z)
COMMON LLJQ(800)
COMMON 1X1(3048), PX1(8656), TH(3), PX2(370), AREA, B(3,2),
1      XM(3,3), S(15,15), X(3,5), Y(3,5), X1, X2, X3, X4, X5,
2      X6, X7, X8, X9, Y4, Y5, Y6, Y7, Y8, Y9, T(3,3),
3      TU1(3,5), TU2(3,5), PX3(1216)
DIMENSION U(3,5,2),V(9),W(6),LO(10),IPERM(3)
EQUIVALENCE (X1,V),(Y4,W),(X,U),(TH(1),T1),(TH(2),T2),(TH(3),T3)
DATA LO/1,3,5,7,9,2,4,6,8,10/,IPERM/2,3,1/
FAC=1./((120.*AREA)
T(1,1)=(6.*T1+2.*T2+2.*T3)*FAC
T(1,2)=(2.*T1+2.*T2+ T3)*FAC
T(1,3)=(2.*T1+ T2+2.*T3)*FAC
T(2,2)=(2.*T1+6.*T2+2.*T3)*FAC
T(2,3)=( T1+2.*T2+2.*T3)*FAC
T(3,3)=(2.*T1+2.*T2+6.*T3)*FAC
T(2,1)=T(1,2)
T(3,1)=T(1,3)
T(3,2)=T(2,3)
DO 1 I=1,2
U(1,1,I)= B(1,I)-2.*B(3,I)
U(2,1,I)= B(1,I)
U(3,1,I)= -B(1,I)
U(1,2,I)= B(2,I)
U(2,2,I)= B(2,I)-2.*B(3,I)
U(3,2,I)=-B(2,I)
U(1,3,I)=-B(3,I)
U(2,3,I)=-B(3,I)
U(3,3,I)=3.*B(3,I)
U(1,4,I)=0.
U(2,4,I)=4.*B(3,I)
U(3,4,I)=4.*B(2,I)
U(1,5,I)=4.*B(3,I)
U(2,5,I)=0.
1 U(3,5,I)=4.*B(1,I)
IF(LSIDES.EQ.1) GOTO 11
DO 10 M=2,LSIDES
L=IPERM(M)
DO 10 I=1,3
DO 10 K=1,2
U(I,M,K)=U(I,M,K)+U(I,M+2,K)*.5
10 U(1,L,K)=U(1,L,K)+U(I,M+2,K)*.5
11 DO 2 I=1,3
DO 2 J=1,LNODES
TU1(I,J)=0.
TU2(I,J)=0.
DO 2 K=1,3
TU1(1,J)=TU1(I,J)+T(I,K)*X(K,J)

```

LMB 7/09

```

2 TU2(I,J)=TU2(I,J)+T(I,K)*Y(K,J)
DO 5 J=1,LNODES
M=L0(J)
L=L0(J+5)
DO 3 N=1,3
U1=TU1(N,J)
U2=TU2(N,J)
V(N)=XM(1,1)*U1+XM(3,1)*U2
V(N+3)=XM(2,1)*U1+XM(3,2)*U2
V(N+6)=XM(3,1)*U1+XM(3,3)*U2
W(N)=XM(2,2)*U2+XM(3,2)*U1
3 W(N+3)=XM(3,2)*U2+XM(3,3)*U1
DO 4 I=J,LNODES
N=L0(I)
K=L0(I+5)
S(N,M)=X(1,I)*X1+X(2,I)*X2+X(3,I)*X3+Y(1,I)*X7+Y(2,I)*X8+Y(3,I)*X9
S(M,N)=S(N,M)
S(K,L)=Y(1,I)*Y4+Y(2,I)*Y5+Y(3,I)*Y6+X(1,I)*Y7+X(2,I)*Y8+X(3,I)*Y9
4 S(L,K)=S(K,L)
DO 5 I=1,LNODES
K=L0(I+5)
S(K,M)=Y(1,I)*X4+Y(2,I)*X5+Y(3,I)*X6+X(1,I)*X7+X(2,I)*X8+X(3,I)*X9
5 S(M,K)=S(K,M)
RETURN
END

```

```

SUBROUTINE SLCCCT ( NBF,NSF,NT )
IMPLICIT REAL*8 (A-H,O-Z)
COMMON LLJQ(800)
COMMON IX1(3048), PX1(8656), TH(3), PX2(370), AREA, B(3),
1 A(3), XM(3,3), ST(15,15), PX3(84), P(21,15), H(21),
2 U(21), Q(3,6), TX(3), TY(3), HT(3), T(3,3,3), QS(3,3),
3 XS(2,2), SCOND(15,6,4), PX4(432)
DIMENSION IPERM(3),NKN(4,3)
DATA IPERM/2,3,1/, NKN/2,5,3,6, 8,2,9,3, 5,8,6,9/
NDF=NBF+NSF
T0 = (TH (1)+TH (2)+TH (3))/3.
FAC = T0**3*AREA/15120.
DO 150 I = 1,3
J = IPERM(I)
K=IPERM(J)
X = A(I)**2+B(I)**2
U(I) = -(A(I)*A(J)+B(I)*B(J))/X
X =OSQRT(X)
HT(I) = 4.0*AREA/X
TY(I) = -0.5*B(I)/X
TX(I) = 0.5*A(I)/X
A1 = A(I)/AREA
A2 = A(J)/AREA
B1 = B(I)/AREA
B2 = B(J)/AREA
Q(1,I) = B1*B1
Q(2,I) = A1*A1
Q(3,I) = 2.*A1*B1
Q(1,I+3) = 2.*B1*B2
Q(2,I+3) = 2.*A1*A2
Q(3,I+3) = 2.*(A1*B2+A2*B1)
QS(I,I) = T0/20.*TH (I)/30.
QS(J,K) = TJ/20.-TH (I)/120.
QS(K,J) = QS(J,K)
X=TH (I)/T0
Y=TH (J)/T0
X2=X**2
Y2=Y**2
XY=X*Y
T(1,1,I)=X2*(10.*X+6.*Y+6.)+Y2*(3.*X+Y+1.)+3.*X+Y+3.*XY+1.
T(2,2,I)=X2*(X+3.*Y+1.)+Y2*(6.*X+10.*Y+6.)+X+3.*Y+3.*XY+1.
T(3,3,I)=X2*(X+Y+3.)+Y2*(X+Y+3.)+6.*X+6.*Y+3.*XY+10.
T(1,2,I)=X2*(2.*X+3.*Y+1.5)+Y2*(3.*X+2.*Y+1.5)+X+Y+2.*XY+.5
T(1,3,I)=X2*(2.*X+1.5*Y+3.)+Y2*(X+.5*Y+1.)+3.*X+1.5*Y+2.*XY+2.
T(2,3,I)=X2*(.5*X+Y+1.)+Y2*(1.5*X+2.*Y+3.)+1.5*X+3.*Y+2.*XY+2.
T(2,1,I)=T(1,2,I)
T(3,1,I)=T(1,3,I)
150 T(3,2,I)=T(2,3,I)
DO 200 I = 1,3
J = IPERM(I)
K = IPERM(J)
II = 3*I
JJ = 3*J
KK = 3*K
A1 = A(I)
A2 = A(J)
A3 = A(K)
B1 = B(I)
B2 = B(J)
B3 = B(K)
U1 = U(II)
U2 = U(JJ)
U3 = U(KK)

```

LMB 7/09

```

W1 = 1.-U1
W2 = 1.-U2
W3 = 1.-U3
B1D = 2.*B1
B2D = 2.*B2
B3D = 2.*B3
A1D = 2.*A1
A2D = 2.*A2
A3D = 2.*A3
C21 = B1-B3*U3
C22 = -B1D+B2*W2+B3*U3
C31 = A1-A3*U3
C32 = -A1D+A2*W2+A3*U3
C51 = B3*W3-B2
C52 = B2D-B3*W3-B1*U1
C61 = A3*W3-A2
C62 = A2D-A3*W3-A1*U1
C81 = B3-B2D-B2*U2
C82 = B1D-B3*B1*W1
C91 = A3-A2D-A2*U2
C92 = A1D-A3*A1*W1
DO 200 N = 1,3
L = 6*(I-1) + N
Q11 = Q(N,I)
Q22 = Q(N,J)
Q33 = Q(N,K)
Q12 = Q(N,I+3)
Q23 = Q(N,J+3)
Q31 = Q(N,K+3)
Q2333 = Q23-Q33
Q3133 = Q31-Q33
P(L ,I1-2) = 6.*(Q11+W2*Q33+U3*Q2333)
P(L ,I1-1) = C21*Q23+C22*Q33-B3D*Q12+W2D*Q31
P(L ,I1 ) = C31*Q23+C32*Q33-A3D*Q12+A2D*Q31
P(L ,JJ-2) = 6.*(Q22+W3*Q2333)
P(L ,JJ-1) = C51*Q2333+B3D*Q22
P(L ,JJ ) = C61*Q2333+A3D*Q22
P(L ,KK-2) = 6.*(1.+U2)*Q33
P(L ,KK-1) = C81*Q33
P(L ,KK ) = C91*Q33
P(L ,I+9 ) = 0.
P(L ,J+9 ) = HT(J)*Q33
P(L ,K+9 ) = HT(K)*Q2333
P(L+3 ,I1-2) = 6.*(Q11+U3*Q3133)
P(L+3 ,I1-1) = C21*Q3133-B3D*Q11
P(L+3 ,I1 ) = C31*Q3133-A3D*Q11
P(L+3 ,JJ-2) = 6.*(Q22+U1*Q33+W3*Q3133)
P(L+3 ,JJ-1) = C51*Q31+C52*Q33+B3D*Q12-B1D*Q23
P(L+3 ,JJ ) = C61*Q31+C62*Q33+A3D*Q12-A1D*Q23
P(L+3 ,KK-2) = 6.*(1.+W1)*Q33
P(L+3 ,KK-1) = C82*Q33
P(L+3 ,KK ) = C92*Q33
P(L+3 ,I+9 ) = HT(I)*Q33
P(L+3 ,J+9 ) = 0.
P(L+3 ,K+9 ) = HT(K)*Q3133
P(N+18,I1-2) = 2.*(Q11+U3*Q12+W2*Q31)
P(N+18,KK-1) = ((B1D-B2D)*Q33+C82*Q23+C81*Q31)/3.
P(N+18,KK ) = ((A1D-A2D)*Q33+C92*Q23+C91*Q31)/3.
200 P(N+18,K+9 ) = HT(K)*Q12/3.
NK = 12 - NBF
IF (NK.LE.0) GO TO 240
DO 220 N = 1,NK
K = 13 - N

```

```

DO 220 L = 1,4
J = NKN(L,N)
IF (L.LE.2) C = TX(K-9)
IF (L.GT.2) C = TY(K-9)
DO 220 I = 1,21
220 P(I,J) = P(I,J) + C*P(I,K)
240 IF(NSF.LE.0) GO TO 300
DO 260 K = 1,3
J = K + NBF
L = 3*K
A1 = A(K)/AREA
B1 = B(K)/AREA
DO 260 I = 1,19,3
P(I ,J ) = P(I ,L ) + B1
P(I+1,J ) = P(I+1,L )
P(I+2,J ) = P(I+2,L ) + A1
P(I ,J+3) = -P(I ,L-1)
P(I+1,J+3) = -P(I+1,L-1) + A1
260 P(I+2,J+3) = -P(I+2,L-1) + B1
300 DO 400 J=1,NDF
DO 340 L=19,21
H(L)=0.
DO 340 M=1,3
N=(M-4)*6+L
H(N ) = T(1,1,M)*P(N,J)+T(1,2,M)*P(N+3,J)+T(1,3,M)*P(L,J)
H(N+3) = T(2,1,M)*P(N,J)+T(2,2,M)*P(N+3,J)+T(2,3,M)*P(L,J)
340 H(L )=H(L)+T(3,1,M)*P(N,J)+T(3,2,M)*P(N+3,J)+T(3,3,M)*P(L,J)
DO 360 N = 1,19,3
U(N )=XM(1,1)*H(N)+XM(2,1)*H(N+1)+XM(3,1)*H(N+2)
U(N+1)=XM(2,1)*H(N)+XM(2,2)*H(N+1)+XM(3,2)*H(N+2)
360 U(N+2)=XM(3,1)*H(N)+XM(3,2)*H(N+1)+XM(3,3)*H(N+2)
DO 400 I = 1,J
X = 0.
DO 380 N = 1,21
X = X + U(N)*P(N,I)
ST(I,J) = X*FAC
400 ST(J,I) = ST(I,J)
IF(NSF.LE.0) GO TO 1000
DO 550 K = 1,3
I = K + NBF
DO 550 L = 1,3
FAC = QS(K,L)*AREA
J = L + NBF
ST(I ,J ) = ST(I ,J ) + FAC*XS(1,1)
ST(I+3,J+3) = ST(I+3,J+3) + FAC*XS(2,2)
ST(I ,J+3) = ST(I ,J+3) + FAC*XS(1,2)
550 ST(J+3,I ) = ST(I ,J+3)
DO 600 N = 1,6
K = 15 - N
L = K + 1
PIVOT = ST(L,L)
DO 600 I = 1,K
C = ST(I,L)/PIVOT
ST(I,L) = C
DO 600 J = I,K
ST(I,J)=ST(I,J)-C*ST(L,J)
600 ST(J,I)=ST(I,J)
DO 700 I=1,15
DO 700 J=1,6
700 SCOND(I,J,NT)=ST(I,J+9)
1000 RETURN
END

```



```

SUBROUTINE QOCOS (N,X,Y,Z,T)
IMPLICIT REAL*8 (A-H,O-Z)
LMB 7/09

THIS SUBROUTINE COMPUTES THE DIRECTION COSINES OF THE LOCAL
ELEMENT SYSTEM OF A QUADRILATERAL (N=4) OR SINGLE TRIANGLE (N=1)

DIMENSION X(1), Y(1), Z(1), T(1)
X1 = X(2)+X(3)-X(N)-X(1)
Y1 = Y(2)+Y(3)-Y(N)-Y(1)
Z1 = Z(2)+Z(3)-Z(N)-Z(1)
X2 = X(3)+X(N)-X(1)-X(2)
Y2 = Y(3)+Y(N)-Y(1)-Y(2)
Z2 = Z(3)+Z(N)-Z(1)-Z(2)
S1 = X1**2+Y1**2+Z1**2
C = (X1*X2+Y1*Y2+Z1*Z2)/S1
X2 = X2 - C*X1
Y2 = Y2 - C*Y1
Z2 = Z2 - C*Z1
S1 = DSQRT (S1)
S2 = DSQRT (X2**2+Y2**2+Z2**2)
X1 = X1/S1
Y1 = Y1/S1
Z1 = Z1/S1
X2 = X2/S2
Y2 = Y2/S2
Z2 = Z2/S2
T(1) = X1
T(2) = X2
T(3) = Y1*Z2-Y2*Z1
T(4) = Y1
T(5) = Y2
T(6) = Z1*X2-Z2*X1
T(7) = Z1
T(8) = Z2
T(9) = X1*Y2-X2*Y1
RETURN
END

```

```

SUBROUTINE NLOAD ( X,Y,Z,P1,P2,P3,D1,D2,D3,PE,AREA ,
A,B,TEMP,FAC,TH)
LMB 7/09
1
IMPLICIT REAL*8 (A-H,O-Z)
DIMENSION PE (3,5),Q(3,3),TEMP(3),TH(3),A(3),B(3)
Q(1,1)=D1*X
Q(1,2)=D2*X
Q(1,3)=D3*X
Q(2,1)=D1*Y
Q(2,2)=D2*Y
Q(2,3)=D3*Y
Q(3,1)=D1*Z+P1
Q(3,2)=D2*Z+P2
Q(3,3)=D3*Z+P3
D=AREA/24.
DO 1 I=1,3
PE(I,1)=(2.*Q(I,1)+ Q(I,2)+ Q(I,3))*D
PE(I,2)=( Q(I,1)+2.*Q(I,2)+ Q(I,3))*D
1 PE(I,3)=( Q(I,1)+ Q(I,2)+2.*Q(I,3))*D
SUMF=0.
TP=TEMP(1)+TEMP(2)+TEMP(3)
DO 10 I = 1,3
SUMF = SUMF+TH(I)*(TP*TEMP(I))
FACT=FAC*SUMF
DO 20 I =1,3
PE(1,I)=FACT*B(I)+PE(1,I)
20 PE(2,I)=FACT*A(I)+PE(2,I)
RETURN
END

```

```

SUBROUTINE OVER3
IMPLICIT REAL*8 (A-H,O-Z)
COMMON/CV/NUMEL,NUPTS,NUBPTS,IBANDP,MBAND,NBLOC,NDFRE,NODES,LVECT
COMMON/SS/IGEN,JSHEAR,JSHEAR,NRED,IREACT,NTRUSS,ISIG
COMMON M,N,PK1,P(100,3),B(100,3),A(100,100),Q(300)
DIMENSION PV(5,850,3)
EQUIVALENCE (P(1,1),PV(1,1,1))
IRED=0
M=MBAND
N=NBLOC
M1=M-1
DO 1 I=1,M
DO 1 J=1,M
1 A(I,J)=0.
CALL CHOL(M1)
CALL WIND (1,4)
CALL FPASS (M1)
CALL BPASS (M1)
CALL QTAPE (-1,4,PV,Q,0)
CALL WIND (3,1)
CALL RLOAD (1,3,PV,1,LVECT,850)
IF(LVECT.EQ.1) GO TO 4
DO 8 LV=1,LVECT
PRINT 13, LV
PRINT 11
DO 8 K=1,NUPTS
8 PRINT 12,K,(PV(J,K,LV),J=1,NDFRE)
GO TO 20
4 IRED=IRED+I
CALL RESID (M1,IRED,NRED,IREACT)
IF (IRED.LT.NRED) GOTO 4
11 FORMAT(5H0NODE2X,2HD1 11X,2HD2 11X,2HD3 11X,2HD4 11X,2HD5)
12 FORMAT(I4,1P5E13.4)
13 FORMAT(1H1,2HDISPLACEMENTS FOR LOAD CASE 15,17H INITIAL SOLUTION)
20 RETURN
END

```

LMB 7/09
LMB 7/09

```

SUBROUTINE FORMK(II,M1)
IMPLICIT REAL*8 (A-H,O-Z)
COMMON/CV/NUMEL,NUPTS,NUBPTS,IBANDP,MBAND,NBLOC,NDFRE,NODES,LVECT
COMMON/SS/IGEN,JSHEAR,JSHEAR,NRED,IREACT,NTRUSS,ISIG
COMMON M,N,PK1,P(100,3),B(100,3),A(100,100),D(5,5,20),Q(20),
1 E(5,5,20)
INTEGER Q
DO 1 I=1,M1
K=I+1
DO 1 J=K,MBAND
1 A(I,J)=0.
DO 2 J=1,MBAND
2 A(MBAND+J)=0.
JJ=(II-1)*IBANDP
DO 7 IK=1,IBANDP
IF (IGEN.GT.0) GO TO 3
PRINT 906,IK,II
3 READ (2) IT,(Q(I),I=1,IT)
LT=25*IT
READ (2) ((E(I,J,K),I=1,5),J=1,5),K=I,IT)
READ (2) ((D(I,J,K),I=1,5),J=1,5),K=1,IT)
DO 7 K=1,17
IX=(Q(K)-JJ-1)*NDFRE
JX=(IK-1)*NDFRE
I1=NDFRE
IF(IX.GE.MBAND) IX=IX-MBAND
DO 7 L=1,NDFRE
IF(IX.EQ.JX) I1=L
LX=IX+L
DO 7 I=1,I1
MX=JX+I
7 A(LX,MX)=D(L,I,K)+A(LX,MX)
906 FORMAT(2I4)
RETURN
END

```

LMB 7/09

```

SUBROUTINE CHOL(M1)
IMPLICIT REAL*8 (A-H,O-Z)
COMMON/CV/NUMEL,NUPTS,NUBPTS,IBANDP,MBAND,NBLOC,NDFRE,NODES,LVECT
COMMON/SS/IGEN,ISHEAR,JSHEAR,NRED,IREACT,NTRUSS,ISIG
COMMON M,N,PX1,P(100,3),B(100,3),A(100,100)
DO 11 ICHOL=1,N
CALL FORMK(ICHOL,M1)
IF (IGEN.GT.0) GO TO 12
PRINT 20,ICHOL
12 DO 5 J=1,M
L1=J-1
DO 5 I=J,M
SUM = 0.
2 IF (J.EQ.1) GOTO 4
DO 3 L=1,L1
3 SUM = SUM+A(J,L)*A(I,L)
4 IF (I.EQ.J) A(I,J) =DSQRT(A(I,J)-SUM)
5 IF (I.NE.J) A(I,J) = (A(I,J)-SUM)/A(J,J)
C BEGIN DECOMPOSITION OF LOWER TRIANGLE CASE 1
IF (ICHOL.EQ.N) GOTO 8
DO 7 I=1,M1
K1=I+1
DO 7 J=K1,M
K2=J-1
SUM=0.0
IF (K1.GT.K2) GOTO 7
DO 6 K=K1,K2
6 SUM = SUM+A(J,K)*A(I,K)
7 A(I,J) = (A(I,J)-SUM)/A(J,J)
8 CALL INOUTA ( 1,ICHOL )
IF (ICHOL.EQ.N) GOTO 11
DO 10 J=1,M1
DO 10 I=J,M1
K1=I+1
SUM=0.
DO 9 K=K1,M
9 SUM=SUM+A(J,K)*A(I,K)
10 A(I,J)=-SUM
11 CONTINUE
20 FORMAT(I5)
RETURN
END

```

LMB 7/09

```

SUBROUTINE INOUTA (IGO,ICHOL)
IMPLICIT REAL*8 (A-H,O-Z)
COMMON M,N,PX1,P(100,3),B(100,3),A(100,100)
DIMENSION X(10000)
EQUIVALENCE (A(1,1),X(1))
COMMON /BTAPE/ LCPJ(100),MCPJ(100)
GO TO (1,3),IGO
1 K = 0
DO 2 J=1,M
DO 2 I=1,M
K = K + 1
X(K) = A(I,J)
WRITE (8:LCPJ(ICHOL)) (X(I),I=1,K)
GO TO 4
3 K = M*M
READ (8:LCPJ(ICHOL)) (X(I),I=1,K)
4 K = M*M + 1
L = M + 1
DO 5 J=1,M
DO 5 I=1,M
K = K - 1
A(L-I,L-J) = X(K)
5 RETURN
END

```

```

SUBROUTINE FPASS ( M1 )
IMPLICIT REAL*8 (A-H,O-Z)
COMMON/CV/NUMEL,NUPTS,NUBPTS,IBANDP,MBAND,NBLOC,NDFRE,NODES,LVECT
COMMON / BTAPE / LCPJ(100), MCPJ(100)
COMMON M,N,PX1,P(100,3),B(100,3),A(100,100),Q(300)
CALL WIND ( 4,3 )
CALL QTAPE (-2,4,P,Q,0 )
DO 4 ICHOL=1,N
CALL INOUTA ( 2,ICHOL )
DO 20 LV=1,LVECT
20 B(1,LV)=P(1,LV)/A(1,1)
OO 2 LV=1,LVECT
OO 2 I=2,M
K=I-1
OO 1 J=1,K
1 P(I,LV)=P(I,LV)-A(I,J)*B(J,LV)
2 B(I,LV)=P(I,LV)/A(I,I)
IF (ICHOL.EQ.N) GOTO 4
CALL QTAPE (-2,4,P,Q,0 )
DO 3 LV=1,LVECT
DO 3 I=1,M1
L=1+1
DO 3 J=L,M
3 P(I,LV)=P(I,LV)-A(I,J)*B(J,LV)
4 CALL QTAPE ( 3,9,B,Q,ICHOL )
CALL WIND (3,4)
CALL WIND ( 4,1 )
RETURN
END

```

LMB 7/09

```

SUBROUTINE SWITCH
IMPLICIT REAL*8 (A-H,O-Z)
COMMON/CV/NUMEL,NUPTS,NUBPTS,IBANDP,MBAND,NBLOC,NDFRE,NODES,LVECT
COMMON M,N,PX1,P(100,3),B(100,3),A(100,100)
MD=M/2
MJ=M+1
DO 1 I=1,MD
LI=M-I+1
DO 3 LV=1,LVECT
C=P(I,LV)
P(I,LV)=P(LI,LV)
3 P(LI,LV)=C
MJ=MJ-1
DO 1 J=1,MJ
LJ=M-J+1
C=A(J,I)
A(J,I)=A(LI,LJ)
A(LI,LJ)=C
1 CONTINUE
MJ=M+1
DO 2 I=1,MD
LI=M-I+1
MJ=MJ-1
JJ=1+1
DO 2 J=JJ,MJ
LJ=M-J+1
C=A(I,J)
A(I,J) = A(LJ,LI)
A(LJ,LI) = C
2 CONTINUE
RETURN
END

```

LMB 7/09

```

SUBROUTINE BPASS(M1)
IMPLICIT REAL*8 (A-H,O-Z)
COMMON/CV/NUMEL,NUPTS,NUBPTS,IBANDP,MBAND,NBLDC,NDFRE,NODES,LVECT
COMMON / BTAPE / LCPJ(100), MCPJ(100)
COMMON M,N,PX1,P(100,3),B(100,3),A(100,100),Q(300)
DO 7 I1=1,N
ICHOL=N+1-I1
CALL INOUTA ( 2,ICHOL )
CALL QTAPE (-3,9,P,Q,ICHOL )
CALL SWITCH
IF(I1.EQ.1) GOTO 3
DO 2 LV=1,LVECT
DO 2 I=1,M1
L=I+1
DO 2 J=L,M
2 P(I,LV)=P(I,LV)-A(I,J)*B(J,LV)
3 DO 10 LV=1,LVECT
10 B(1,LV)=P(1,LV)/A(1,1)
DO 5 LV=1,LVECT
DO 5 I=2,M
K=I-1
DO 4 J=1,K
4 P(I,LV)=P(I,LV)-A(I,J)*B(J,LV)
5 B(1,LV)=P(1,LV)/A(1,I)
DO 6 LV=1,LVECT
DO 6 I=1,M
IZ=M-I+1
6 P(I,LV)=B(IZ,LV)
7 CALL QTAPE ( 2,4,P,Q,0 )
CALL WIND ( 4,3 )
RETURN
END

```

LMB 7/09

```

SUBROUTINE RESID ( M1,IRED,NRED,IREACT )
IMPLICIT REAL*8 (A-H,O-Z)
COMMON/CV/NUMEL,NUPTS,NUBPTS,IBANDP,MBAND,NBLOC,NDFRE,NODES,LVECT
COMMON IX1(2),PX2,B(5,850,1),R(5,800)
DIMENSION Y(5,850)
EQUIVALENCE (R(1,1),Y(1,1))
IF ( IRED.NE.1 ) GOTO 21
DO 8 LV=1,LVECT
PRINT 13,LV
PRINT 11
DO 8 K=1,NUPTS
8 PRINT 12,K,( B(J,K,LV),J=1,NDFRE)
21 IF ( NRED.EQ.0 ) GOTO 5
DO 2 LV=1,LVECT
CALL QLAYER ( LV,0 )
CALL RLOAD (-1,2,B,1,LV,850 )
DO 2 I=1,NUPTS
DO 2 J=1,NDFRE
X=B(J,I,LV)
2 B(J,I,LV)=X-R(J,I)
CALL WIND ( 4,1 )
CALL QTAPE ( 1,4,B,PX1,0 )
CALL FPASS ( M1 )
CALL BPASS ( M1 )
CALL QTAPE (-1,4,B,PX1,0 )
CALL WIND ( 3,1 )
DO 4 LV=1,LVECT
CALL RLOAD (-1,3,Y,1,1,850 )
DO 4 K=1,NUPTS
DO 4 L=1,NDFRE
4 B(L,K,LV)=B(L,K,LV)+Y(L,K)
DO 7 LV=1,LVECT
PRINT 10,LV,IRED
PRINT 11
DO 7 K=1,NUPTS
7 PRINT 12,K,( B(J,K,LV),J=1,NDFRE)
CALL WIND ( 3,1 )
CALL RLOAD ( 1,3,B,1,LVECT,850 )
DO 6 LV=1,LVECT
IF ( IRED.GE.NRED.AND.IREACT.GT.0 ) CALL QLAYER ( LV,1 )
6 CONTINUE
10 FORMAT(1M1,27HDISPLACEMENTS FOR LOAD CASE15,15H ITERATION NO. ,15)
11 FORMAT (5H0NODE 2X,2HD1 11X,2HD2 11X,2HD3 11X,2HD4 11X,2HD5)
12 FORMAT (I+,1P5E13,4)
13 FORMAT(1M1,27HDISPLACEMENTS FOR LOAD CASE15,17H INITIAL SOLUTION)
RETURN
END

```

LMB 7/09

```

SUBROUTINE QLAYER ( LV,IPRINT )
IMPLICIT REAL*8 (A-H,O-Z)
COMMON/CV/NUMEL,NUPTS,NUBPTS,IBANDP,MBAND,NBLOC,NDFRE,NODES,LVECT
COMMON IX1(2),PX1,B(5,850,1),R(5,800),DM(5,5,20),DD(5,5,20),IQ(20)
COMMON/SS/IGEN,ISHEAR,JSHEAR,NRED,IREACT,NTRUSS,ISIG
CALL WIND ( 2,1 )
DO 1 I=1,NUPTS
DO 1 J=1,NDFRE
1 R(J,I)=0.
NUEQS=NBLOC*IBANDP
DO 7 J=1,NUEQS
READ (2) IT,(IQ(I),I=1,IT)
LT=25*IT
IF ( IPRINT.EQ.0 ) READ (2) (((DM(I,L,K),I=1,5),L=1,5),K=1,IT)
IF ( IPRINT.EQ.0 ) READ (2) (((DD(I,L,K),I=1,5),L=1,5),K=1,IT)
IF ( IPRINT.EQ.1 ) READ (2) (((DD(I,L,K),I=1,5),L=1,5),K=1,IT)
IF ( IPRINT.EQ.1 ) READ (2) (((DM(I,L,K),I=1,5),L=1,5),K=1,IT)
IF ( J.GT.NUPTS ) GOTO 7
DO 4 II=1,IT
I=IQ(II)
IF ( I.EQ.J ) GOTO 3
DO 2 L=1,NDFRE
DO 2 K=1,NDFRE
2 R(K,J) = R(K,J)+DD(L,K,II)*B(L,I,LV)
3 DO 4 L=1,NDFRE
DO 4 K=1,NDFRE
4 R(K,I) = R(K,I)+DD(K,L,II)*B(L,J,LV)
7 CONTINUE
IF ( IREACT.EQ.0 ) GOTO 6
PRINT 10,LV
PRINT 11
DO 5 K=1,NUPTS
5 PRINT 12,K,(R(J,K),J=1,NDFRE)
10 FORMAT ( 1M1,42HODDAL FORCES INCLUDING REACTIONS LOAD CASE,15 )
11 FORMAT ( 4H PT.12X,2HR19X,2HR29X,2HR39X,2HR49X,2HR5 )
12 FORMAT ( 14,11X,1P5U11,4 )
6 RETURN
END

```

LMB 7/09

LMB

LMB

LMB

LMB

```

SUBROUTINE OVER4
IMPLICIT REAL*8 (A-H,O-Z)
COMMON/CV/NUMEL,NUPTS,NUBPTS,IBANDP,MBAND,NBLOC,NDFRE,IFLAG,LVECT
COMMON/SS/IGEN,ISHEAR,JSHEAR,NRED,IREACT,NTRUSS,ISIG
COMMON IQ(4),NODES,NTYPE,NQUAD,NTRI,IC(800),BX(5,800),
1 PP(800,6),OU,AD(3,4),BD(3,4),TD(3,36),TR(3,36),
2 IQ(3,3,4),XMQ(3,3,4),TH(5),TPC(6),PX1(134),S(37,13),
3 PT(13),PX2(152),DB(5),XM(3,3),XB(3,3),SM(3,3),
4 SB(3,3),ZT(3,3,4),G1(3,3,4),ZQ(3,5),GQ(3,5),
5 SCOND(15,6,4),PX3(9),X(4),Y(4)
DIMENSION SIGN(2),SIG(3,2),ST(8),DU23(23),OU324(324)
EQUIVALENCE (DU,OU23(1)),(DU,OU324(1))
DATA SIGN/1,-1/
CALL WIND ( 2,1 )
CALL WIND ( 3,3 )
CALL WIND ( 4,1 )
OO 7 LV=1,LVECT
CALL WIND ( 1,1 )
IF ( NTRUSS.EQ.NUMEL ) GOTD 56
CALL RLOAD (-1,3,BX,1,1,800 )
C.....INITIALIZE PP,THE MATRIX STORING AVERAGED MOMENTS AND STRESSES.....
DO 1 I=1,NUPTS
IC(I)=0
DO 1 J=1,6
1 PP(I,J)=0.
C.....SUM OVER NUMBER OF ELEMENTS.....
IF ( ISIG .GT. 0 ) GO TO 800
PRINT 90,LV
PRINT 93
GO TO 56
800 PRINT 801,LV
PRINT 802
NEL = 0
56 DO 50 JQ=1,NUMEL
READ (1) IQ,NODES,NTYPE,NQUAD
IF ( NODES.GT.2 ) GOTD 55
READ (1) DU23
IQ(3)=JQ
IF ( LV.EQ.1 ) WRITE (2) (IQ(I),I=1,3),DU23
GOTO 50
55 READ (1) OU324
TH(5) = DU
IF ( NTYPE.GT.0 ) READ (1) X,Y
DO 8 I=1,NODES
K=IQ(I)
8 IC(K)=IC(K)+1
IF ( ISHEAR.EQ.6 ) READ (1) SCOND
IF ( NDDDES.EQ.4 ) READ (1) S
IF ( NDOES.EQ.4 ) READ (1) PT
C.....COMPUTE INTERIOR NODAL PT. DISPL. FOR QUAD. AND NODAL PT. DISPL. F
C.....TRI. IN ELEMENT COOROS.....
IF (TH(5).LT..000001) GO TO 50
IF (XMQ(1,1,1).LT..001 .OR. XMQ(2,2,1).LT..001) GO TD 50
CALL GDISPL
C.....COMPUTE AND TRANSFORM ELEMENT STRESSES AND MOMENTS.....
DO 11 J=1,5
11 DB(J)=TH(J)*.3/12.
DO 10 NTRI=1,NQUAD
IF ( NTYPE.LE.0 ) CALL MEMBR
IF ( NTYPE.GT.0 ) CALL MEMBG ( NTRI,X,Y,PT,XM,TPC )
CALL MOMTR ( 9,ISHEAR )
DO 6 I=1,3
DO 6 J=1,3
SB(I,J)=0.
SM(I,J)=0.
OO 6 K=1,3
SB(1,J)=SB(1,J)+XMQ(I,K,NTRI)*XB(K,J)
6 SM(1,J)=SM(1,J)+XMQ(1,K,NTRI)*XM(K,J)
K=NTRI
KK=(NTRI-1)*9
DO 10 J=1,3
L=KK*(J-1)*3
NS=1
IF ( NS.GT.0 ) L=KK+6
C=TR(1,L-1)
R=TR(1,L*2)
CS=DSQRT(C**2+R**2)
C=C/CS
R=R/CS
C2=C*C
S2=R*R
SC=R*C
C2MS2=C2-52
F=SM(1,J)
G=SM(2,J)
H=SM(3,J)
IF(NTYPE.LE.0) GO TO 30
ZT(1,J,K)=F
ZT(2,J,K)=G
ZT(3,J,K)=H
GD TO 40
30 ZT(1,J,K)=C2*F+S2*G-2.*SC*H
ZT(2,J,K)=S2*F+C2*G+2.*SC*H
ZT(3,J,K)=SC*(F-G)+C2MS2*H
40 F=SB(1,J)
G=SB(2,J)
H=SB(3,J)
G1(1,J,K)=C2*F+S2*G-2.*SC*H
G1(2,J,K)=S2*F+C2*G+2.*SC*H
10 G1(3,J,K)=SC*(F-G)+C2MS2*H
IF(NDDDES.EQ.4) GOTD 13
DO 12 J=1,3
DO 12 I=1,3
GQ(I,J)=G1(I,J,1)*DB(J)
12 ZQ(I,J)=ZT(I,J,1)*TH(J)
GOTO 15
13 OO 14 I=1,3
C.....COMPUTE AVERAGE MOMENTS AND STRESSES FOR QUAD.....
GQ(I,1)=(G1(I,1,1)+G1(I,2,4))*5*DB(1)
GQ(I,2)=(G1(I,2,1)+G1(I,1,2))*5*DB(2)
GQ(I,3)=(G1(I,2,2)+G1(I,1,3))*5*DB(3)
GQ(I,4)=(G1(I,2,3)+G1(I,1,4))*5*DB(4)
GQ(I,5)=(G1(I,3,1)+G1(I,3,2)+G1(I,3,3)+G1(I,3,4))*25*DB(5)
ZQ(I,1)=(ZT(I,1,1)+ZT(I,2,4))*5*TH(1)
ZQ(I,2)=(ZT(I,2,1)+ZT(I,1,2))*5*TH(2)
ZQ(I,3)=(ZT(I,2,2)+ZT(I,1,3))*5*TH(3)
ZQ(I,4)=(ZT(I,2,3)+ZT(I,1,4))*5*TH(4)
14 ZQ(I,5)=(ZT(I,3,1)+ZT(I,3,2)+ZT(I,3,3)+ZT(I,3,4))*25*TH(5)
C.....ADD NODAL PT. MOMENTS AND STRESSES IN PP.....
DO 16 J=1,NODES
K=IQ(J)
DO 16 L=1,3
M=L+3
PP(K,L)=PP(K,L)+GQ(L,J)
16 PP(K,M)=PP(K,M)+ZQ(L,J)
C.....PRINT AVERAGE MOMENTS AND STRESSES FOR QUAD.....

```

```

PRINT 101,JQ
NPT=3
IF(NODES.EQ.4) NPT=5
  NQ = 1
  IF(NPT.EQ.5.AND.IGEN.GT.2) NQ = 5
  IF ( ISIG .GT. 0 ) GO TO 60
  DO 3 L = NQ, NPT
    M=0
    IF(LL.LT.5) M=IQ(L)
  3 PRINT 20,((GQ(I,J),J=L+L),I=1,3),((ZQ(I,J),J=L+L),I=1,3),M
  GO TO 50
60 CONTINUE
C.....COMPUTE STRESSES AT EACH NODE
DO 81 LL = NQ,NPT
DO 80 II = 1,2
C.....TOP(II=1), BOTTOM(II=2)
DO 80 IL = 1,3
80 SIG(IL,II) = ZQ(IL,LL)/TH(LL)*(GQ(IL,LL)*6./TH(LL)**2)*SIGN(II)
M = 0
IF (LL.LT.5) M=IQ(LL)
PRINT 810, ((SIG(IL,II),IL=1,3),II=1,2),M
810 FORMAT (1P6E11.3,I4)
IF ( LL.LT.NPT) GO TO 81
IF ( NPT.EQ.5 ) GO TO 82
C.....AVERAGE THE STRESS RESULTANTS FOR TRI. ELEMENT
DO 85 IL = 1,3
GQ(IL,5) = (GQ(IL,1)+GQ(IL,2)+GQ(IL,3))/3.
85 ZQ(IL,5) = (ZQ(IL,1)+ZQ(IL,2)+ZQ(IL,3))/3.
TH(5) = (TH(1)+TH(2)+TH(3))/3.
82 CONTINUE
WRITE (4) JQ
NEL = NEL+1
DO 83 II = 1,2
DO 84 IL = 1,3
84 SIG(IL,II)=ZQ(IL,5)/TH(5)*(GQ(IL,5)*6./TH(5)**2)*SIGN(II)
FAC1 = (SIG(1,II)+SIG(2,II))*0.5
FAC2 =DSQRT(((SIG(1,II)-SIG(2,II))*0.5)**2+SIG(3,II)**2)
SMAX = FAC1+FAC2
SMIN = FAC1-FAC2
TMAX = (SMAX-SMIN)/2.
IF (SMIN .EQ. SIG(2,II)) GO TO 87
ANG=- 57.295779513*DATAN(SIG(3,II)/(SIG(2,II)-SMIN))
GO TO 88
87 ANG = 90.
88 WRITE (4) SMAX,SMIN,TMAX,ANG
83 CONTINUE
81 CONTINUE
50 CONTINUE
20 FORMAT (1P6E11.3,I4)
IF ( NTRUSS.EQ.NUMEL ) GO TO 825
IF (IGEN.GT.2) GO TO 7
IF ( ISIG .GT. 0 ) GO TO 7
PRINT 91,LV
PRINT 92
DO 5 I=1,NUPTS
XP=IC(I)
IF (XP.EQ.0.) GO TO 5
DO 4 J=1,6
4 PP(I,J)=PP(I,J)/XP
PRINT 110,I,((PP(K,L),L=1,6),K=I,I)
5 CONTINUE
7 CONTINUE
IF ( ISIG.LE.0) GO TO 824

```

```

CALL WIND ( 4,3 )
DO 822 LV = 1,LVECT
PRINT 820,LV
PRINT 821
DO 822 JJJ = 1,NEL
READ (4) JQ
READ (4) (ST(I),I=1,4)
READ(4) (ST(I),I=5,8)
PRINT 823,JQ,(ST(I),I=1,8)
823 FORMAT (I4,1P8E11.3)
822 CONTINUE
824 CONTINUE
IF ( NTRUSS.EQ.0 ) GO TO 8000
CALL WIND ( 2,4 )
CALL WIND ( 3,1 )
825 DO 700 LV=1,LVECT
CALL WIND ( 2,1 )
PRINT 94,LV
CALL RLOAD ( -1,3,8X,1,I,800 )
DO 600 JQ=1,NTRUSS
CALL AXIAL ( 0,IQ,8X )
IF ( Q.LT.0.0 ) PRINT 95,IQ(3),Q
IF ( Q.GE.0.0 ) PRINT 96,IQ(3),Q
600 CONTINUE
700 CONTINUE
90 FORMAT(2M1 ,38HELEMENT STRESS RESULTANTS FOR LOAD CASE,14)
I01 FORMAT (12M ELEMENT NO,I4,50X,4HNODE)
91 FORMAT (70HIAVERAGED NODAL STRESS RESULTANTS,W,R,T,SURFACE COORDI
1NATES,LOAD CASE,I4)
92 FORMAT (5H0NODE 2X,2HN2 9X,2HM1 9X,3HM12 8X,2HN1 9X,2HN2 9X,1HS)
93 FORMAT (1H0 2X,2HM2 9X,2HM1 9X,3HM12 8X,2HM1 9X,2HN2 9X,1HS /)
94 FORMAT (1H17X,43HAXIAL STRESSES FOR TRUSS ELEMENTS LOAD CASE,14 )
95 FORMAT ( 7X,23HAXIAL STRESS FOR MEMBER,15,4H IS 1PE12.4,
* 12H COMPRESSION )
96 FORMAT ( 7X,23HAXIAL STRESS FOR MEMBER,15,4H IS 1PE12.4,
* 8H TENSION )
110 FORMAT (I4,1P6E11.3)
907 FORMAT(30I4)
801 FORMAT(2M1 ,43HELEMENT STRESSES (TOP-BOTTOM) FOR LOAD CASE,14)
802 FORMAT(1H0,2X,2HN1,9X,2HN2,10X,1HS,8X,2HN1,9X,2HN2,9X,1HS /)
820 FORMAT(2M1 ,45HPRINCIPAL STRESSES (TOP-BOTTOM) FOR LOAD CASE,I4)
821 FORMAT(5H0ELEM,2X,4HSMAX,7X,4HSMIN,8X,4HTMAX,5X,3HANG,8X,4HSMAX,
* 7X, 4HSMIN,8X,4HTMAX,5X,3HANG)
8000 RETURN
END

```

22MAR75

```

SUBROUTINE GDISPL
IMPLICIT REAL*8 (A-H,O-Z)
COMMON IQ(4),IX1(1),NTYPE,NQUAD,IX2(801),B(5,800),PX1(4825),
1 TU(3,36), TR(3,36), TQ(3,3,4), PX2(47), UM(5,4),
2 VM(5,4), BP(9,4), PX3(58), S(37,13), PT(13), R2(13),
3 P(39), D(5,5,4), PA4(512)
LMB 7/09
IP=IQ(1)
JP=IQ(2)
KP=IQ(3)
IF(NQUAD.EQ.4) GOTO 10
DO 11 I=1,5
D(I,1,1)=B(I,IP)
D(I,2,1)=B(I,JP)
11 D(I,3,1)=B(I,KP)
GOTO 12
10 LP=IQ(4)
C.....GROUP DISPL. OF CORNER NNODES IN P.....
DO 1 M = 1,3
P(M )=TQ(M,1,1)*B(1,IP)+TQ(M,2,1)*B(2,IP)+TQ(M,3,1)*B(3,IP)
P(M+5 )=TQ(M,1,2)*B(1,JP)+TQ(M,2,2)*B(2,JP)+TQ(M,3,2)*B(3,JP)
P(M+10)=TQ(M,1,3)*B(1,KP)+TQ(M,2,3)*B(2,KP)+TQ(M,3,3)*B(3,KP)
1 P(M+15)=TQ(M,1,4)*B(1,LP)+TQ(M,2,4)*B(2,LP)+TQ(M,3,4)*B(3,LP)
DO 4 M=4,5
P(M )=B(M,IP)
P(M+5 )=B(M,JP)
P(M+10)=B(M,KP)
4 P(M+15)=B(M,LP)
C.....COMPUTE DISPL. AT INTERIOR NODES.....
DO 13 I=6,13
13 R2(I)=0.0
NDOFC = 13
IF ( NTYPE.GT.0 ) NDDFC = 5
DO 3 I=1,NDOFC
L=19+I
R2(I)=PT(I)/S(L+1,I)
DO 2 K=1,L
2 R2(I)=R2(I)-S(K,I)*P(K)
3 P(I+20)=R2(I)
C.....STORE ALL THREE DISPL. COMPONENTS AT MID SIDE NODES IN P.....
DO 5 I=1,4
J=(I-1)*2
K=(I-1)*3
P(K+26)=R2(J+6)
5 P(K+27)=R2(J+7)
P(28)= (P( 3)+P(23))/2.
P(31)= (P( 8)+P(23))/2.
P(34)= (P(13)+P(23))/2.
P(37)= (P(18)+P(23))/2.

```

```

C.....STORE DISPL. COMPONENTS FOR EACH TRI. IN D.....
DO 6 I=1,5
D(I,1,1)=B(I,IP)
D(I,2,1)=B(I,JP)
D(I,4,1)=P(I+28)
D(I,5,1)=P(I+25)
D(I,3,1)=P(I+20)
D(I,1,2)=B(I,JP)
D(I,2,2)=B(I,KP)
D(I,4,2)=P(I+31)
D(I,5,2)=P(I+28)
D(I,3,2)=P(I+20)
D(I,1,3)=B(I,KP)
D(I,2,3)=B(I,LP)
D(I,4,3)=P(I+34)
D(I,5,3)=P(I+31)
D(I,3,3)=P(I+20)
D(I,1,4)=B(I,LP)
D(I,2,4)=B(I,IP)
D(I,4,4)=P(I+25)
D(I,5,4)=P(I+34)
6 D(I,3,4)=P(I+20)
C.....TRANSFORM NODAL PT. DISPL. TO ELEMENT COORDS.....
12 DO 8 K=1,NQUAD
KK=(K-1)*9
DO 7 J=1,5
IF (J.LT.4) L=KK+(J-1)*3
UM(J,K)=TD(1,L+1)*D(1,J,K)+TD(1,L+2)*D(2,J,K)+TD(1,L+3)*D(3,J,K)
VM(J,K)=TD(2,L+1)*D(1,J,K)+TD(2,L+2)*D(2,J,K)+TD(2,L+3)*D(3,J,K)
IF (J.GT.3) GOTO 7
I=(J-1)*3
BP(I+1,K)=TD(3,L+1)*D(1,J,K)+TD(3,L+2)*D(2,J,K)+TD(3,L+3)*D(3,J,K)
BP(I+2,K)=TR(1,L+1)*D(4,J,K)+TR(1,L+2)*D(5,J,K)
BP(I+3,K)=TR(2,L+1)*D(4,J,K)+TR(2,L+2)*D(5,J,K)
7 CONTINUE
8 CONTINUE
DO 20 I=1,4
J=(I-1)*2
K=(I-1)*5
PT(J+1)=P(K+1)
20 PT(J+2)=P(K+2)
RETURN
END

```



```

SUBROUTINE MEMBR
IMPLICIT REAL*8 (A-H,O-Z)
COMMON IX1(5),NTYPE,NQUAD,NTRI,IX2(800),PX1(8801),AD(3,4),
1      BD(3,4),PX2(293),TPC(6),UM(5,4),VM(5,4),PX3(36),U(5),
2      V(5),PX4(699),XM(3,3),PX5(498)
C.....GROUP MEMBRANE DISPL. IN U AND V.....
DO 1 I=1,5
  U(I)=UM(I,NTRI)
  V(I)=VM(I,NTRI)
C.....MODIFY STRAIN DISPL. MATRIX IF ELEMENT IS A CST.....
  IF (NQUAD.EQ.4) GOTO 2
  U(4)=(U(2)+U(3))/2.
  V(4)=(V(2)+V(3))/2.
  U(5)=(U(1)+U(3))/2.
  V(5)=(V(1)+V(3))/2.
C.....COMPUTE STRAINS IN X DIR.....
  2 AREA2=-1./(AD(3,NTRI)*BD(1,NTRI))
  E=BD(1,NTRI)*AREA2
  A=AD(1,NTRI)*AREA2
  C=AD(2,NTRI)*AREA2
  D=AD(3,NTRI)*AREA2
  ITEST=NTRI+1
  IF (ITEST.GT.4) ITEST=1
  XM1=TPC(6)*TPC(NTRI)
  XM2=TPC(6)*TPC(ITEST)
  XM3=TPC(6)*TPC(5)
  XM(1,1)=(U(1)-U(2))*E-XM1
  XM(1,2)=(U(1)-U(2))*E-XM2
  XM(1,3)=(-U(1)+U(2)+4.*(-U(4)+U(5)))*E-XM3
C.....COMPUTE STRAINS IN Y DIR.....
  XM(2,1)=(A-2.*D)*V(1)+C*V(2)-D*V(3)+4.*D*V(5)-XM1
  XM(2,2)=A*V(1)+(C-2.*D)*V(2)-D*V(3)+4.*D*V(4)-XM2
  XM(2,3)=-A*V(1)-C*V(2)+3.*D*V(3)+4.*C*V(4)+4.*A*V(5)-XM3
C.....COMPUTE SHEAR STRAINS.....
  XM(3,1)=(V(1)-V(2))*E+(A-2.*D)*U(1)+C*U(2)-D*U(3)+4.*D*U(5)
  XM(3,2)=(V(1)-V(2))*E+A*U(1)+(C-2.*D)*U(2)-D*U(3)+4.*D*U(4)
  XM(3,3)=(-V(1)+V(2)+4.*(-V(4)+V(5)))*E
  1 -A*U(1)-C*U(2)+3.*D*U(3)+4.*C*U(4)+4.*A*U(5)
RETURN
END

```

LMB 7/09

```

SUBROUTINE MOMTR ( NBF,ISHEAR )
IMPLICIT REAL*8 (A-H,O-Z)
COMMON IX1(7), NTRI, IX2(800), PX1(8801), AD(3,4), BD(3,4),
1      PX2(339), BP(9,4), PX3(10), R(12), A(3), B(3), U(3),
2      HT(3), TX(3), TY(3), D(3,6), PX4(660), XB(3,3),
3      PX5(120), SCOND(15,6,4), C(6), D(3)
DIMENSION IPERM(3),NKN(2,3)
DATA IPERM/2,3,1/, NKN/2,5, 8,2, 5,8/
DO 2 I=1,9
  2 R(I)=BP(I,NTRI)
  IF ( ISHEAR.NE.6) GOTO 10
  DO 6 I=1,6
    C(I)=0.
    L= 8*I
    DO 3 K=1,L
      3 C(I)=C(I)-SCOND(K,I,NTRI)*R(K)
      6 R(I+9)=C(I)
      R(2)=R(2)-C(4)
      R(5)=R(5)-C(5)
      R(8)=R(8)-C(6)
      R(3)=R(3)+C(1)
      R(6)=R(6)+C(2)
      R(9)=R(9)+C(3)
  10 DO 1 I=1,3
    D(I)=0.
    B(I)=BD(1,NTRI)
    1 A(I)=AD(I,NTRI)
    IF ( ISHEAR.NE.6) GOTO 5
    DO 4 J=1,3
      O(1)=D(1)+B(J)*C(J)
      D(2)=D(2)+A(J)*C(J+3)
      4 O(3)=D(3)+A(J)*C(J)+B(J)*C(J+3)
      5 AREA = A(3)*B(2)+A(2)*B(3)
      DO 120 I = 1,3
        J = IPERM(I)
        X = A(I)**2+B(I)**2
        U(I) = -(A(I)*A(J)+B(I)*B(J))/X
        X =DSQRT(X)
        TX(I) = 0.5*A(I)/X
        TY(I) = -0.5*B(I)/X
        HT(I) = 4.0*AREA/X
        A1 = A(I)/AREA
        B1 = B(I)/AREA
        A2 = A(J)/AREA
        B2 = B(J)/AREA
        O(1,J) = B1*B1
        O(2,J) = A1*A1
        O(3,J) = 2.*A1*B1
        O(1,I+3) = 2.*B1*B2
        O(2,I+3) = 2.*A1*A2
      120 O(3,I+3) = 2.*(A1*B2+A2*B1)
        N = 12 - NBF
        IF (N.LE.0) GO TO 160
        DO 140 N = 1,N
          K = 13 - N
          L1 = NKN(1,N)
          L2 = NKN(2,N)
      140 R(K) = (R(L1)+R(L2))*TX(K-9)+(R(L1+1)+R(L2+1))*TY(K-9)

```

LMB 7/09

```

160 DO 200 I = 1,3
  J = IPERM(I)
  K = 1PERM(J)
  II = 3*I
  JJ = 3*J
  KK = 3*K
  A2 = A(J)
  A3 = A(K)
  B2 = B(J)
  B3 = B(K)
  U2 = U(J)
  U3 = U(K)
  W2 = 1.-U2
  W3 = 1.-U3
  C21 = -(2.*W2)*B2-(2.*U3)*B3
  C22 = B2*W2-B3*U3
  C31 = -(2.*W2)*A2-(2.*U3)*A3
  C32 = A2*W2-A3*U3
  C51 = 4.*B3-B2*B3*W3
  C52 = B2-B3*W3
  C61 = 4.*A3-A2*A3*W3
  C62 = A2-A3*W3
  C81 = B3-4.*B2-B2*U2
  C82 = B2*U2-B3
  C91 = A3-4.*A2-A2*U2
  C92 = A2*U2-A3
  C021 = -B2-(3.*U3)*B3
  C022 = B3+(3.*W2)*B2
  C031 = -A2-(3.*U3)*A3
  C032 = A3+(3.*W2)*A2
  DO 200 N = 1,3
    Q11 = Q(N,I)
    Q22 = Q(N,J)
    Q33 = Q(N,K)
    Q12 = Q(N,I+3)
    Q23 = Q(N,J+3)
    Q31 = Q(N,K+3)
    Q1 = Q22-Q33
    Q2 = Q22-Q23
    Q3 = Q33-Q23
    Q4 = Q23-Q1
    Q5 = Q23-Q1
    XR(N,I) = (-6.*Q11+3.*((U3-W2)*Q1+(U3-W2)*Q23))*R(II-2)
  1 + (6.*Q22+3.*W3*Q4)*R(JJ-2) + (6.*Q33+3.*U2*Q5)*R(KK-2)
  2 + ((C21*Q1+C22*Q23+4.*(B2*Q31-B3*Q12)) *R(II-1)
  3 + (C31*Q1+C32*Q23+4.*(A2*Q31-A3*Q12)) *R(II)
  4 + (C51*Q22+C52*Q3) *R(JJ-1) + (C61*Q22+C62*Q3) *R(JJ)
  5 + (C81*Q33+C82*Q2) *R(KK-1) + (C91*Q33+C92*Q2) *R(KK)
  6 + HT(K)*Q4*R(K+9) + HT(J)*Q5*R(J+9))/2.
200 XB(N,I)=-XB(N,I)-U(N)/AREA
  RETURN
  END

```

```

SUBROUTINE MEMBQ(NTRI,X,Y,P,XM,TEMP)
  IMPLICIT REAL*8 (A-H,O-Z)
  DIMENSION X(4), Y(4), P(13), XM(3,3),TEMP(6)
  DIMENSION EPSX(4), EPSY(4), SS(4), TT(4), LOC(2,4)
  DATA LOC / 1, 2, 2, 3, 3, 4, 4, 1 /
  DATA SS /-1.,1.,1.,-1./, TT /-1.,-1.,1.,1./
  IF(NTRI.GT.1) GO TO 300
  R12 = X(1) - X(2)
  R13 = X(1) - X(3)
  R14 = X(1) - X(4)
  R23 = X(2) - X(3)
  R24 = X(2) - X(4)
  R34 = X(3) - X(4)
  Z12 = Y(1) - Y(2)
  Z13 = Y(1) - Y(3)
  Z14 = Y(1) - Y(4)
  Z23 = Y(2) - Y(3)
  Z24 = Y(2) - Y(4)
  Z34 = Y(3) - Y(4)
  VOL=R13*Z24-R24*Z13
  CALL QM5C2 ( R13,R24,Z13,Z24,VOL,X5,X6,X7,X8,Y5,Y6,Y7,Y8 )
  EPSXY = X5*P(1)+Y5*P(2)+X6*P(3)+Y6*P(4)+X7*P(5)+Y7*P(6)+X8*P(7)+
    Y8*P(8)
  DO 200 I = 1, 4
    CALL QM5C1 ( SS(I),TT(I),R12,R13,R14,R23,R24,R34,Z12,Z13,Z14,Z23,
      Z24,Z34,VOL,X1,X2,X3,X4,XC,Y1,Y2,Y3,Y4,YC,XJAC,X(1),
      X(2),X(3),X(4),Y(1),Y(2),Y(3),Y(4) )
    EPSX(I) = Y1*P(1)+Y2*P(3)+Y3*P(5)+Y4*P(7)
  200 EPSY(I) = X1*P(2)+X2*P(4)+X3*P(6)+X4*P(8)
    SXAV = ( EPSX(1)+EPSX(2)+EPSX(3)+EPSX(4) ) * 0.25
    SYAV = ( EPSY(1)+EPSY(2)+EPSY(3)+EPSY(4) ) * 0.25
  300 DO 400 I=1,2
    L = LOC(I,NTRI)
    XM(1,I)=EPSX(L)-TEMP(6)*TEMP(L)
    XM(2,I)=EPSY(L)-TEMP(6)*TEMP(L)
  400 XM(3,I) = EPSXY
    XM(1,3)=SXAV-TEMP(6)*TEMP(5)
    XM(2,3)=SYAV-TEMP(6)*TEMP(5)
    XM(3,3) = EPSXY
  RETURN
  END

```

LMB 7/09

```

SUBROUTINE QM5C1 ( S,T,R12,R13,R14,R23,R24,R34,Z12,Z13,Z14,Z23,
.           Z24,Z34,VOL,X1,X2,X3,X4,XC,Y1,Y2,Y3,Y4,YC,XJAC,R1,R2,
.           R3,R4,Z1,Z2,Z3,Z4 )
C..... THIS ROUTINE IS CALLED BY QM5 STIFFNESS AND STRESS ROUTINES
IMPLICIT REAL*8 (A-H,O-Z)
XJ =VOL*S*(R34*Z12-R12*Z34)+T*(R23*Z14-R14*Z23)
XJAC=XJ/8.0
SM=1.0-S
SP=1.0+SM
TM=1.0-T
TP=1.0+T
X1=(-R24+R34*S+R23*T)/XJ
X2=( R13-R34*S-R14*T)/XJ
X3=( R24-R12*S+R14*T)/XJ
X4=(-R13+R12*S-R23*T)/XJ
Y1=( Z24-Z34*S-Z23*T)/XJ
Y2=(-Z13+Z34*S+Z14*T)/XJ
Y3=(-Z24+Z12*S-Z14*T)/XJ
Y4=( Z13-Z12*S+Z23*T)/XJ
RS=0.25*(-TM*R1+TM*R2+TP*R3-TP*R4)
ZS=0.25*(-TM*Z1+TM*Z2+TP*Z3-TP*Z4)
RT=0.25*(-SM*R1-SP*R2+SP*R3+SM*R4)
ZT=0.25*(-SM*Z1-SP*Z2+SP*Z3+SM*Z4)
XC=-2.0*(T*SM*SP*RS-S*TM*TP*RT)/XJAC
YC= 2.0*(T*SM*SP*ZS-S*TM*TP*ZT)/XJAC
RETURN
END

```

LMB 7/09

```

SUBROUTINE QM5C2 ( R13,R24,Z13,Z24,VOL,X5,X6,X7,X8,Y5,Y6,Y7,Y8 )
IMPLICIT REAL*8 (A-H,O-Z)
C..... THIS ROUTINE IS CALLED BY QM5 STIFFNESS AND STRESS ROUTINES
Y5 = Z24/VOL
X6 = R13/VOL
X7 = R24/VOL
Y8 = Z13/VOL
X5 =-X7
Y6 =-Y8
Y7 =-Y5
X8 =-X6
RETURN
END

```

LMB 7/09

```

SUBROUTINE AXIAL ( Q,IQ,BX )
IMPLICIT REAL*8 (A-H,O-Z)
COMMON /AX/ THQ(4),ANG,TPC(6),X(4),Y(4),Z(4)
DIMENSION IQ(4),BX(5,800),THQ23(123)
EQUIVALENCE (THQ(1),THQ23(1))
HEAD (2) (IQ(1),1)=1,3,1,THQ23
XP=X(2)-X(1)
YP=Y(2)-Y(1)
ZP=Z(2)-Z(1)
Q=DSQRT( XP*XP+YP*YP+ZP*ZP )
X1=XP/Q
X2=YP/Q
X3=ZP/Q
M=IQ(1)
N=IQ(2)
XR=BX(1,N)-BX(1,M)
YR=BX(2,N)-BX(2,M)
ZR=BX(3,N)-BX(3,M)
Q=(X1*XR+X2*YR+X3*ZR)*THQ(2)/Q
TEMP=0.5*(TPC(1)+TPC(2))
Q1=THQ(2)*TPC(6)*TEMP
Q = Q-Q1
RETURN
END

```

LMB 7/09

```

//P224132X JOH (Z255,96,1,1,1),*D-45R TRACOR JJP ',TIME=1,CLASS=R,
// REGION=24UK,MSGLEVEL=(1,1)
//STEP1 EXEC FORTGLG
// PARM.LKED='OVLY,LIST,LET,MAP,SIZE=(128K,24K)'
//LKED,SHELL7 DD DSN=D4S,JJP.ONE,DISP=(OLD,KEEP)
//LKED.SYSIN DD *
INCLUDE SMELL7(SHELL7,QTAP,RLDAD,WIND,OVER1,SEARCH,OVER2,SUBSPH, X
BLAYER,UDSMEL,TRUSS,SSTQM5,QM5STF,QM5C1,QM5C2,CLST10, X
SLCCT,QDCOS,NLOAD,OVER3,FORMK,CHOL,INOUTA,FPASS,SWITCH, X
BPASS,RESID,QLAYER,OVER4,GDISPL,MEMBR,MOMTR,MEMBU,AXIAL)
ENTRY SHELL7
INSERT SHELL7,QTAP,RLDAD,WIND,QM5C1,QM5C2
OVERLAY ALPHA
INSERT OVER1,SEARCH
OVERLAY ALPHA
INSERT OVER2,SUBSPH,BLAYER,QDSMEL,TRUSS,SSTQM5,QM5STF, X
CLST10,SLCCT,QDCOS,NLOAD
OVERLAY ALPHA
INSERT OVER3,FORMK,CHOL,INOUTA,FPASS,SWITCH,BPASS,RESID,QLAYER
OVERLAY ALPHA
INSERT OVER4,GDISPL,MEMBR,MOMTR,MEMBU,AXIAL
/*
//GO.FT01F001 DD DSN=&FILE1,UNIT=SYSDA,SPACE=(CYL,(1,1),RLSE),
// DISP=(NEW,DELETE),DCB=(BUFNO=1,RECFM=VS,LRECL=5004,BLKSIZE=5008)
//GO.FT02F001 DD DSN=&FILE2,UNIT=SYSDA,SPACE=(CYL,(1,1),RLSE),
// DISP=(NEW,DELETE),DCB=(BUFNO=1,RECFM=VS,LRECL=5004,BLKSIZE=5008)
//GO.FT03F001 DD DSN=&FILE3,UNIT=SYSDA,SPACE=(CYL,(1,1),RLSE),
// DISP=(NEW,DELETE),DCB=(BUFNO=1,RECFM=VS,LRECL=5004,BLKSIZE=5008)
//GO.FT04F001 DD DSN=&FILE4,UNIT=SYSDA,SPACE=(CYL,(1,1),RLSE),
// DISP=(NEW,DELETE),DCB=(BUFNO=1,RECFM=VS,LRECL=5004,BLKSIZE=5008)
//GO.FT08F001 DD DSN=&FILE8,UNIT=SYSDA,SPACE=(CYL,(1,1)),
// DISP=(NEW,DELETE),DCB=(BUFNO=1,RECFM=VS,LRECL=804,BLKSIZE=808)
//GO.FT09F001 DD DSN=&FILE9,UNIT=SYSDA,SPACE=(CYL,(1,1)),
// DISP=(NEW,DELETE),DCB=(BUFNO=1,RECFM=VS,LRECL=2404,BLKSIZE=2408)
//GO.SYSIN DD * DATA FOR SHELL7 FOLLOWS

```